Treatment of Pancreatic Cancer using Gemcitabine-loaded Superparamagnetic Iron Oxide Nanoparticles (SPIONs)

Thesis submitted in accordance with the requirements of the University of Liverpool for the degree of Doctor of Medicine

By

Sumit Nandi

MRCS (Eng), MBBS (London)

[January 2020]

Declaration

I declare that this thesis and the research upon which it is based is the result of my own work. Wherever I have incorporated the work of other, it has clearly been stated.

This work has not already been accepted in substance for any degree, nor is it being concurrently submitted in candidature for any degree in this or another University.

Sumit Nandi

[January 2020]

Abstract

Introduction:

Despite advances in the surgical management of pancreatic cancer, particularly adjuvant chemotherapy, pancreatic cancer continues to carry a dismal prognosis. Nanotechnology offers the possibility for patient tailored therapy while providing novel methods of targeted drug delivery. Our aim was to develop a superparamagnetic iron oxide nanoparticle capable of targeted release of chemotherapy in pancreatic cancer cell lines using either specific antibodies or through exploitation of their superparamagnetic properties, both in static and dynamic *in vitro* models.

Methodology:

Micellar superparamagnetic iron oxide nanoparticles, incorporating a gemcitabine pro-drug, conjugated to anti-carbohydrate antigen 19-9 antibodies were manufactured using a self-assembly methodology. Cellular uptake was assessed using co-localisation fluorescent microscopy. Antigen expression of cell lines was determined using indirect immunofluorescence. Antibody targeting was assessed using EZ4U cytotoxicity assay in Bx PC-3 (anti-carbohydrate antigen 19-9 antigen expressive) and Mia Pa Ca-2 (non-anti-carbohydrate antigen 19-9 expressive) cell lines.

Complete RPMI media was circulated through custom-made $25cm^2$ flasks containing $2x10^6$ monolayers of Mia Pa Ca-2 cells at $37^oC/5\%CO_2$. Cells were subjected to control media or 2% gemcitabine-loaded superparamagnetic iron oxide nanoparticles, with or without a magnet for 16/24/48/72 hours. Light and fluorescent microscopy was used to visualise the monolayer and gemcitabine-loaded SPION uptake. LDH assay was performed as a measure of cell lysis.

Results:

The 50% inhibitory concentration of superparamagnetic iron oxide nanoparticles conjugated to

anti-carbohydrate antigen 19-9 antibodies was significantly improved with specific antibody targeting in BxPC-3 cells (354nM vs 1,175nM) but absent in MiaPaCa-2 cells (3,510nM vs 3,090nM).

Light microscopy confirmed destruction of monolayers and co-localisation fluorescent microscopy, after up to 72 hours of flow, showed cellular uptake of rhodamine-tagged gemcitabine-loaded SPIONs, especially adjacent to a magnet. Lactate dehydrogenase assay optical densities were higher, indicating increased cell lysis, in flow systems subjected to gemcitabine-loaded SPIONs with use of a magnet: 16 hours (0.751 v 0.139nm; $p<0.001$); 24 hours (0.798 v 0.226; $p<0.05$); 48 hours (1.716 v 1.375; $p=0.01$) and 72 hours (1.645 v 1.330; $p=0.11$). There was no significant difference in corresponding static experiments.

Conclusions:

We have developed a novel nanohybrid to target antigen expressing pancreatic cancer cells using a specific antibody tag. When loaded with modified gemcitabine, these SPIONs act as delivery vehicles capable of intracellular drug release. They can be successfully drawn from circulation and destroy monolayers within a flow system. Magnetic targeting provides greatest improvements over static conditions at early time points and is still superior at 72 hours. Bio-magnetic targeting in custom-made nano-vehicles provides a potential novel theranostic solution in pancreatic cancer. This could reduce off target effects leading to increased chemotherapy agent efficacy and offer the prospect for new treatments in pancreatic cancer.

Acknowledgements

I am forever grateful to all those who have helped and advised me to complete my thesis. In particular, I would like to thank my primary supervisor Professor Chris Halloran, who has been extremely supportive throughout my time in research. I am greatly thankful to my secondary supervisor, Professor Eithne Costello, who has been always been willing to share her invaluable expertise. I thank Mr Paul Sykes, who has handed over great knowledge in continuing this exciting project.

The project is indebted to the Department of Chemistry at the University of Liverpool, especially Professor Matthew Rosseinsky, Dr Erol Hasan, Dr Mike Barrow and other Rosseinsky group members for their close collaboration in helping me with the nanotechnology.

I am thankful to all my scientific colleagues at the NIHR Liverpool Pancreas Biomedical Research Unit for their teaching and patience.

I have been very fortunate to complete my studies with the financial support from a Freemasons One Year Research Fellowship through the Royal College of Surgeons, England and The Royal Liverpool University and Broadgreen Hospitals Research and Development Fund.

Table of contents

1. Introduction

1.1 Nanotechnology and Nanomedicine

Nanotechnology is rapidly developing; its uses are wide-ranging and provide novel approaches in all areas of science. It is the branch of science and engineering that studies and exploits the unique behaviour of materials at a scale of approximately 1-100 nanometres [1]. It promises huge potential in fields as diverse as healthcare, IT and energy generation and storage. Nanomedicine is the application of nanotechnology to achieve breakthroughs exclusively in healthcare. It exploits the improved and often novel physical, chemical, and biological properties of materials at the nanoscale, and offers the potential to enable early detection, prevention, improved diagnosis and imaging, treatment and follow-up of diseases. Nanomedicine embraces a wide range of applications from in vivo and in vitro diagnostics to therapy including targeted delivery and regenerative medicine [2]. It has the potential to have far-reaching benefits in diseases such cancer, diabetics, cardiovascular diseases, multiple sclerosis, Alzheimer's and Parkinson's disease and inflammatory and/or infectious diseases, and impact individuals and their families. Given the immense potential impact of nanomedicine on public well-being and on economic growth, large sums of money are funded towards research projects in nanomedicine. The European Technology Platform on Nanomedicine [3], supported by the European Union, has pledged €550 million in 116 projects involving nanomedicine advances, through its through its 7th Framework Programme for Research and Development (FP7) until 2020 [1].

1.1.1 Applications of Nanomedicine in Oncology

Cancer is a leading cause of death worldwide, accounting for 9.6 million deaths (around 13% of all deaths) in 2018 with global deaths from cancer projected to continue rising, with an estimated 13.1 million deaths in 2030 [4-6]. More than 90% of cancer-related deaths are attributed to metastasis. Research advances in nanomedicine are centred to the development of specific treatments that can detect and destroy primary and secondary (i.e. metastasis) tumours.

Nanomedicine holds the wide-ranging possibilities from earlier diagnostics and improved imaging to better, more efficient, and more targeted therapies [3]. The use of nanomaterials to treat and image cancer is arguably the most active area of nanomedicine research. As a nascent and emerging field that holds great potential for precision oncology, nanotechnology has been envisioned to improve drug delivery and imaging capabilities through precise and efficient tumour targeting, safely sparing healthy normal tissue. In the clinic, nanoparticle formulations such as the first-generation Abraxane® in breast and metastatic pancreatic cancer have shown advancement in drug delivery while improving safety profiles [7], [1]. However, effective accumulation of nanoparticles at the tumour site is sub-optimal due to biological barriers that must be overcome. Nanoparticle delivery and retention can be altered through systematic design considerations in order to enhance passive accumulation or active targeting to the tumour site. In tumours where passive targeting is possible, modifications in the size and charge of nanoparticles play a role in their tissue accumulation. For tumours in which active targeting is required, precision oncology research has identified targetable biomarkers, with which nanoparticle design can be altered through bioconjugation using antibodies, peptides, or small molecule agonists and antagonists [1, 7-9].

1.1.2 Nanomedicine in cancer imaging

Properties of certain nanomaterials can be harnessed to improve the resolution and accuracy of mapping lesions. Consequently, surgeons can thus rely on this to appropriately select patients and plan the surgical removal of a tumour. This has been demonstrated mainly by manipulating the magnetic qualities of certain nanomaterials in the use of imaging tumours with magnetic resonance [10, 11].

1.1.3 The use of nanoparticles in drug delivery in cancer treatment

Due to their small size and surface area characteristics, they exhibit unique electronic, optical, and magnetic properties that can be exploited for drug delivery [12]. It is ideal in cancer therapy that anti-cancer therapeutic compounds are delivered to targeted tumour cells to exert their effects. Conventional chemotherapy agents that are administered systemically are distributed

throughout the body via the bloodstream and are subjected to hydrolysis and enzymatic degradation, subsequently leading to rapid excretion through the urinary system. Furthermore, owing to suboptimal targeting, the accumulation of the chemotherapeutic agent in tumour cells is limited. Targeted delivery of drug molecules with nanoparticles can improve biodistribution, increase circulation half-life, and protect drugs from the microenvironment, thus increasing efficacy and reducing side effects [13]. Nanoparticles, through the enhanced permeability and retention (EPR) effect, preferentially accumulate in tumours [14, 15]. This phenomenon can translate into higher therapeutic efficacy and lower toxicity for nanoparticle therapeutics, as shown in Gradisher et al. study of conventional versus nanoparticle-based paclitaxel delivery in metastatic breast cancer. [16]. Even though nanomedicine is a relatively new branch of science, many novel nanoparticle drug delivery platforms have been developed over the past three decades. These platforms generally fall into the following categories: liposomes, nanoparticle albumin bound (nab) technology, polymeric nanoparticles, dendrimers, metal nanoparticles, and molecular targeted nanoparticles. [17]. This thesis will focus on the use of metal-based nanoparticles, focusing on iron oxide core nanoparticles.

1.1.4 Targeting of cancer using nanomaterials

Nanotechnology offers many possibilities for targeting cancer, as there are several differing materials available combined with the ability to construct tailor-made particles to address a specific function. Nanoparticles can be synthesised to encapsulate and deliver a diverse range of therapeutic compounds, including chemotherapy agents and DNA/RNA. Therefore, specific targeting should allow a higher concentration of a nanoparticle to accumulate within the vicinity of the tumour and hence reduces systemic side effects of conventional chemotherapy [11]. Broadly there are two methods for targeted drug delivery using nanoparticles: passive and active. Passive targeting takes advantage of the leaky vasculature of tumours. Due to the small size of the nanomaterial, it is thought to preferentially accumulate at the site of the tumour, a phenomenon known as the enhanced permeability retention effect. Libutti et al have demonstrated in a phase I clinical trial that a novel PEGylated colloidal gold nanoparticle

carrying recombinant human tumor necrosis factor alpha (rhTNF), when injected intravenously in patients with advance breast cancer, may be administered systemically at doses of rhTNF that were previously shown to be toxic. Furthermore, even at the highest dose rhTNF's dose-limiting toxic effect of hypotension was not seen. This demonstrated increased tumour accumulation without the systemic side effects [18]. Active targeting of cancer is facilitated by conjugation of the particle with a specific ligand (e.g. antibody) or an external stimulus to guide the nanoparticle to the desired location, for example, a magnetic field to direct nanomaterials with magnetism.

Nanomaterial	Key features	Potential Use
Iron oxide	Superparamagnetism, (magnetised only in the presence of an external magnetic field, termed SPIONs).	Targeting (accumulation using an external magnetic field to the desired site). Treatment as alternating magnetic field causes the particles to heat up, resulting in thermal ablation of adjacent cells. Imaging (MRI contrast).
Gold	Affinity for binding thiols, disulphides, phosphates and amines allow simple conjugation with peptides, proteins, and antibodies.	Biological applications as use in targeted cancer therapy. Photothermal treatment to ablate specific tissue.
Quantum dots	Fluorescence.	Imaging in vivo. Nanocarrier for drug delivery. Multimodal probe to monitor the biodistribution of drugs.
Carbon	Chemically stable. High tensile strength and conductivity. Numerous points of attachment, allowing for precise grafting of active chemical groups.	Drug delivery. Thermal ablation therapy.
Liposomes	Lipid vesicles either unilamellar or multilamellar with an aqueous compartment Structure allows for delivery of a cargo loaded in the aqueous compartment or embedded in the lipid bilayer	Therapy Imaging
Dendrimers	Three dimensional, hyperbranched globular nanopolymeric architectures Narrow polydispersity index, control over molecular structure and availability of multiple functional groups at the periphery and cavities Terminal functionalities provide a platform for tailor made conjugation of drug and targeting moieties	Drug targeting and delivery MRI contrast agents

Table 1: Summary of commonly used nanomaterials in oncological applications. (SPIONs: superparamagnetic iron oxide nanoparticles; MRI: magnetic resonance imaging.

1.2 Superparamagnetic iron oxide nanoparticles

Superparamagnetic iron oxide nanoparticles (SPIONs) are small synthetic γ-Fe_2O_3 (maghemite), Fe_3O_4 (magnetite) or α-Fe_2O_3 (hermatite) particles with a core diameter ranging from 10 to 100nm. Mixed oxides of iron with transition metal ions such as copper, cobalt, nickel, and manganese, are known to exhibit superparamagnetic properties and fall into the category of SPIONs [12, 19, 20]. However, magnetite and maghemite nanoparticles are the most widely used SPIONs in various biomedical applications. SPIONs have an organic or inorganic coating, on or within which a drug is loaded, and they are then can guided by an external magnet to their target tissue. This thesis will focus on the relevant biomedical aspects of SPIONs rather than the material chemistry processes used in their manufacture.

1.2.1 Superparamagnetism

SPIONs exhibit the phenomenon of superparamagnetism, that is, on application of an external magnetic field, they become magnetised up to their saturation magnetisation then, on removal of the magnetic field, they no longer exhibit any residual magnetic interaction. This property is size-dependent and generally arises when the size of nanoparticles is as low as 10 to 20nm [21]. This superparamagnetism, unique to nanoparticles, is very important for their use as drug delivery vehicles because these nanoparticles can literally drag drug molecules to their target site in the body under the influence of an applied magnet field [12]. As described above, once the applied magnetic field is removed, the magnetic particles retain no residual magnetism (at room temperature) and hence are likely to easily disperse, thus preventing uptake by phagocytes and increasing their circulatory half-life. Furthermore, due to a negligible tendency to agglomerate, SPIONs pose no danger of thrombosis or blockage of blood capillaries [12, 19, 20].

1.2.2 Size

The size of nanoparticles largely determines their half-life in the circulation. Particles with sizes smaller than 10 nm are mainly removed by renal clearance, whereas particles larger than 200nm become concentrated in the spleen or are taken up by phagocytic cells of the body, in both

instances leading to decreased plasma concentrations [22]. However, particles with a size range of 10 to100nm are considered to be optimal, as they can easily escape the reticuloendothelial system and sustain longer circulation times. They are also able to penetrate through very small capillaries [12, 23]. The small size of SPIONs is responsible for the enhanced permeability and retention (EPR) effect, which causes concentration of the particles in target tumour tissue. SPIONs with a particle size smaller than 2 nm are not suitable for medical use, as they diffuse through cell membranes, damaging intracellular organelles and thus exhibiting potentially toxic effects. Controlling the size of SPIONs during manufacturing is an important consideration for use in biomedical application. The techniques most employed for measuring the particle size of SPIONs are transmission electron microscopy and dynamic light scattering [23, 24].

1.2.3 Drug loading

Drug loading can be achieved either by conjugating the therapeutic molecules on the surface of SPIONs or by co-encapsulating drug molecules along with magnetic particles within the coating. The primary requirement, despite the loading method is that the active drug's functionality is not compromised. Furthermore, the drug-loaded nanoparticles should also release the drug at the appropriate site and at a desired rate. Several approaches have been developed for conjugation of therapeutic agents or targeting ligands on the surface of these nanoparticles and they can be grouped under two categories: firstly, conjugation by means of cleavable covalent linkages onto the surface of polymer-coated SPIONs and secondly, by means of physical interactions [25] such as electrostatic, hydrophobic/hydrophilic and affinity interactions.

1.2.4 SPION targeting approaches

SPIONs can be properly engineered to reach their target tissue with minimum nonspecific cellular interactions. Targeting strategies can be grouped into three classes: passive, active and magnetic.

1.2.4.1 Passive targeting

Passive targeting, as described before, takes advantage of the innate size of the nanoparticles as well as the unique characteristics provided by the tumour microenvironment [26]. Tumour cells exhibit leaky vasculature due to incomplete angiogenesis compared to healthy cells. This is also known as the enhanced permeability and retention effect [14, 15].

1.2.4.2 Active targeting

Active targeting involves targeting ligands which are coupled at the surface of magnetic nanoparticles to interact with receptors that are overexpressed at their target sites. Such particles accumulate in larger quantities in target cells due to an attraction of these ligands onto the receptors and subsequent improvement of internalisation into cells. Various active targeting agents engineered and attached to the SPION surface not only ensure specific target binding but also minimize the dose required and nonspecific cellular interactions [9, 26, 27].

1.2.4.3 Magnetic targeting

Magnetic focusing uses external magnets to create a suitable magnetic field gradient over the targeted area and ensure significant accumulation of drug-loaded SPIONs [28]. The strength of the applied magnetic field can be altered to modulate release of the drug in the desired fashion, resulting in maximum therapeutic benefits [29]. Accumulation of SPIONs within malignant cells was found to be dependent on duration of exposure to the external magnetic field [30].

1.2.5 Pharmacokinetics

For SPIONs to be considered an effective modulation to biomedical treatments, it must have appropriate pharmacokinetic properties. Especially, their absorption into various cells, biodistribution and excretion from the body.

1.2.5.1 Cellular uptake and biodistribution

Literature reports several processes for cellular uptake of SPIONs. When administered intravenously, the SPIONs are predominantly taken up by phagocytes in the reticuloendothelial systems of the liver, spleen, and lymph tissue [31]. The SPIONs must cross the vascular

endothelium, in order to reach their target site(s) [32]. Particle size, surface coating, and surface charge are major determinants of the biodistribution, pharmacokinetics, and possible toxicity of SPIONs [22]. Tissue distribution is mainly affected by particle size. SPIONs with a particle size smaller than 50 nm evade opsonisation, thus increasing their circulation time and hence are gradually taken up by macrophages in the reticuloendothelial system (predominantly within the liver). In addition to particle size, the coating material used on iron oxide particles also determines the rate of hepatic clearance. In general, SPIONs covered with coating materials which hinder access of water to the iron oxide core show slower degradation and hence an increased half-life in blood [9, 12]. Surface charge, in addition to particle size and the coating material, affects the uptake of SPIONs by different cells. For example, positively charged SPIONs adhere nonspecifically to cells because the majority of the cell membranes have a net negative charge, whereas strong negative charges on the surface of magnetic particles facilitate their uptake by the liver [13, 19, 27, 33].

1.2.5.2 Metabolism and excretion from biological systems

An ideal drug delivery system, after delivering its payload to the target site, should be eliminated from the biological system with minimal harmful systemic effects. The uptake, distribution, metabolism, and excretion of dietary iron is highly regulated in biological systems. Specialized mechanisms which govern the body's iron regulation processes are also thought to be involved in handling iron oxide nanoparticles. There remain only few reports in the literature clarifying their biotransformation in biological systems. Once internalised, lysosome-mediated degradation is generally considered to be the main intracellular metabolic mechanism involved in the degradation of SPIONs [34] [35, 36]. The most desirable pathway for SPIONs to be excreted from biological systems is via the kidney, because this route involves minimal intracellular catabolism, reducing the probability of generating reactive oxygen species and hence associated toxicity. Renal excretion represents the safest route of elimination for SPIONs. However, the shape, hydrodynamic size, surface coating, and surface charge of SPIONs play a major role in regulating their renal clearance [19, 29].

1.2.6 Utility as drug delivery vehicles

SPIONs have emerged as an attractive prospect for targeted delivery of drugs because of their unique magnetic qualities. Their role as contrast agents in MRI has already been established [19] and increasingly are being investigated for their potential application in the delivery of chemotherapeutic drugs, radionuclides, and anti-inflammatory agents, as well as in gene delivery [7, 9, 25]. Magnetic fluid hyperthermia is another approach where SPIONs can be utilised for localized production of heat, resulting in destruction of cancer cells [37].

1.2.6.1 Diagnostic use

The only clinical use for which commercial SPION-based products are available is as MRI contrast agents for the diagnosis of human disease. SPIONs have been used as contrast agents for at least 20 years and have emerged as an suitable alternative to gadolinium-based MRI contrast agents, particularly in patients with renal dysfunction [19]. As this report is focused on the therapeutic usage of SPIONs, diagnostic applications are not discussed in detail.

1.2.7 Role in cancer therapy

Chemotherapeutic agents are well known to exert a multitude of unwanted systemic side effects due to their lack of target specificity. SPIONs can deliver chemotherapy drugs into malignant cells while sparing healthy cells. This also leads to reduction of the dose required because the drug is delivered directly to target cells. A number of anticancer drugs, including paclitaxel, methotrexate, mitoxantrone, and doxorubicin, have been conjugated with magnetic nanoparticles to increase their target specificity [9, 29, 38]. Further strategies can be utilised to increase the specificity of targeting cancer cells. These include, coating of SPIONs with polymers have resulted in increased interaction of these particular nanoparticles with human cancer cells, as well as reduced cytotoxicity in healthy cells [25, 39]. Cole et al. have shown polyethylene glycol (PEG)-modified, cross-linked, and starch-coated iron oxide nanoparticles have been found to enhance magnetic tumour targeting [40].

1.2.8 Potential for theranostics

Theranostics is a new field of medicine which combines specific targeted therapy based on specific targeted diagnostic tests providing a personalised and precision medicine approach. The theranostics paradigm involves using nanotechnology to unite diagnostic and therapeutic applications to form a single agent, allowing for diagnosis, drug delivery and treatment response monitoring. This is a particularly exciting prospect of SPIONs. As increasingly sophisticated multifunctional SPIONs are developed, as does the potential uses. Such nanocomplexes, can not only serve the purpose of being drug delivery vectors, but also have applications in another diagnostic or therapeutic aspect. Such examples include additional uses in MRI imaging [41] targeted thermosensitive chemotherapy [42], magnetically targeted photodynamic therapy [43], and fluorescence imaging [44].

1.2.9 Thermal ablation

A drug-free approach to combating malignant cells involves localised heating of these cells from the inside. Cells begin to show signs of apoptosis when their inside temperature is raised in the range of 41–47°C. Necrosis results when the temperature reaches approximately 50°C. Targeted hyperthermia involves administration of magnetic nanoparticles, such as SPIONs, which are taken up by cells through endocytotic pathways and become concentrated in intracellular endosomal vesicles. When subjected to a high frequency AC magnetic field, these particles become heated because of Neel or Brownian relaxation losses in single-domain particles, resulting in localised cellular destruction [45]. The main drawback of this approach is ensuring the selective delivery of these nanoparticles to the desired cells to be target and the nanoparticles' optimisation of their thermal properties to produce an effective magnetic hyperthermic effect. Coating tends to decrease heating efficiency, hence should be kept to a minimum [46].

Figure 1: Common oncological applications for SPIONs [adapted (Palanisamy and Wang 2019)]

1.2.10 Potential disadvantages of using SPIONs as drug vectors

There several disadvantages with the use of SPIONs as drug delivery vehicles, which are briefly discussed below.

1.2.10.1 Creating a suitable magnetic field gradient

For successful implementation for SPION-based therapy is the development and maintenance of a suitable magnetic field to ensure effective localisation of the particles within the targeted cells and tissues; and furthermore, their successful internalisation with the desired cells. Blood circulation naturally offers resistance to a magnetic field developing [12]. Blood vessels and organs deep within the body cannot be targeted by external magnets because as the distance between the magnet and targeted area increases, the strength of the magnetic field at the desired site decreases. Only those areas which are close to the surface can be properly targeted using an external magnet. To overcome this limitation, research groups have been adopting superconducting magnets, which can exert strong magnetic fields. These magnetic fields have been found to penetrate the skin surface to a depth of 20 mm [47]. Magnetic stents or implants, which can create strong local magnetic fields, have also been used to increase the concentration

of drug-loaded magnetic nanoparticles at the desired site [48], however, an invasive surgical procedure is required and carries a morbidity risk [49].

1.2.10.2 Burst effect

Ideally, SPIONs should release their entire payload of the cytotoxic agent at the site of action, however, one limitation is the burst release of drug bound at the surface of the SPION. Any defective surface engineering leads to a premature release of a significant proportion of the drug load, which can lead to unnecessary systemic toxicity, that is, non-targeted release into the blood circulation. Certain strategies have shown to reduce the so-called burst effect, such as the use of crosslinked polymer coating [50] or utilising a starch coating [51].

1.2.10.3 Low bioavailability

Intravenous administration is the route of choice for SPIONs, currently, commercially available SPION-based MRI contrast agents are generally given by the intravenous route. Although intravenous administration of these iron oxide nanoparticles ensures 100% systemic bioavailability, their specific uptake by target cells is an issue of concern because of nonspecific uptake by the reticuloendothelial system and non-specific binding to plasma proteins. However, with adequate surface engineering and the attachment of suitable targeting ligands, along with magnetic focussing, it is possible to enhance the uptake of drug-loaded SPIONs by target tissue, as previously discussed [7, 9, 11, 49, 52].

1.2.10.4 Toxicity

Obviously, as SPION-driven drug delivery systems are relatively novel, despite showing promise, scrutiny is placed on pharmacokinetic and toxicity profiles. SPIONs are known to be excreted via endogenous metabolic iron pathways to maintain homeostasis [53]. Liu et al has performed significant research to demonstrate a low hazard potential for SPIONs with no murine deaths or transient adverse clinical signs [54]with no histological iron-positive pigments in macrophages of major organs, such as the liver, lungs, spleen, brain, kidney and heart [54]. A few reports have suggested some toxicological effects for SPIONs. Iron overload at the target

site is one of the causes of SPION-associated toxicity. After digestion of the coating, high levels of bare iron oxide nanoparticles at the target site can cause an imbalance in homeostasis. This can alter local cellular responses, leading to effects such as: DNA damage, inflammatory response, oxidative stress, genetic changes, disruption of cytoskeletal organization of cells, and unwanted cytotoxicity [12, 52]. After cellular uptake of SPIONs, they can be digested by lysosomes, resulting in release of free iron. These free iron ions (Fe^{2+}) can react with hydrogen peroxide or oxygen in the mitochondria to form reactive free radicals which can cause cellular and genetic toxicity [39, 55]. Strategies to reduce this unwanted effect is to coat the SPIONs, commonly used are crosslinked polymers and dextran or starch.

1.2.11 Summary and future direction for SPIONs in cancer therapy

There are several novel and progressive drug delivery systems, including SPIONs. However, there are numerous factors that make SPIONs an extremely promising prospect as a drug delivery vehicle. There are relatively simple to assemble and have shown a low toxicity profile to date. They can be multifunctional in nature and can be specific manufactured to a high degree to target a specific cell type. Furthermore, their unique magnetic qualities enable another targeting mechanism, using an external magnetic field, which other nanomaterials do not possess. Carcinomas near the body surface, like squamous cell carcinoma, malignant melanoma, Kaposi's sarcoma, and breast carcinoma, are likely to benefit the most from SPION-based therapy because magnetic targeting works best in these regions [12]. They have shown potential applications in a wide variety of biomedical fields, both diagnostic and therapeutic. Disappointingly, despite decades of research and the outlined advantages there remains no SPION-based drug delivery product on the market. There are limitations which must be overcome to successfully launch a commercially available SPION-based product in the clinic. With the discovery of supermagnets, it has become possible to create a suitable magnetic field gradient deep inside the skin surface, which can lead to increased targeting capability of SPIONs. Further research is required especially towards the pharmacokinetics biodistribution and toxicity of SPIONs *in vivo*. Nevertheless, there is a remarkable rate of studies and research

involving SPIONs, that it is only a matter of time before SPION-based drug treatments are available in the clinic.

1.3 Functionalisation of nanoparticles using antibodies

1.3.1 Antibody structure and function and Specificity

Antibodies are found in the serum and other bodily fluids of vertebrates that react specifically with antigens. Antibodies belong to the immunoglobulin family; and the term antibody and immunoglobulin can be used interchangeably. Immunoglobulins are defined as a family of globular proteins that comprise antibody molecules and molecules having patterns of molecular structure (antigenic determinants) in common with antibodies. The term immunoglobulin can be used to refer to any antibody-like molecule, regardless of its antigen-binding specificity [56]. However, this text will only deal with the IgG molecule. The primary function of an antibody is to bind to a foreign molecule (antigen). In humans, there is a vast array of antibodies due to millions of different amino acid sequence combinations. However, the antibodies remain structurally similar (grossly Y-shaped molecules). Antibodies are the most diverse proteins known. Due to the differing amino acid sequences in the arms of various antibody molecules, each different antibody can bind specifically one unique epitope. Thus, the arms of an antibody molecule confer the versatility and specificity of responses that a host can mount against antigens. The stem region of an antibody molecule decides its biological activity and defines whether the response against a particular antigen will lead to complement-mediated lysis, enhanced phagocytosis, or (in some cases) allergy [56]. These activities start once antibodies bind to antigen. The structure of an antibody is related to its function; its structure explains the binding versatility, binding specificity and biological activity. Pioneering experiments performed by Porter and Edelman [57, 58] discovered the finer structure of antibodies. Their research led to the 1972 Nobel in Medicine or Physiology. Whilst fragmenting the whole antibody molecule, Edelman discovered two subunits in equimolar ratios. He designated the

larger subunit (50 kiloDalton [kD]) as the heavy, or H, chain and the smaller subunit (23 kD) as the light, or L, chain; with the molecular weight of the original IgG molecule is 150 kD.

1.3.2 Antibody specificity

The antibody structure is further elaborated by the discovery of each chain consisting of a large region that was constant in different types of antibodies (even from unrelated species) and a similar-sized region that was highly variable. This large region, known as the constant (C) region, has amino acid sequences in the carboxyl terminal end of the chains that are almost identical; whereas the opposite end (amino terminal end) shows great variability in amino acid sequencing, called the variable (V) region [56]. This finding applies to both the light and heavy chains, leaving four distinguishable domains: variable light (VL), variable heavy (VH), constant heavy (CH1-3) and constant light (CL). As amino acid sequencing determines the 3D structuring of proteins, the unique sequence of each variable region leads to the large diversity of structure, which accounts for antibody specificity. Variability of the amino acid sequences in the V regions is not random but precisely organised.

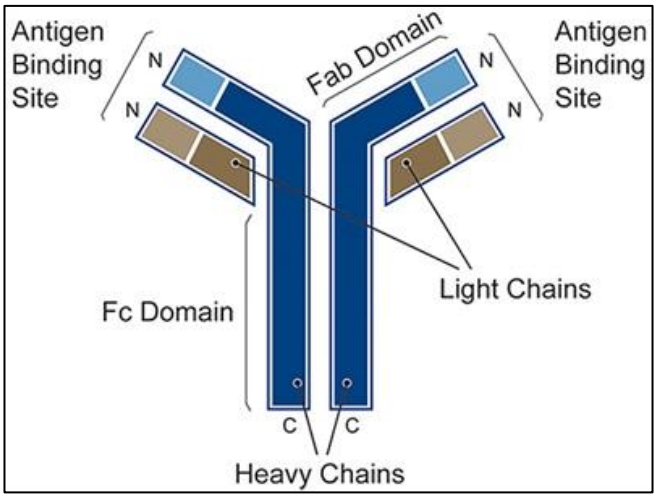

Figure 2: showing the various sites of an antibody. Two light chains and two heavy chains. The antibody has an amine terminal (N) and carboxyl terminal (C). The darker areas represent the constant regions and the lighter areas the variable regions (Bio-Rad 2014).

1.3.3 Conjugation of antibodies to nanoparticles

The conjugation of different moieties to the nanoparticle widens their application and provides them with new or enhanced properties. A variety of ligands have been explored for such purposes, including aptamers, peptides and carbohydrates, although antibodies are perhaps the most frequently employed [59, 60]. The conjugation of nanoparticles with antibodies combines the properties of the nanoparticles themselves with the specific and selective recognition ability of the antibodies to antigens [61]. This is to improve the targeting specify of the nanoparticle to its desired cell. This is one method of active targeting of nanoparticles. Furthermore, the chemistry applications in order to conjugate antibody attachments onto nanoparticles is not discussed in this text.

1.4 Pancreatic Cancer

1.4.1 Overview

Pancreatic cancer is the 11th most common cancer worldwide and, in the UK, with around 338,000 new global cases annually and around 10,000 cases in the UK between 2014-16. There are around 9,200 pancreatic cancer deaths in the UK every year, and is the 5th most common cause of cancer death in the UK, accounting for 6% of all cancer deaths in 2017 [5]. Since the early 1970s, pancreatic cancer mortality rates have remained stable in the UK. Over the last decade, pancreatic cancer mortality rates have increased by 5% in the UK [5]. The causes for pancreatic cancer remain unknown. Several environmental factors have implicated, but tobacco use is the only causative factor with evidence: the risk of developing pancreatic cancer is 2.5 to 3.6 times higher in smokers, where the risk increases with greater tobacco use and longer exposure [62]. Some studies have shown an increased incidence of pancreatic cancer among patients with diabetes mellitus or chronic pancreatitis and data is limited for on the possible roles of alcohol, coffee consumption and aspirin use [63-65].

1.4.2 Poor prognosis

Pancreatic ductal adenocarcinoma (PDAC) is considered as the most common pathological type of pancreatic cancer and contributes to 94% of pancreatic cancers [66]. PDAC remains difficult to diagnose, as symptoms are often vague and only later when recognisable symptoms, such as jaundice, weight loss and abdominal pain arise. Unfortunately, by the time of diagnosis, many patients experience either a locally advanced stage or distant metastasis, and then become ineligible candidates for major potentially curable surgery. The current terrible outcomes for patients with pancreatic cancer can in part attributed to: the difficulty in obtaining an early diagnosis; the inability to detect pre-cancerous lesions (pancreatic intraductal neoplasms) and the lack of any reliable serum biomarker(s) with accuracy to detect early either pre-malignant lesions [67] or a developing invasive malignancy. Consensus shows that patients with pancreatic cancer were often observed with 90% KRAS mutations, 50 to 80% inactivating mutations in CDKN2A, SMAD4, and TP53 [68].

All of this summates into only 20% of patients at the time of diagnosis are suitable for potentially curative resection. Without treatment, survival is approximately 18% at one year and 3.7% at five years [69]. Only 1% of people diagnosed with pancreatic cancer in England and Wales survive their disease for ten years or more (2010-11) [5]. The five-year relative survival rates for pancreatic cancer are the lowest of the 21 most common cancers in England [70]. At present the only chance for long-term survival (29% 5-year survival) is with a combination of curative surgery and adjuvant therapy, however, recurrence occurs in 55% of patients at 2 years and 70% at 5 years [71, 72].

These dismal statistics indicate that is an urgent need to ensure better diagnosis and treatment for PDAC to improve any survival benefit. Novel approaches, such as the use of nanotechnology applications may be a potential theranostic solution.

1.4.3 Molecular biology of pancreatic ductal adenocarcinoma

PDACs are complex, with the tumoural mass comprising a multitude of different cell types. Its surrounding desmoplastic environment (also known as stroma) is a hallmark of the disease. Stroma contains a number of cellular components including cancer-associated fibroblasts (CAFs), macrophages, lymphocytes and pancreatic stellate cells (PSCs), embedded within a dense and complex extracellular matrix (ECM) [73]. PDAC has the unique property of a high ratio of stroma to epithelial cells, with stroma commonly accounting for more than 90% of the tumour volume [74].

1.4.4 Role of stroma

The role of stroma in PDAC is currently under intense scrutiny. It is widely accepted to promote and facilitate tumour cell proliferation, migration, and invasion [75-77]. However, further research is on-going and is needed to fully comprehend its function [78]. PSCs, which comprise approximately 4% of the cells in the pancreas [79], are the principle cell type responsible for the production of stromal fibrosis. The high proportion of stromal cells causes overexpression of several growth factors and their associated receptors, such as vascular endothelial growth factor (VEGF), epidermal growth factor (EGF), connective tissue growth factor (CTGF) and fibroblast growth factor (FGF). It is these growth factors that have an intricate relationship with the stroma and tumour itself and further modulates the tumour's behaviour. It is apparent that tumour cell-autonomous changes alone are not enough for tumour growth. Tumour cell-extrinsic factors are prominent in the pathogenesis of PDAC [80].

1.4.5 Chemotherapy resistance

The stroma of pancreatic cancer is extensively fibrotic which results in a reduced intra-tumoural vascular density, which in turn causes damaged/collapsed vessels (up to ~75%) and reduced blood flow; poor venous and lymphatic drainage; and increases the tumour's interstitial pressure [81, 82]. This is a contradistinction to most solid tumours and indeed, perfusion Computer Tomography (CT) scans show PDAC as hypodense regions i.e. areas that uptake less injected contrast material than surround normal tissue [83]. Chemotherapy drug delivery to

pancreatic tumour is difficult due to its hypo-vascularity and poor perfusion, furthermore, the dense stroma prevents drugs from penetrating the tissue's interstitium [84-86]. The difficulty in infiltrating the PDAC tumour load, can be exploited by nanotechnology, namely nanoparticles, due to their size predominantly, but also with the addition of an active targeting method e.g. ligand for a specific tumour epitope. In addition, the abundance of immunosuppressive cells leads to low numbers of effector CD8+ T cells in the stroma and consequently limited anti-tumour cytotoxicity [87].

1.4.6 Potential targets for Drug Discovery

The unique microenvironment in PDAC has been shown to play a major role in tumour growth and chemotherapy resistance. Therefore, the elimination of stromal support by destroying the stromal cells or by inhibiting feedback stimulation of cancer growth is in the focus of many evolving therapies, the concept of "anti-stromal" therapy [88]. Given the tumour mass comprise mainly of the fibrotic stroma, the extracellular matrix components or PSCs residing within the stroma could be novel targets for early diagnosis, imaging and targeted therapy [89] as they can affect the biology of the tumour cells and form barriers to drug delivery. Consequently, these stromal targets could be important as starting points for the drug discovery process (target identification and subsequent validation). A selection of the most promising stromal components for drug discovery targeting are summarised in Table 2.

1.4.7 Carbohydrate antigen 19-9

Although both benign and malignant pancreato-biliary tissue produce biomarkers, they are of particular interest in cancer management. Early in the formation of a cancer, they are present in the circulation at usually very low or undetectable levels [7, 90]. The Sialyl Lewis A antigen, or carbohydrate antigen 19-9 (CA 19-9) is the most commonly used biomarker for diagnosis and management of patients with pancreatic cancer. Since the original research by Steinberg in 1990, numerous studies have reported the use of CA 19-9 in the diagnosis of pancreatic cancer [91, 92] and at present, serum CA 19-9 is the only validated tumour marker in widespread clinical use. Several immunochemical markers have been proposed for pancreatic cancer such

as carcinoembryonic antigen (CEA), MUC3, MUC4, MUC1, and CA125, but currently the only one with any practical usefulness is CA 19-9 [93, 94], although not suitable for screening. The reported sensitivity and specificity of CA 19-9 for pancreatic cancer is between 80 to 90 percent [91, 95, 96]. Serum level of this marker rises in benign pancreatobilliary disease, so its specificity for adenocarcinoma is limited.. Nevertheless, the use of CA 19-9 for the differentiation of pancreatic cancer should be applied on an individual case basis, depending on the clinical situation and imaging findings and remains an important adjunct.

1.4.8 Potential uses of nanotechnology against micro-environment targets

Without doubt, understanding of the complex stromal constituents and involvement of numerous signalling pathways in pancreatic cancer progression and desmoplastic reaction is crucial to the development of novel therapies through the drug discovery process. As an increasing number of targets are explored with improved knowledge of the tumour microenvironment, the application of nanotechnology has a huge role to play in validating those targets. Given the vast array of targets available, nanotechnology would allow faster and more reliable extraction of protein targets from samples using proteomic techniques described above. Furthermore, the stromal-tumour interactions may well be directly visualised with the aid of nanoscale imaging, such as fluorescence studies (through quantum dots) and atomic force microscopy. Finally, if encouraging targets are identified, nanomaterials themselves may be used as therapeutic carriers against the target of interest.

Component	**Effect on tumour**	**Mechanism**	**Potential for therapy**
Fibroblasts			
Pancreatic stellate cells (PSCs)	Promote proliferation and invasion	Expression of fibroblast activation protein-α (FAP) [97]	• Depletion of FAP-expressing stromal cells in pancreatic ductal adenocarcinoma (PDAC) resulted in an immune-mediated hypoxic necrosis of both tumour and stroma cells [98]. • Targeting of cancer stroma fibroblasts with FAP-activated promelittin protoxin, showed increased tumour lysis and growth inhibition in xenograft mouse models of breast and prostate cancer [99]. • However, anti-FAP antibodies tested in phase II clinical trials in patients with metastatic *colorectal* cancer did not report encouraging results [100].
	Creates fibrotic environment leading to increased chemotherapy resistance	Increases secretion of collagen I, III, IV; fibronectin, laminin, hydraluronan and growth factors [101]	
ECM			
Collagen I	Activates pancreatic stellate cells	Increased expression of transgelin, increasing desmoplastic reaction and fibrosis [102]	• Mouse models have shown degradation of hyaluronan (with hyaluronidase) relieved vascular collapse and resulted in increased cytotoxicity of gemcitabine [103]. • Subsequent development of PEGPH20 (pegylated recombinant human hyaluronidase) showed partial response in 43% of patients and stable disease in additional 30% patients in phase Ib clinical trials in patients with metastatic disease [104]. • A randomized phase II clinical trial of PEGPH20 in combination with gemcitabine and *nab*-paclitaxel is in progress (NCT01839487) [105] .
Hydraluronan	Increases intra-tumoural fluid pressure and consequent vascular collapse	Causes water retention [106]	
(Tumour-infiltrating) Immune Cells			
Myeloid-derived suppressive cells (MDSCs)	Implicated in tumour progression, chemotherapy resistance and metastasis and regulates effector cells anti-tumour responses by variety of mechanisms [107, 108]	Inhibit $CD8^+$ T cell function via arginase, and reactive oxygen species secretion (direct cell contact) [109]	Targeted depletion of granulocytic MDSCs in PDAC significantly increased intratumoural accumulation of activated $CD8^+$ T cells and apoptosis of tumour epithelial cells *in vitro* and in genetically engineered mouse models. [110]
T-regulatory cells		Secretion of suppressive cytokines e.g. IL-10 and TGFβ [111]	Targeting of downstream targets such as TGFβ.
Tumour associated macrophages	M1 (pro-inflammatory) and M2 (immunosuppressive)	Source of anti-inflammatory cytokines such as IL-10 and have been shown to induce Th2 responses [112]	Tumour regression seen due to depletion in tumour associated macrophages in clinical study combining CD40 antibody with gemcitabine in advanced disease [113].

Table 2: Table summarising the stromal components that could be potential drug discovery targets. (IL-10: interleukin-10; Th2: T-helper 2 cells; TGFβ: transformation growth factor β)

1.5 Gemcitabine

Gemcitabine (2',2'-difluoro 2'-deoxycytidine, dFdC) is an analogue of cytosine arabinoside (Ara-C) from which it differs structurally due to its fluorine substituents on position 2'of the furanose ring. [114]. Gemcitabine is a prodrug which requires cellular uptake, where it is phosphorylated to gemcitabine monophosphate (dFdCMP) by deoxycytidine kinase (dCK). It is subsequently to its active metabolites, gemcitabine di- and triphosphate respectively [114].

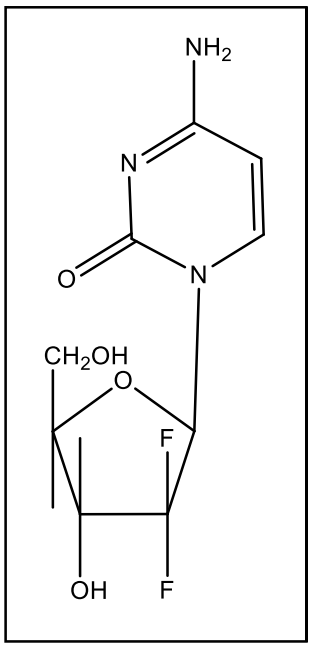

Figure 3: chemical structure of gemcitabine

1.5.1 Intra-cellular actions

Gemcitabine, through its active metabolites has many potential intra-cellular targets to prevent cell growth, mainly targeting DNA synthesis [114]. Gemcitabine triphosphate (dFdCTP) is an inhibitor of DNA polymerase and its incorporation into the DNA chain leads to termination of chain elongation. [115, 116], the non-terminal position of dFdCTP in the DNA chain prevents detection and repair by DNA repair enzymes (masked chain termination) [117, 118]. Furthermore, dFdCTP is known to incorporate into RNA. These molecular events are critical to gemcitabine-induced apoptosis.

1.5.2 Uses in cancer therapy

Gemcitabine displays a wide spectrum of anti-tumour activity. In the UK, the National Institute for Health and Care Excellence (NICE) is currently approved for first-line treatment for locally advanced

or metastatic non-small cell lung cancer (as monotherapy in elderly patients and in palliative treatment; otherwise in combination with cisplatin), treatment of locally advanced or metastatic pancreatic cancer, treatment of advanced or metastatic bladder cancer (in combination with cisplatin), treatment of locally advanced or metastatic epithelial ovarian cancer which has relapsed after a recurrence-free interval of at least 6 months following previous platinum-based therapy (in combination with carboplatin) and treatment of metastatic breast cancer which has relapsed after previous chemotherapy including an anthracycline (in combination with paclitaxel) [119].

1.5.3 Uses in pancreatic cancer

Despite previously being licensed as a single agent for adjuvant therapy for all stages of pancreatic cancer, gemcitabine has been superseded by combination therapies. For resectable disease, adjuvant therapies now involve combination strategies (with capecitabine), demonstrating a 2.5 month improvement in overall survival compared with gemcitabine alone [120]. After being approved by US FDA in 1997, gemcitabine was the first line and gold standard agent for all stages of advanced PDAC. However, combination regimens such as, FOLFURINOX (includes the drugs leucovorin calcium, fluorouracil, irinotecan hydrochloride, and oxaliplatin) or gemcitabine combination therapies are the current first-line option for resectable disease.

At the time of this research, gemcitabine was considered the ‘gold standard’ of treatment against pancreatic cancer and was in use at all stages of the disease. However, as described, more sophisticated oncological regimens have grossly diminished its use, becoming somewhat of a second-line treatment and reserved for advanced stages of the disease.

1.5.4 Limitations of gemcitabine

Gemcitabine has been surpassed as the cornerstone of PDAC treatment for a variety of reasons. The major drawbacks are effects primarily caused by molecular mechanisms limiting its cellular uptake and activation which determines its overall efficacy. There is low bioavailability after its administration, due to rapid inactivation by blood deaminases, resulting in a very short plasma half-life. Furthermore, there is a described development of chemoresistance within weeks of treatment initiation. According to

the U.S Food & Drug Administration (FDA), gemcitabine half-life for short infusions ranged from 32 to 94 minutes, and this increased to 245 to 638 minutes with longer infusions. The values were dependent on depending on age and gender [121]. The main cause for the fast development of cell chemoresistance is induced by down-regulation of deoxycytidine kinase (dCK) or nucleoside transporters [122], predominantly human equilibrative nucleoside transporter-1 (hENT1). Thus, a frequent administration schedule at high doses is required, leading to significant side effects such as hepatotoxicity and nephrotoxicity [123]. The majority of patients with gemcitabine-treated pancreatic adenocarcinoma become resistant after consecutive treatments and fail to derive benefit from chemotherapy.

1.5.5 Gemcitabine resistance

Gemcitabine has a complex pathway of metabolism, and there are many mechanisms that can contribute to gemcitabine cytotoxicity and conversely its resistance [124]. Studies performed on human cancer cell lines have indicated that human equilibrative nucleoside transporter-1 (hENT1) was found to be gemcitabine's dominant cellular transporter [125], which is over-expressed in human pancreatic adenocarcinoma cells. If gemcitabine is not transported into the cell via hENT1 it cannot inhibit cell growth [126, 127]and studies have shown that a decrease in hENT1 expression may result in gemcitabine resistance in PDAC [128, 129]. Increased hENT1 abundance facilitates efficient cellular entry of gemcitabine and confers increased cytotoxicity [130, 131]. Once intra-cellular, gemcitabine is phosphorylated by deoxycytidine kinase in a rate-limiting step. And its deficiency is acknowledged to be one of the main mechanisms responsible for the development of resistance to gemcitabine.

To counteract gemcitabine's poor bioavailability and chemoresistance in PDAC, several novel therapeutic approaches, including chemical modifications of the gemcitabine molecule generating numerous prodrugs, not rendering it dependent on the nucleoside transporter and/or entrapping gemcitabine designs in colloidal systems such as nanoparticles and liposomes may be a successful future more targeted mode of chemotherapy treatment.

1.6 Chemotherapy treatments in pancreatic cancer

The chemotherapy regimens offered to patients is dependent on the stage of the disease, broadly speaking, if the cancer is surgically amenable to resection or not; either due to locally advance disease or metastases. The disease status governs which agents are considered.

1.6.1 Current chemotherapy treatments for pancreatic cancer

Table 3 below summarises the current chemotherapy strategies that are recommended in the UK as per the most recent NICE guidance from 2018.

<table>
<tr><th colspan="3">Resectable or borderline resectable disease</th></tr>
<tr><th>Neoadjuvant therapy</th><th>Surgery</th><th>Adjuvant therapy</th></tr>
<tr><td>Only considered as part of a clinical trial.</td><td>Consider pylorus-preserving resection (for head of pancreas tumours) if can be adequately resected with standard lymphadenectomy.</td><td>Offer adjuvant gemcitabine plus capecitabine to people as soon as they are well enough to tolerate all 6 cycles.
Consider adjuvant gemcitabine for people who are not well enough to tolerate combination chemotherapy.</td></tr>
<tr><th colspan="3">Locally advanced disease</th></tr>
<tr><td colspan="3">Offer systemic combination chemotherapy to people with locally advanced pancreatic cancer who are well enough to tolerate it or consider gemcitabine alone if unable to tolerate combination chemotherapy.</td></tr>
<tr><th colspan="3">Metastatic pancreatic cancer</th></tr>
<tr><th colspan="2">First-line treatment</th><th>Second-line treatment</th></tr>
<tr><td colspan="2">• Offer FOLFIRINOX with performance status 0-1.
• Consider gemcitabine combination therapy (with nab–paclitaxel) for people who are not well enough to tolerate FOLFIRINOX.
• Offer gemcitabine to people who are not well enough to tolerate combination chemotherapy.</td><td>• Consider oxaliplatin-based chemotherapy, for those who have not received as first-line treatment.
• Consider gemcitabine-based chemotherapy as second-line treatment for people whose cancer has progressed after first-line FOLFIRINOX.</td></tr>
</table>

Table 3: Summary of current recommended chemotherapy agents and regimens as indicated by NICE in the UK. Adapted from [132] (FOLFURINOX: includes the drugs leucovorin calcium, fluorouracil, irinotecan hydrochloride, and oxaliplatin; nab-paclitaxel = nanoparticle albumin-bound paclitaxel)

1.6.2 Nanoparticle albumin-bound (nab)-paclitaxel

Nanoparticle albumin-bound (nab)-paclitaxel is paclitaxel linked to albumin nanoparticles which makes it soluble and is an example of application of nanotechnology to cancer treatment; and the only example concerning pancreatic cancer. Nab-paclitaxel (Abraxane®) is a microtubule inhibitor, it was developed to avoid the toxicities of the polyoxyethylated castor oil solvent which is used for unbound paclitaxel because of its poor aqueous solubility [133, 134]. The nanoparticle-driven delivery system has pharmacokinetics and pharmacodynamics of paclitaxel, in part by decreasing its hydrophobicity. The use of nab-paclitaxel, combined with gemcitabine, was founded on molecular profiling of malignant

pancreatic tumours, which identified overexpression of secreted protein acidic and rich in cysteine (SPARC), an albumin-binding protein [135]. Nab-paclitaxel is now used in the UK as first-line combination therapy with gemcitabine for metastatic adenocarcinoma of the pancreas (see table 3).

1.7 Nanotechnology in pancreatic cancer

Nanoparticles provide an attractive approach in the treatment of pancreatic cancer. As discussed, they can be modified to contain a variety of therapeutic agents and also be conjugated to ligands to facilitate active targeting [136]. Furthermore, they confer an option to negotiate the hypo-vascular and densely fibrotic stroma, with which current chemotherapy options has had limited success. Pancreatic cancer expresses a number of potential targets that can be aimed for by conjugated nanoparticles, these include: antibodies (CA-19-9, Carcinoembryonic antigen [CEA], CA-125, bombesin, Epithelial cell adhesion molecule [EpCAM]) and receptor ligands (Urokinase receptor [uPAR], epidermal growth factor receptor [EGFR]) [15, 137]. PDAC has a rather unique micro-environment typified by a dense hypo-cellular stroma, which contains important growth factors, pancreatic stellate cells, fibroblasts and lymphocytes. There is a complex interplay between these elements which promote fibrosis, invasion and migration of the cancer. Furthermore, this barrier is relatively avascular limiting the effects of drugs entering into the mass. Conversely the stroma has an abundance of potentially 'drug-able' targets and the extrapolations of nano-techniques to probe this are immense. Current examples being tested with stromal modulation followed by cytotoxic/immune based therapies are: PEGylated nanoparticles carrying TGF-β inhibitor and follow on liposomal gemcitabine [138]; and PEGylated human recombinant PH20 hyaluronidase [103]. Nanotechnology can facilitate with the identification and validation of targets; and furthermore, once suitable targets are selected can visualise drug interactions and test efficacy of the therapies. Drug discovery is constantly stimulated by new technologies and the rapidly advancing research field of nanotechnology provides a focus on developing novel therapy approaches for various diseases. These applications can have an impact in the discovery of therapies in pancreatic cancer, where new approaches are desperately required. Table 4 summarises promising research into the use of nanotechnology for the treatment of pancreatic cancer.

Nanotechnology	Outcomes	Reference
Nab-paclitaxel or Abraxane® (Abraxis Bioscience): albumin-bound paclitaxel	• Phase I/II trial for pancreatic cancer demonstrated the maximum-tolerated dose for Nab-paclitaxel in combination with gemcitabine. • Improved overall survival in patients treated with nab-paclitaxel plus gemcitabine (12.2 median months of overall survival) compared to gemcitabine alone. • Nab-paclitaxel alone and in combination with gemcitabine was shown to deplete pancreatic stroma in xenograft mouse models. • This led to a 2.8 fold increase in the intra-tumoural concentration of gemcitabine.	[139]
uPAR-targeted magnetic iron oxide nanoparticles IONPs carrying gemcitabine	• Significantly inhibited the growth of orthotopic mice xenografts and allowed detection of residual tumours after treatment using MRI.	[140]
Polymeric micelles consisting of a oxaliplatin-loaded hydrophobic core and poly(ethylene glycol) hydrophilic shell.	• Repeated systemic administration of the nanoparticles significantly reduced tumour growth and metastases in transgenic mouse model.	[141]
Nanoparticle encapsulated with pro-drug of gemcitabine [4-(N) stearoyl gemcitabine]	• Overcome gemcitabine resistance associated with M1 cell overexpression in pancreatic cancer cells.	[142]
PEGylated human recombinant PH20 hyaluronidase (PEGPH20) targeting hyaluronic acid	• Systemic administration in a mouse model; produced marked decrease stroma and subsequent decrease in interstitial tumour pressure and [139] increased tumour blood vessel lumen diameter. • When delivered in combination with gemcitabine there was a strong chemotoxic effect compared to gemcitabine alone.	[103].
Polyethyleneimine / PEG-coated mesoporous silica nanoparticle for molecular complexation to a small molecule TGF-β inhibitor, LY364947 *followed by* PEGylated gemcitabine-carrying liposome	• Two-wave nanotherapy approach improved the delivery of gemcitabine as the first-wave nanocarrier reducing stromal resistance by decreasing pericyte coverage of the vasculature through interference in the pericyte recruiting TGF-β signaling pathway. • This two-wave approach provided effective shrinkage of the tumour xenografts beyond 25 days, compared to the treatment with free drug or gemcitabine-loaded liposomes only.	[138]

Table 4: Table outlining promising research into the use of nanotechnology for the treatment of pancreatic cancer. (uPAR: urokinase plasminogen activator receptor; MRI: magnetic resonance imaging; PEG: poly(ethylene glycol); TGF-β: transforming gene factor)

1.8 Aims of the Study

There were various aims from the research conducted. Firstly, it was to determine the effective cytotoxic effects of the gemcitabine within a novel nanoparticle drug carrier against pancreatic cancer cells *in vitro*. Secondly, was to determine any potential active targeting methods that could be utilised to increase the cytotoxic effects of the gemcitabine-loaded SPIONs. Finally, to determine whether the gemcitabine-loaded SPIONs would be successful in producing any cytotoxic effect whilst circulated within a flow model.

1.9 Plan of the study

- Consistent and reproducible manufacture and storage of gemcitabine-loaded SPIONs
- Growth and maintenance of immortalised pancreatic cancer cell lines
- Assessment of antigen expression of pancreatic cancer cell lines
- Determine cytotoxicity of gemcitabine-loaded SPIONs against cancer cells
- Potentiate any cytotoxicity using a specific targeting ligand: CA 19-9 antibody
- Replicate any 2D results within a 3D culture set-up
- Construct an artificial circulatory system to assess for improved cytotoxicity using magnetic targeting

2 Material and Methods

2.1 Manufacture of nanoparticles

2.1.1 Multifunctional iron oxide nanoparticles

The superparamagnetic iron oxide nanoparticles (SPIONs) used in my experiments have previously been described and optimised by the Rosseinsky Group at the Department of Chemistry, University of Liverpool in close collaboration with Prof. Christopher Halloran at the Department of Molecular and Clinical Cancer Medicine. They were initially used *in vitro* for biological applications by my colleague, Mr Paul Sykes. The production of these tailor-made nanoparticles is described in Olariu et al. [137].

2.1.2 Component parts of the nano-complexes

The SPIONs used in the experiments are comprised of several individually tailored components which are combined to form the completed nano-complexes in a self-assembly methodology. Table 5 summarises component parts of the self-assembled nano-complexes.

Component	Name	Details
Core	Hydrophobically-modified superparamagnetic iron (II,III) oxide nanoparticles (SPIONs)	Arranged in a central cluster
Fluorescent tag	Octadecyl rhodamine	Arranged in the mixed hydrophobic core
Polymer	Amphiphilic poly (2-ethyl)-2-oxazoline	Sterically stabilises the nano-complex. The end-alkyl chain is arranged in the mixed hydrophobic core and the polymer segment organises as the outer hydrophilic shell
Chemotherapy pro-drug	Hydrophobically-modified pro-drug of gemcitabine	Arranged in the mixed hydrophobic core of the nano-complex
Targeting antibody	Either isotype or specific antibodies were attached	Covalently bonded onto the hydrophilic segment of the polymer shell

Table 5: Component parts of the self-assembled nano-complexes used in experiments.

2.1.3 Characterisation of the manufactured nano-complexes

The nano-complexes manufactured were characterised to determine the average diameter, iron concentration of its core and drug (gemcitabine) concentration loaded.

2.1.3.1 Dynamic Light Scattering (DLS)

The hydrodynamic diameters of SPION samples were measured using a Malvern Zetasizer Nano ZS equipped with a helium laser at a wavelength of 633 nm. 1mL sample was used for each measurement. Scattered light was collected at a fixed angle of 173^0 and measurements were performed at 25 °C. The intensity-average hydrodynamic diameters reported are obtained from 3 independent measurements; for each measurement at least 20 repeat runs were used.

This protocol is described in Olariu et al. [137] and were kindly performed by Dr Mike Barrow, Department of Chemistry, University of Liverpool.

2.1.3.2 Zeta potential

The zeta potential of the SPION samples dispersed in deionised water or buffers were measured using a Malvern Zetasizer Nano ZS equipped with a helium laser 633 nm wavelength. An aliquot of 1 mL sample was used for each the measurement. The measurements were performed at 25 °C. The zeta potential values reported are obtained from 3 independent measurements; for each measurement at least 50 repeat runs were used.

This protocol is described in Olariu et al. [137] and were kindly performed by Dr Mike Barrow, Department of Chemistry, University of Liverpool.

2.1.3.3 High performance liquid chromatography

This technique was used to determine the average concentration of iron and drug (gemcitabine) within each batch of SPION samples. The SPIONs that were manufactured for the use in my experiments had an iron core concentration of 1mM/mg and pro-drug gemcitabine concentration of 0.2mg/ml.

2.1.3.4 Overview of nanoparticle manufacture

In brief, independently synthesized hydrophobic SPIONs (Figure 4F) and amphiphilic poly (2-ethyl-2-oxazoline) (PEtOX) (Figure 4A) were self-assembled together with a fluorescent dye (Octadecyl Rhodamine B) in a 10:1:0.01 mass ratio respectively to yield a multifunctional NP (Figure 4G). The PEtOX polymer via its hydrophobic segment, hydrophilic and carboxylic end functional groups can form important interactions with Rhodamine B, proteins, antibodies and gemcitabine. To manufacture

drug-loaded particles, gemcitabine was modified through conjugation of a hydrophobic alkyl chain with the gemcitabine molecule using a pH sensitive acetal bond (Figure 4B). This resulting amphiphilic compound was then added to the nanoparticle components in a ratio of 4:1 resulting in a self-assembled drug-laden nanoparticle.

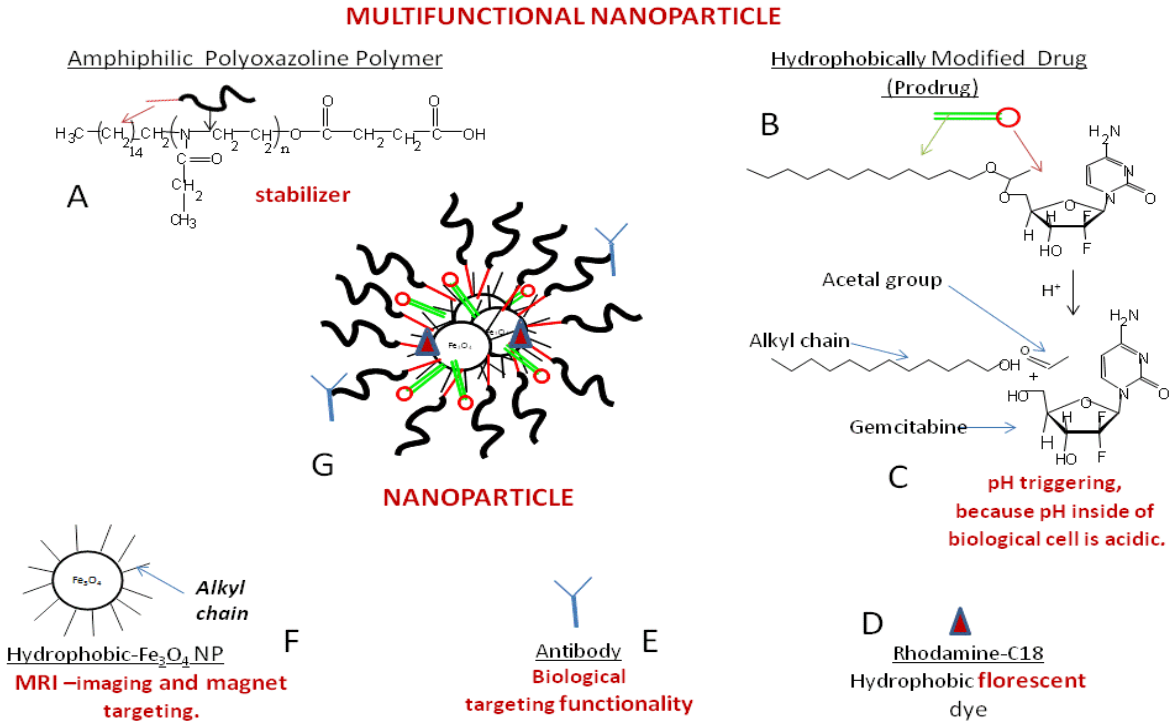

Figure 4: Composition of multifunctional SPION. A – Schematic of amphiphilic PEtOX, B – Modified Gemcitabine, C –Gemcitabine released from the acetal group and alkyl chain, D – Rhodamine fluorescent dye, E – Antibody, F – Oleic acid coated iron oxide cores conjugated with alkyl chains, G – The assembled NP *(Illustration courtesy Dr E. Hasan, Department of Chemistry, University of Liverpool, UK)*

2.1.3.5 Laboratory manufacture of nanoparticle complexes

I was kindly demonstrated the above chemistry protocol by Dr Erol Hasan, Department of Chemistry, University of Liverpool. I was able to manufacture nanoparticles in the tissue laboratory using the self-assembly components. 4mg of pro-drug gemcitabine and 20mg of polymer was added to 2ml of Tetrahydrofuran (THF). 2µg of Rhodamine was added and thoroughly mixed. 20ml of distilled water (dH_20) was added, and solution was placed in a 37ºC water bath and ultrasonically mixed for 15 minutes. This was then added to a dialysis tube and submerged into phosphate buffered saline [PBS], covered with aluminium foil and left in dialysis for 48 hours. The PBS was changed after 24 hours. The

SPION complexes used throughout the experiments were stable in distilled water or PBS and were effective for use for 3 months after production.

2.2 Cell lines and culture

2.2.1 Cell culture of primary immortalised cancer cell lines

Several commercially available cell lines were used during my laboratory work. All cell lines were grown within media supplemented with additional supplements. Table 6 summarises the media, additional supplements and other reagents used during cell culture. These cell lines and their passaged clones were checked for genotyping to ensure no unwanted mutations and also for mycoplasma contamination.

Supplement / Reagent	Supplier
RPMI-1640 Medium (with $NaHCO_3$)	Sigma-Aldrich Company Ltd, Dorset, UK
Dulbecco's Modified Eagle Medium (DMEM) 1x (high glucose with added sodium pyruvate)	Gibco © Life Technologies Ltd, Paisley, UK
Foetal bovine serum (FBS) – Origin: South America.	Gibco © Life Technologies Ltd, Paisley, UK
Penicillin-Streptomycin (10,000 units penicillin; 10mg streptomycin per ml)	Sigma-Aldrich Company Ltd, Dorset, UK
L-Glutamine (200nM)	Sigma-Aldrich Company Ltd, Dorset, UK
Trypsin-EDTA solution	Sigma-Aldrich Company Ltd, Dorset, UK
HEPES (1M) buffer solution	Gibco © Life Technologies Ltd, Paisley, UK
2-Mercaptoethanol	Sigma-Aldrich Company Ltd, Dorset, UK
Phosphate-buffered saline (PBS) [pH 7.4, 1x]	Gibco © Life Technologies Ltd, Paisley, UK
Dimethyl Sulfoxide (DMSO)	Fisher Scientific, Leicestershire, UK

Table 6: Reagents and supplements used in cell culture

Table 7 summarises the cell lines used, their characteristics and the media they were kept in.

Name	Tissue Origin	Disease	Supplier	Media	CA 19-9 expression
BxPC-3	Pancreas	Adenocarcinoma	ATCC ® #CRL-1687	RPMI + 10% FBS + 1% L-Glut + 1% Pen-Strep	Yes
PANC-1	Pancreas/duct	Epithelioid carcinoma	ATCC ® #CRL-1469	RPMI + 10% FBS + 1% L-Glut + 1% Pen-Strep	Yes
CFPAC-1	Pancreas; derived from metastatic liver	Ductal adenocarcinoma; cystic fibrosis	ATCC ® #CRL-1918	RPMI + 10% FBS + 1% L-Glut + 1% Pen-Strep	Yes
SUIT-2	Pancreas	Adenocarcinoma	ATCC ® #CRL-1687	RPMI + 10% FBS + 1% L-Glut + 1% Pen-Strep	Yes
MIA PaCa-2	Pancreas	Carcinoma	ATCC ® #CRL-1420	RPMI + 10% FBS + 1% L-Glut + 1% Pen-Strep	No

Table 7: Cell lines and their characteristics. [ATCC ®: American Tissue Culture Collection]

The above cell lines outlined in Table 3 were grown and maintained within a 37ºC / 5% CO_2 incubator. Cell lines were regularly inspected under light microscopy to monitor their health and confluence. Cell lines were sub-cultured (using trypsin) 2-3 times a week and frozen stocks made as required, for later use. Cell lines with passage numbers below 20 were maintained for experimental use. Results presented are for the cell lines of interest: Mia Pa Ca-2 and BxPC-3 only. These cell lines were used as they were easily and successfully passaged numerous times throughout my experiments, and as will be reported, showed contrasting expression to CA 19-9 antibody.

2.2.2 Cryostorage of cells

Confluent T75 flasks were passaged and cells centrifuged at 1000rpm for 10 minutes then pellets re-suspended in complete medium + 5% DMSO (storage medium) in cryotubes. Cryotubes were stored in -80ºC overnight then transferred to -150ºC liquid nitrogen.

2.2.3 Recovery of cells from cryostorage

Cryotubes were removed from liquid nitrogen and placed within a 37ºC water bath. Once cells were thawed, they were immediately placed with a T25 flask containing warmed media. The following day

the flask was washed with warmed PBS and fresh media replaced to remove the DMSO. Once cells were confluent, they were transferred to a T75 flask.

2.3 Production of monoclonal antibodies from hybridoma culture

Anti-CA 19-9 hybridoma was purchased from ATCC for culture and production of purified monoclonal antibody, which could be used for conjugated onto the SPION complexes.

2.3.1 Culture of hybridoma

The culture of the hybridoma is very similar to the cell culture methods of pancreatic cancer cells, except the hybridoma grow in suspension, so centrifugation is used in lieu of trypsin when passaging. The anti-CA19-9 hybridoma was maintained within a complete culture medium of DMEM with L-Glut; FBS (20%). The hybridoma is thawed using a 37ºC water bath and generously sprayed with 70% ethanol. The cells are transferred to a 15 ml Falcon tube containing complete media. The cells then are centrifuged at 1000-1500rpm for 5min. These steps are performed as quickly as possible to prevent unnecessary stress to the cells. The media is removed, and the pellet re-suspended in 10ml fresh complete media and transferred to a T75 flask. The cells were maintained in a 37ºC/5% CO_2 incubator.

2.3.2 Cryostorage of hybridoma cell lines

This was performed using 5% DMSO in complete media with a cell count of $1x10^6$ cells/ml. Cells were transferred to cryovials and immediately place in -80C freezer within a Mr Frostee ® container. The following day the cryovials transferred to liquid nitrogen (-150C) for long term storage.

2.3.3 Passage and reducing amount of serum content in complete media

Once growing well, the cells were sub-cultured 2-3 times a week at ratios between 1:2 and 1:4. The cells were passaged using centrifugation with supernatant removed and cells re-suspended in an appropriate volume of fresh media into a new T75 flask. Each passage step, the amount of serum content in the complete media was reduced, to allow for simpler and purer antibody to be produced downstream. For example, half the cells passaged were kept at 20% FBS baseline for stock and the other half grown in media with serum free media (plain DMEM) added to reduce the serum content to 10%. The serial

dilutions of serum continued until the amount of FBS was 2.5% - now ready for downstream applications.

2.3.4 Antibody purification

Cells in the low concentration of serum are centrifuged at 1500rpm for 10 minutes and re-suspended in the commercial provided binding buffer. The protocol for protein purification using *Nab protein A spin columns* was adhered to.

2.3.5 Antibody production concentrations

These were gathered using Nano Drop analyser against 450nm protein standard setting.

2.3.6 SDS-Page

To demonstrate successful production of a pure IgG antibody, the eluted fractions from the spin column process were loaded for SDS-page analysis against the relevant commercially available antibody.

2.4 Functionalisation of SPIONs

2.4.1 Carbodiimide-coupling chemistry

An antibody was attached to the polymer surface of the SPION complex. This was achieved by using a reaction named carbodiimide-coupling using, in order, the chemicals 1-Ethyl-3-(3-dimethylaminopropyl) carbodiimide (EDC) and N-Hydroxysuccinimide (NHS). It is a commonly performed process often used to activate carboxylic acids towards amide formations. In these experiments, the carboxylic acid group lies on the polyoxazoline polymer and the amine group on the antigen binding site of an antibody.

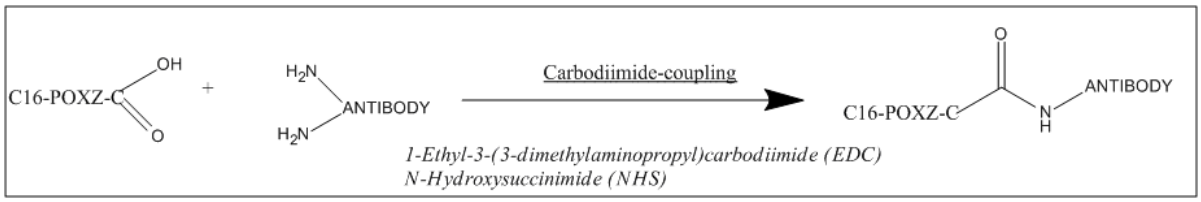

Figure 5: Carbodiimide-coupling chemistry to conjugate an antibody to the polymer coating of the SPION complex.

This process was kindly performed and demonstrated by Dr Michael Barrow and Dr Erol Hasan of the Department of Chemistry, University of Liverpool, and later performed by me.

2.5 Different preparations of SPION manufactured.

Due to the self-assembly process of manufacturing the tailor-made SPIONs a combination of components can be prepared. Additionally, the SPION can be functionalised with an antibody – this increases their size. Consequently, several nanoparticles can be produced for experimental use. I was able to attach different types of commercially available antibodies: isotype IgG and CA19-9. The various combinations of SPION manufactured is shown below in table 8.

Nanohybrid complex	Gemcitabine-loaded	Antibody attached (functionalised)
NH1.0	×	×
NH1.2	✓	×
NH1.2:ISO	✓	Isotype IgG
NH1.2:CA 19-9	✓	Anti-CA-19-9

Table 8: Different combinations of nanohyrbids synthesised. [NH = nanohybrid, 1 = 1mM/ml iron content; 2 = 0.2mg/ml gemcitabine pro-drug concentration].

2.6 MTS cytotoxicity assays

MTS Assay uses a colorimetric method for the sensitive quantification of viable cells. It is based on a single ready-to-use reagent. The MTS assay can be used to assess cell proliferation, cell viability and cytotoxicity.

2.6.1 Preparation of cells

Confluent flasks of cells are trypsinised and centrifuged at 1000rpm for 5 minutes. A cell count performed using TC20™ Automated Cell Counter (Bio-Rad Laboratories Ltd, Hertfordshire, UK) to achieve a final cell concentration of $1x10^5$ per ml. 100µL per well of cell-containing media plated into a 96-well plate with the outer wells usually filled with 100µL of media only, to prevent any evaporation effect. Therefore, each well contains $1x10^4$ cells. One column of the plate is left bare and another filled

with media only – these are used as controls later. The plated cells are incubated at 37ºC / 5% CO_2 overnight to be used the following day.

2.6.2 Treatment / transfection of cells

The next day, the media is removed and replaced with treatment media, at increasing dosage. Once complete, the plates are replaced into the incubator until the plate is ready to be analysed.

2.6.3 Preparation of reagents

All MTS assays were performed using EZ4U Cell Proliferation Assay (Biomedica, Oxford Biosystems, Oxford, UK). The kit contained a substrate (SUB) and activator (ACT). Firstly, these were warmed to room temperature and then the SUB dissolved in 2.5ml ACT. The mixed SUB and ACT solution then added to complete medium at 1:10 concentration and thoroughly mixed within a sterile trough – this suspension is added to the cells. The media from the 96-well plate is removed and discarded and 100µL of the above suspension containing the reagents is added to *all* the columns.

2.6.4 Plate reading

The cells are incubated again for up to 4 hours. Usually the plate reading at 2 hours is used for statistical analysis, as it tended to give the most consistent reading dependent on each cell line and treatment. The 96-well plate of interest is read using a plate absorbance reader at 450nm with 620nm used as a reference. To improve the accuracy of the results absorbance from a substrate blank in medium is subtracted from all other values. The process is displayed in figure 6.

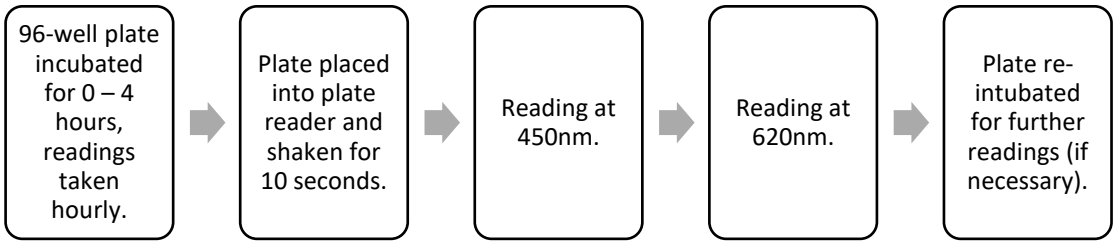

Figure 6: Flow diagram showing the steps of plate reading for a MTS assay.

The MTS cell proliferation assays were used to investigate the percentage of cell viability of cell lines against controls with no active chemotherapy agent (PBS or non-drug-loaded SPIONs) and with

conditions with gemcitabine, either free or bound to SPIONs, at increasing concentrations. These experiments allowed calculation of each cell lines' 50% inhibitory concentration or IC_{50}.

2.7 Immunofluorescence

2.7.1 Indirect immunofluorescence

This method was utilised to assess the antigen expression of cell lines against a variety of antibodies, commercially bought or produced from hybridoma sub-culture. I thank Paul Sykes and Dr Carlos Rubbi (Lecturer in Cancer Biology, Molecular and Clinical Cancer Medicine) for aiding in the optimisation of my protocol.

2.7.1.1 Cleaning coverslips

Circular 13mm diameter [thickness 0.16 – 0.19mm] coverslips (Academy, University of Liverpool Stores) are firstly cleaned. Several coverslips can be cleaned at a time in an ethanol/hydrochloric acid mixture (200ml 70% EtOH + 6ml concentrated HCl) for at least one hour, with gentle periodic shaking. Following the de-greasing the coverslips are rinsed 10 times and transferred to a $10cm^2$ petri dish for use within a class II hood. The coverslips are rinsed again with 70% EtOH, which is then thoroughly aspirated and finally washed with tissue grade PBS prior to use with cells. If immediate use of the coverslips was not required, the coverslips was kept in 70% EtOH in a sterile container whilst working in a class II hood, for later use.

2.7.1.2 Preparation of cells

The de-greased and sterile 13mm diameter coverslips are carefully transferred, usually using curved Watchmakers forceps, from a $10cm^2$ petri dish to a sterile 24-well plate, with an individual coverslip in each well. Cells are added to each well at density $7x10^4$/ml; 1ml of cells in complete medium is added to each well to completely immerse the coverslip. The 24-well plate is incubated overnight (27ºC/5% CO_2) to allow the cells to grow on the coverslip and for use the following day.

2.7.1.3 Fixation of cells

Before fixation, cells (grown on coverslips within a 24-well plate) are rinsed twice using tissue culture grade PBS. Fixation is performed using formalin solution, neutral buffered, 10% (Sigma-Aldrich Ltd, Dorset, UK) – 500µL is added to each well and gently shaken upon a table-top rocker at room

temperature for 10-15 minutes. The formalin solution is then aspirated and thoroughly rinsed with PBS + 0.02% Tween-20 (Sigma-Aldrich Ltd, Dorset, UK) (PBS-T).

2.7.1.4 Blocking

A 2% bovine serum albumin in PBS-0.02% Tween solution is made and filtered through a 0.22μm PES filter (Merck Millipore Ltd, County Cork, Ireland) to remove any protein aggregates, which diminish the final immunofluorescence (IF) image. Again, 500μL of the blocking solution is added to each well to immerse the coverslip and gently shaken for 30 minutes upon a table-top rocker at room temperature.

2.7.1.5 Antibody incubation and washings

All washes are using PBS-0.02% Tween and all antibodies are diluted in blocking solution (2% BSA in PBS-0.02% Tween). Following 30 minutes of blocking, the solution is washed off thoroughly. The antibody concentrations used for immunofluorescence are show in table 9.

Antibody	Starting concentration	Recommended dilution	Dilution [Total protein in µg]						
			1:10	*1:20*	*1:50*	*1:100*	*1:200*	*1:500*	*1:1000*
Anti-Ca19-9 [CA 19-9-203]	0.2mg/ml	1:50 – 1:100	-	8	4	2	1	0.4	0.2
Anti-CEACAM7 [BAC2]	1mg/ml	1:100	-	-	20	20	5	2	1
ISO IgG	0.4mg/ml	n/a	-	-	8	4	2	0.8	0.4
Goat anti-mouse IgG, DyLight 488 - secondary	1mg/ml	1:200 – 1:1000	-	-	20	10	5	2	1
Hb CEA	0.03 – 0.1mg/ml	n/a	3-10	1.5-5	0.75-2.5	0.37-1.25	-	-	-
Hb CA 19-9	0.03 – 0.1mg/ml	n/a	3-10	1.5-5	0.75-2.5	0.37-1.25			

Table 9: Antibody concentrations for immunofluorescence. Shaded boxes are range of stock antibodies made in 1% BSA (based in 0.02% PBS-T) and used for immunofluorescence experiments. (IgG: immunoglobulin G, Hb: hybridoma)

2.7.1.5.1 Primary antibody

Each antibody used is diluted appropriately, for example, dependent on commercial recommendations, in blocking solution. A hydrophobic surface is prepared using a parafilm-wrapped 24-well plate lid. A 20µL drop of the diluted primary antibody is placed onto the parafilm surface. Coverslips are lifted from each well carefully, inverted, and placed onto the relevant primary antibody drop – this ensures the cells are in contact with the antibody. The primary antibody is incubated within a humid chamber for 1 hour.

2.7.1.5.2 Secondary antibody

Following primary antibody incubation, the coverslips are lifted from the parafilm surface, inverted, and replaced into the 24-well plate. The cells are washed for 8 minutes (4 x 2 minutes) with PBS-0.02% Tween. A fresh parafilm surface is adhered to the lid a 24-well plate and the same process used as per the primary antibody. Again, the secondary antibody is incubated for one hour within a humid chamber at room temperature, but in the dark, as the secondary antibody is fluorescent. The secondary antibody used in all the IF experiments is goat anti-mouse IgG, DyLight-488 (Thermo Scientific, Rockford, IL, USA).

2.7.1.5.3 DAPI staining

Once both antibody incubations are complete, the coverslips are lifted from the parafilm, inverted, and returned to the 24-well plate. The coverslips are washed and rocked again for 8 minutes as previously described, however, in the final rinse, is 0.1-0.5µg/ml DAPI (Sigma-Aldrich Ltd, Dorset, UK) added at dilution 1:5000.

2.7.1.5.4 Mounting

Mowiol® 4-88 (Sigma-Aldrich Ltd, Dorset, UK) is used as the mounting medium, with the addition of 0.5µg/ml DAPI. For each coverslip, 5µl of mounting medium is placed onto a rectangular Superfrost ® Plus glass slide (Thermo Scientific, Cramlington, UK), usually three coverslips can be accommodated on one glass slide. The coverslips are carefully lifted from the 24-well plate, excess liquid dried onto blue roll and placed onto the drop of mounting medium.

The glass slides are placed at 4ºC overnight to allow the mounting medium to harden. The following day the coverslips are held in place onto to the glass slide using toluene-based lacquer.

2.7.2 Fluorescent microscopy

All IF images were obtained using Zeiss Axio Imager Z1 (Carl Zeiss Ltd UK, Cambridgeshire, UK). This microscope is suited for comprehensive high-resolution 3D evaluation of fixed cells. Prepared slides are cleaned with 70% EtOH and are visualised under the microscope to a maximum magnification of 63x with immersion oil Immersol 518 F fluorescence free (Carl Zeiss Ltd UK, Cambridgeshire, UK) to visualise single cells. DAPI (nuclear staining) and 488nm (secondary antibody) channels are used for all IF work. Commonly Z-stack images were obtained.

2.7.2.1 MicroManager

Images directly from the Zeiss Axio Imager Z1 were saved using MicroManager (https://www.micro-manager.org/wiki/Download_Micro-Manager_Latest_Release) version 1.4.20. This software allowed for exposure time, binning, Z-stacks, channels, magnification and brightness all to be altered to improve image capture.

2.7.2.2 ImageJ

Saved stack files from fluorescent microscopy were manipulated using software ImageJ 1.48 (imagej.nih.gov/ij/download/). This allowed for colouring of channels (blue for DAPI; green for 488nm fluorescence).

2.8 Experiments using Operetta® CLS High-Content Analysis System

These protocols were entirely novel equipment and components used, therefore it required optimisation guided from previous attempts. These experiments were performed by me, Ms Hannah Murphy (MRes student) and Ms Sarah Brumskill (PhD student at Redx Pharma at University of Liverpool).

2.8.1 Visualisation of receptor-mediated endocytosis of SPIONS in a 2D model

MIaPaCa-2 cells were plated at various cell densities in 96 well plates ranging from $1x10^3$ cells per well to $1x10^6$ cells per well. Cells were incubated for 48 hours to form a monolayer. Hoechst [1mg/ml] [excitation rate- 350nm and emission rate-461nm] was diluted with PBS to various concentrations [2µg/ml, 5µg/ml, 10µg/ml and 20µg/ml] and incubated at room temperature for 7 minutes. Cells were washed thoroughly, and SPIONs were added at dilution of 1:10, 1:20, 1:50 and 1:100. The plate was placed onto the Operetta CLS High-Content Analysis System (Perkin Elmer, Llantrisant, UK) and incubated for 17 hours. Cells were visualised and analysed using Harmony ® High Content Imaging and Analysis Software (Perkin Elmer, Llantrisant, UK).

2.8.2 Formation of condensed spheroids

BxPC-3 cells were plated at a density of $1.0x10^3$ cells per well using 96 well ultra-low adherent (ULA) plates (Thermo Scientific, Cramlington, UK). To visualise the formation of the spheroid, the ULA plate was immediately placed on the Operetta CLS High-Content Analysis System, where the cells remained incubated at 37°C/5% CO_2. In our experiments, we utilised the Operetta® and its the ability to perform confocal imaging on live cells. Using the Harmony ® High Content Imaging and Analysis Software, we were able to view the continual formation of spheroids, over 12 hours.

2.8.3 Dissociation of formed spheroids using gemcitabine-loaded SPIONs

Spheroids were formed using the aforementioned protocol. Gemcitabine-loaded SPIONs were diluted at a concentration of 10% and added to the spheroids. DMEM phenol red free media (Gibco Life Technologies) was used in all spheroid formation experiments. The spheroids (with the transfected SPIONs) were visualised for 13 hours using the Operetta.

2.9 Artificial circulation experiments

These experiments were performed in close collaboration with Professor John Hunt (Head of Unit, Musculoskeletal Biology, University of Liverpool). The purpose of these experiments was to investigate the efficiency of the cytotoxicity of gemcitabine-loaded SPIONs within an artificial flow system, mimicking a blood circulation. It will serve as a pre-cursor to *in vivo* experimentation.

2.9.1 Manufacture of flow T25 flasks

Cell culture 25cm^2 flasks with plug seal caps (VWR, Leicestershire, UK) were modified by drilling two holes either side of the flask and securing a threaded female Luer connector in the defects created. The modification of flasks was kindly made by Mr James Blackhurst (Engineer for the Clinical Engineering Group, Institute of Ageing and Chronic Disease) at the Central University Workshop, Ground Floor Duncan Building, shown in figure7. The completed flow T25 flasks are sterilised with 70% EtOH, irradiated under ultraviolet light and washed with PBS prior to any introduction of cells.

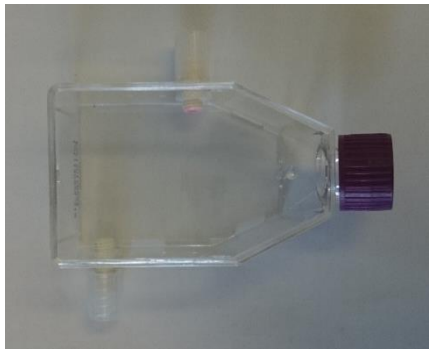

Figure 7: Figure demonstrating specifically modified T25 flask

2.9.2 Preparation of pancreatic cancer cells

Pancreatic cancer cell lines (MIA PaCa-2 or BxPC-3) were seeded into sterilised flow T25 flasks at density 2x10^6 cells per flask (or 4x10^5 cells/ml with 5ml of media per flask). The cells are grown overnight in a 37^{o}C/5% CO_2 incubator until at least 90% confluence, forming a dense monolayer – which is to be used for the flow experiments. Before exposure to any treatment, the monolayer is imaged using light microscopy.

2.9.3 Construction of flow system

The entire system (except the peristaltic pump) is maintained within a large 37°C/5% CO_2 incubator with the Musculoskeletal Biology laboratory on the ground floor of the Duncan Building. All component parts are autoclaved (5th floor UCD Building, University of Liverpool) prior to use with cellular material.

2.9.3.1 Peristaltic pump and tubing

A laboratory bench peristaltic pump was used, 323D peristaltic pump with a three-roller 313D flip-top pump head (Watson-Marlow Ltd, Cornwall, UK). Throughout the whole system 1.6mm gas permeable tubing was used (Watson-Marlow Ltd, Cornwall, UK). The peristaltic pump drove at a flow rate between 80 to 120rpm.

2.9.3.2 Set-up of flow system

The peristaltic pump controls the flow of media around the circuit. A 250ml media bottle (DWK Life Sciences, Mainz, Germany) contained 250ml media (with or without nanoparticle treatment) is connected to the peristaltic pump via 1.6mm gas permeable tubing. Distal to the pump the media is split into two parallel circuits through the flow T25 flasks containing pancreatic cancer cells. One T25 flask has two magnets (University of Liverpool Stores) underneath it. This creates a variable of cells exposed to a magnetic field and cells without a magnetic field. Once the media has flowed through both flasks, over each cell monolayer, the media flows back into the media bottle, to start the circuit again. The whole circuit is exposed to the incubator's environment (namely 5% CO_2) via a 0.22µm filter, to prevent environmental micro-organisms entering the system. The diameter and length of tubing through each limb of the parallel circuit is constant. The completed system is shown in figure 8.

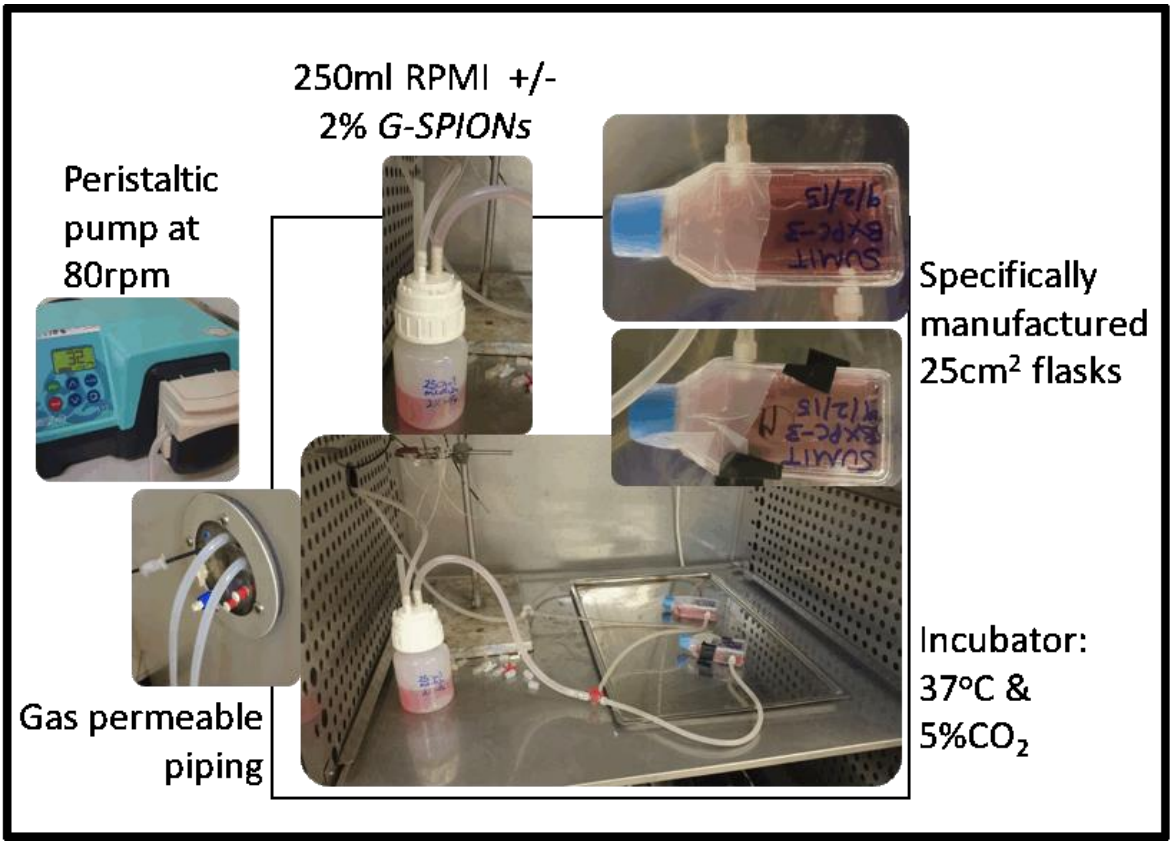

Figure 8: Figure demonstrating set-up of artificial circulatory model. Demonstrating the continuous 250ml media within the media bottle and two T25 flasks in continuous circuit with the nearest flask in the image with two magnets taped on its underside. G-SPIONs = gemcitabine-loaded SPIONs.

2.9.4 Flow experiments

Prior to attaching the flow T25 flasks to the circuit, the tubing is flushed with 70% EtOH and then PBS using a different media bottle. The flasks and media-containing bottle are plumbed into the circuit and the peristaltic flow commenced. The experiment is ran for a certain time period with the below variables in table 10.

Time point	Treatment	Magnet	Flow
16 / 24 / 48 / 72 hours	Media with 2% nanoparticle treatment ***or*** media only.	Magnetic field underneath flask present ***or*** absent.	Exposed to 80rpm flow of media ***or*** static only

Table 10: Variables pancreatic cancer cells are exposed to during experiments with an artificial circulatory model.

2.9.5 Cell work following flow experiment

After a certain time point, the flow experiment is discontinued and the specially manufactured T25 flasks are un-plumbed and are left in a 37°C/5% CO_2 incubator overnight.

2.9.5.1 Extraction of media from T25 flask

The following day the media residing in the flask is removed carefully (not to disturb any adherent cells) and centrifuged at 600g for 10 minutes. The supernatant (1ml) of the spun-down media is removed, placed in a labelled cryovial and stored at -80^{o}C. This supernatant will be used later in a lactate dehydrogenase (LDH) assay, as a measure of cell lysis occurring during the experiment within the flask.

2.9.5.2 Light microscopy

The cell monolayer within the flask is gently washed with warmed PBS, to remove clumps of cells, and imaged under the light microscope. Therefore, both pre-flow and post-flow light microscopy images are obtained and can be used for comparison.

2.9.5.3 DAPI staining

Once light microscopy images are taken, the washed cells are fixed using formalin solution, 10% (Sigma-Aldrich Ltd, Dorset, UK) for 15 minutes on a table-top rocker. Following that, the formalin solution is washed off with PBS three times, with the third wash step containing DAPI (Sigma-Aldrich Ltd, Dorset, UK) at dilution 1:1000 for 10 minutes on a table-top rocker. The PBS with DAPI is removed and the cells washed further with PBS. Finally, the cells are stored in PBS, in the dark, at 4^{o}C, for later use in fluorescent microscopy to visualise the uptake of SPION within cells.

2.9.6 Lactate dehydrogenase assay

This was performed to evaluate of cell death or cytotoxicity by the quantification of plasma membrane damage, by measuring the enzyme lactate dehydrogenase (LDH), which is released into cell culture medium upon damage of the plasma membrane. The media obtained and cryo-stored from the flow experiments was used in the LDH assay. The protocol from the LDH-cytotoxicity assay Kit II (Abcam, Cambridge, UK) was rigidly followed. This protocol utilised the advanced WST reagent for the detection of LDH released from damaged cells. The assay uses an enzymatic coupling reaction where LDH oxidises lactate to generate reduced

nicotinamide adenine dinucleotide (NADH), which consequently reacts with WST to generate a yellow colour. The intensity of the colour correlates directly with the number of cells lysed within the media.

2.9.7 Fluorescent microscopy of remaining cellular monolayer

The remaining fixed monolayer of cells were visualised under the Zeiss Axio Imager Z1microscope (Carl Zeiss Ltd UK, Cambridgeshire, UK) to obtain fluorescent microscopy images. This was performed to show the cellular uptake of the rhodamine-labelled SPIONs in pancreatic cancer cells, the nuclei already stained using DAPI.

2.10 Statistical Analysis

All statistical analysis of the laboratory-based experiments was performed using software GraphPad Prism 5.0. This software was also used to generate relevant publication quality tables and graphs.

3 Results I: Nanoparticles

3.1 Characteristics of SPIONs manufactured

3.1.1 Size of SPIONs manufactured

Dynamic light scattering (DLS) technique was used to determine the size of the gemcitabine-loaded SPIONs before and after the attachment of an CA 19-9 antibody. The average diameter of particle manufactured without antibody conjugation was 143.7nm and with an antibody attachment was 197.9nm – see figures 9 and 10.

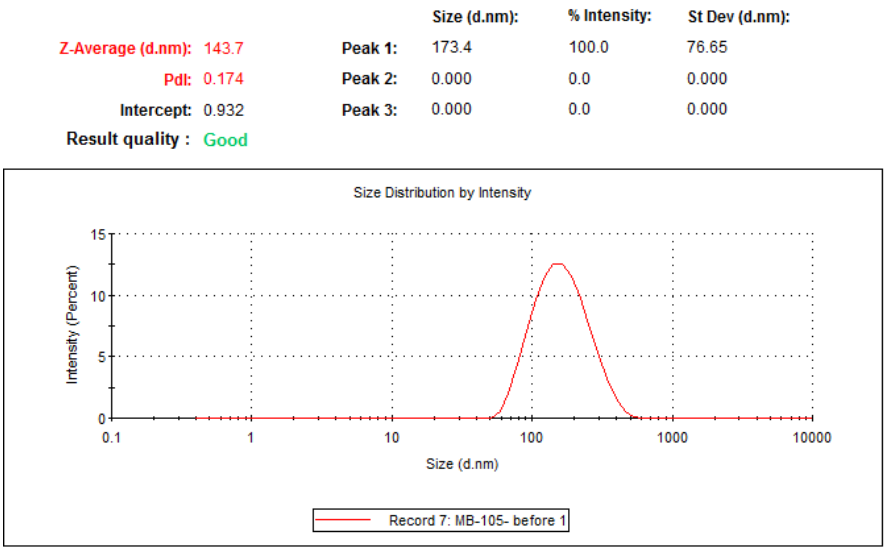

Figure 9: DLS curve demonstrating average SPION size without CA 19-9 antibody attachment. The average value is 143.7nm in diameter. (n=5)

		Size (d.nm):	% Intensity:	St Dev (d.nm):
Z-Average (d.nm): 197.9	Peak 1:	259.5	100.0	126.9
PdI: 0.233	Peak 2:	0.000	0.0	0.000
Intercept: 0.930	Peak 3:	0.000	0.0	0.000
Result quality : Good				

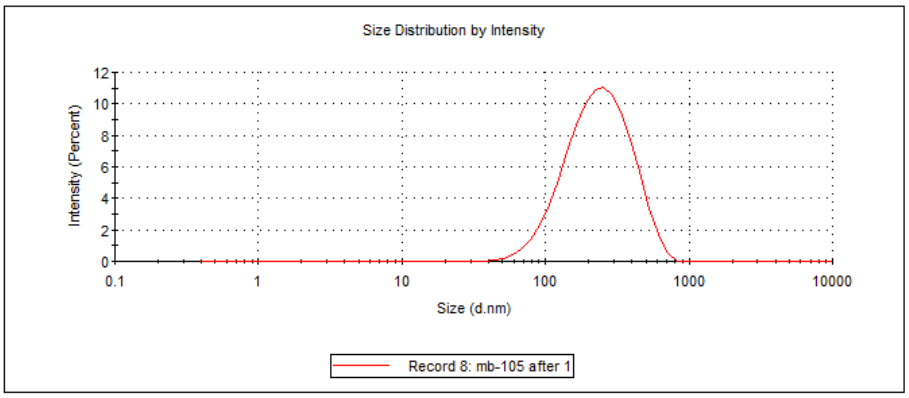

Figure 10: DLS curve demonstrating average SPION size *with* CA 19-9 antibody attachment. The average value is 197.9nm in diameter. (n=5)

These experiments were kindly performed by Dr Mike Barrow, Department of Chemistry, University of Liverpool.

3.1.2 Solubility and stability of SPIONs manufactured

The manufactured SPIONs are successfully stable in solution of either PBS or distilled water for several months. SPIONs loaded with gemcitabine maintained their cytotoxicity if used within three months of production. The SPIONs used for cell experiments were stored in PBS and kept refrigerated at 4ºC before use.

3.1.3 High performance liquid chromatography

The range of gemcitabine pro-drug that is attached to the SPION complex had a mean of 8.15×10^{-2}mg/ml and iron concentration of 120.15µg/ml.

3.2 Magnetic qualities

The superparamagnetic properties of the SPIONs were proven, with the SPIONs aggregating over the area of an external magnet. The SPIONs aggregated in the desired area by 10 minutes. This has been described previously in experimentation performed by Mr Thompson Gana and Mr Paul Sykes as precursor work and not repeated by me.

3.3 Antibody attachments

3.3.1 Production and purification of monoclonal antibodies

The antibody produced from the cultured anti-CA19-9 hybridoma was positively purified and stored. They were successfully used in later experimentation (results shown in following chapter).

3.3.2 SDS-page for anti-CA 19-9 antibody

To demonstrate successful production of a pure IgG antibody (figure 11), the eluted fractions from the spin column process were loaded for SDS-page analysis against the relevant commercially available antibody.

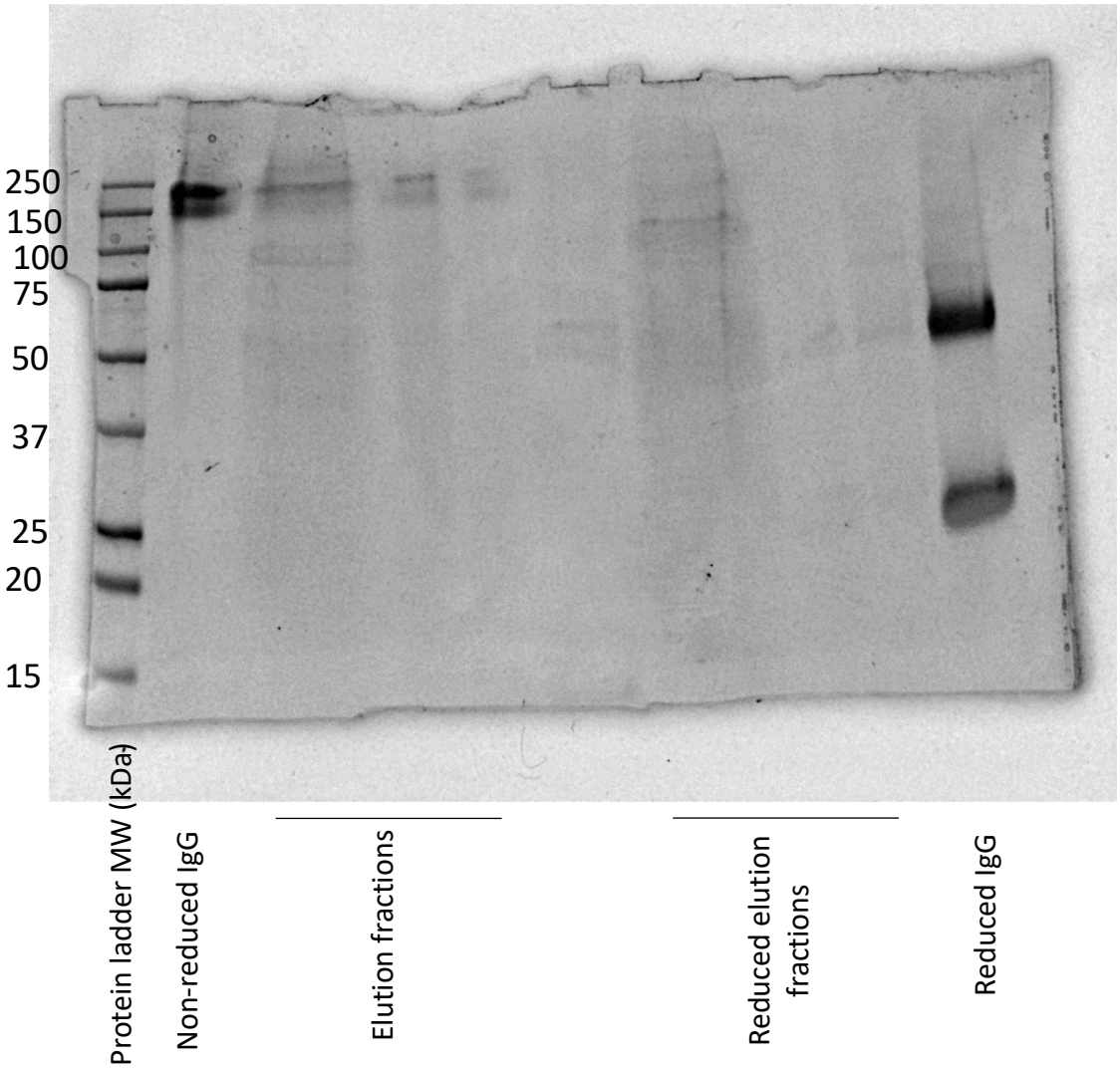

Figure 11: SDS page showing successful production and reduction of pure IgG produced from anti-CA 19-9 antibody hybridoma

3.4 Summary

These results demonstrate that we were able to make consistent ‘raw materials’ for further translational experiments. The SPIONs produced were colloidally stable, of a consistent size under 200nm (which as earlier described is of interest for the clinic) and loaded with a adequate concentration of gemcitabine pro-drug. In addition, the cells grown throughout the experiments, were consistently of high quality, ensuring free of infection (including mycoplasma) and showed correct genotype. Finally, the antibodies to be used for targeting ligands for the SPIONs were successfully manufactured and repeatedly attached onto the SPION.

4 Results II: Cytotoxicity of pancreatic cancer cell lines in 2D culture

4.1 Cell Culture

4.1.1 Successful culture of pancreatic cancer cell lines

A variety of pancreatic cancer cell lines were used for my experiments and continuously successfully passaged. In the whole, these were free from infection, whenever infection was suspected given its microscopic appearances, they were discarded. For the experiments I used BxPC-3 and Mia Pa Ca-2 cells. The following figures 12 and 13 demonstrate light microscopy images of healthy cells that were successfully cultured shown against stock images from ATCC (American Type Culture Collection).

4.1.2 BxPC-3 cells

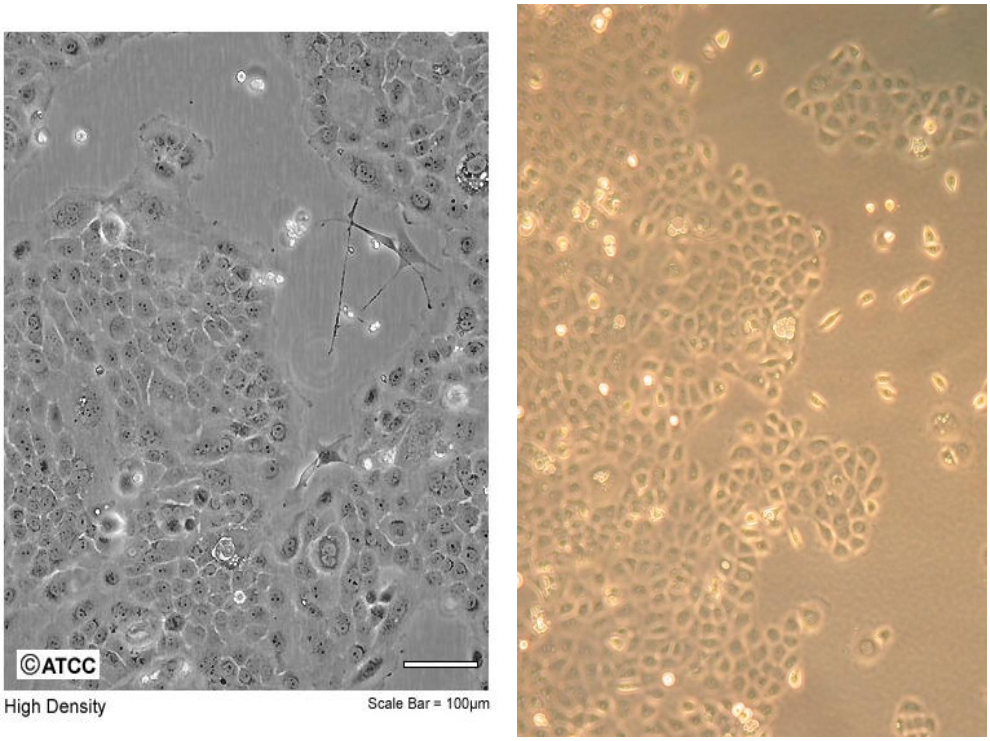

Figure 12: Light microscopy image of healthy high density BxPC-3 cells (right) successfully cultured shown against stock commercial image (left).

4.1.3 Mia Pa Ca-2 cells

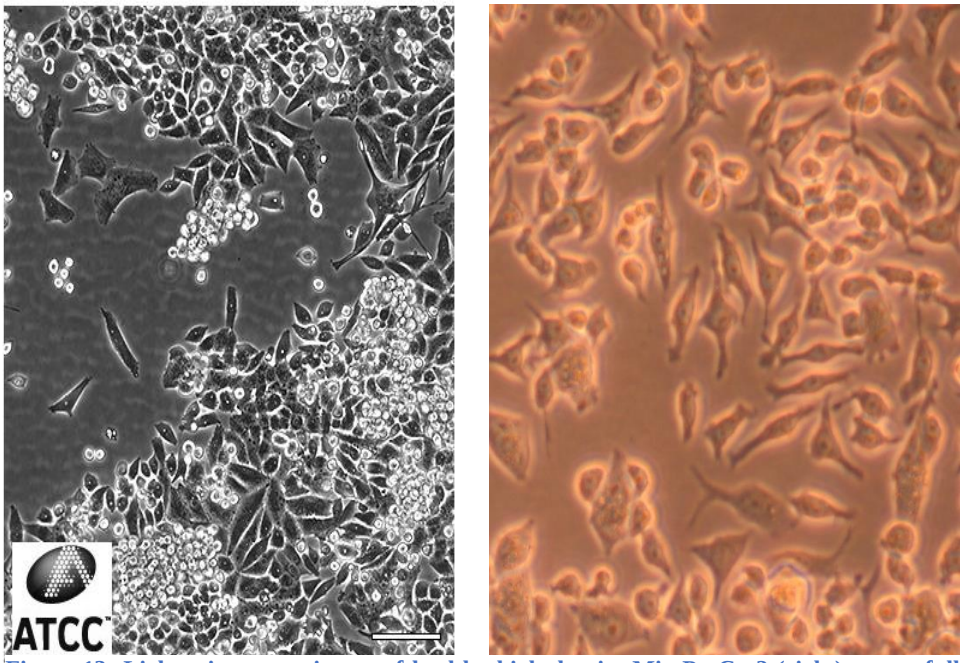

Figure 13: Light microscopy image of healthy high density Mia Pa Ca-2 (right) successfully cultured shown against stock commercial image (left).

4.2 Indirect immunofluorescence

This was performed to assess the antigen status of common pancreatic cancer cell lines. Mia Pa Ca-2 and BxPC-3 cells were subjected to a variety of antibodies. This included a stock generic isotype IgG, commercially available or stock CA19-9 (stCA19-9) and CA19-9 antibody cultured and purified from a hybridoma. The following figures show fluorescent microscopy images obtained using Zeiss Axio Imager Z1 (Carl Zeiss Ltd UK, Cambridgeshire, UK). These experiments were initially performed by my colleague Mr Paul Sykes and were successfully replicated. The antigen expression for CA 19-9 for both Mia Pa Ca-2 and Bx PC-3 cells are shown in figures 14 and 15.

4.2.1 Mia Pa Ca-2 cells show no expression for CA19-9 antibodies

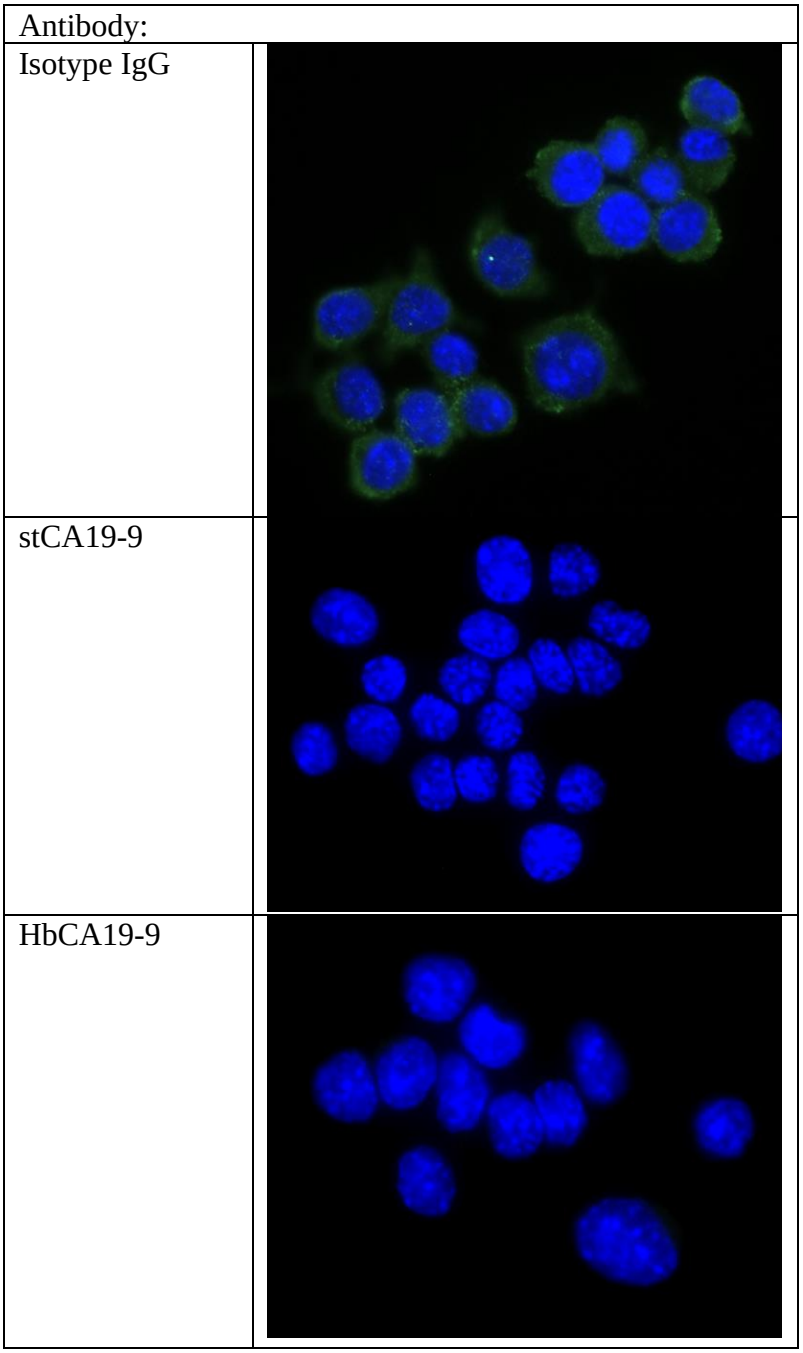

Figure 14: Fluorescent microscopy showing the indeterminate expression of Mia Pa Ca-2 cells to isotype IgG antibody, but no expression against both the stock (stCA 19-9) and hybridoma-produced CA19-9 (HbCA19-9) antibody. Fluorescent microscopy images at x63 magnification (n=3).

4.2.2 BxPC-3 cells are strongly positive expressive for CA19-9 antibodies

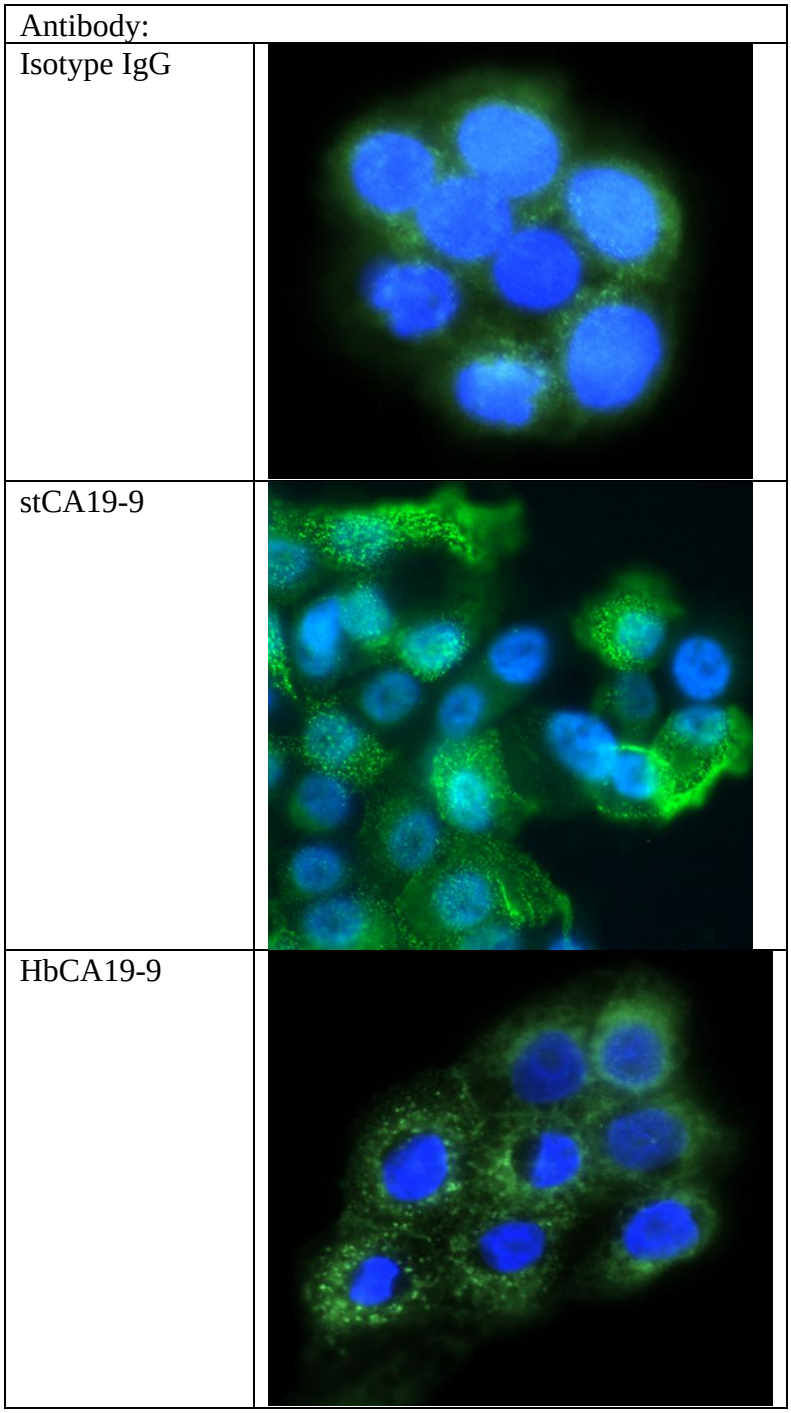

Figure 15: Fluorescent microscopy showing the indeterminate expression of BxPC-3 cells to isotype IgG antibody, but strong expression against both the stock (stCA 19-9) and hybridoma-produced CA19-9 (HbCA19-9) antibody. Fluorescent microscopy images at x63 magnification (n=3).

4.2.3 Antigen expression of Mia Pa Ca-2 and BxPC-3 cell lines

The opposing antigen expressiveness of these cell lines against CA 19-9 antibodies suited them to be ideal to use in forward experimentation to examine the antibody mediated uptake of our nano-complexes.

4.3 MTS assay results

4.3.1 Treatments used

The MTS cell proliferation assays were used to investigate the percentage of viability of cell lines against controls with no active chemotherapy agent (PBS or non-drug-loaded SPIONs) and with conditions with gemcitabine, either free or bound to SPIONs. Finally, against nano-complexes loaded with gemcitabine and functionalised with an antibody – either a non-specific isotype IgG or a targeting CA 19-9 antibody. These experiments allowed calculation of each cell lines' 50% inhibitory concentration or IC_{50} after 72 hours of applied treatment.

4.3.2 No reduction in cell viability without gemcitabine

No cytotoxic effect was seen without gemcitabine, either with PBS or nano-complexes without gemcitabine loading. This highlighted the non-toxic effect of the nanocomplex alone. Data not shown.

4.3.3 Mia Pa Ca-2 cells

Mia Pa Ca-2 cells were proven to be non-expressive for CA 19-9 antigen in earlier immunofluorescence experiments described in 4.2.1. They were prepared as per section 2.6 and subjected to the above treatments described in 4.3.1. Figure 16 demonstrates the different cytotoxicity effects to the cells when subjected to differing SPION treatments for a period of 72 hours. It demonstrates that the IC_{50} value does not change despite what treatment the cells are exposed to. The non-antigen expressive cells are not influenced by any antibody attachment: when exposed to nanohybrids with a specific CA 19-9 tag (3,090nM) versus nanohybrids with a non-specific isotype tag (3,535nM) or non-antibody tagged nanohybrids (4,051nM). The cells were exposed to the different treatments for 72 hours before being analysed for MTS cytotoxicity assays. Finally, when plain gemcitabine was used the IC_{50} was only

41.79nM – data curve not shown due to scaling. These results were not statistically significant with a p-value of 0.27.

4.3.4 BxPC-3 cells

Figure 17 demonstrates the different cytotoxicity effects to the cells when subjected to differing treatments. The IC_{50} value falls considerably when exposed to nanohybrids with a specific CA 19-9 tag (354nM) versus nanohybrids with a non-specific isotype tag (1,175nM) or non-antibody tagged nanohybrids (1,123nM). The cells were exposed to the different treatments for 72 hours before being analysed for MTS cytotoxicity assays. Finally, when plain gemcitabine was used the IC_{50} was only 4.99nM – data curve not shown due to scaling. These results were statistically significant with a p-value of <0.001. This data proves that reduced cell viability can be accelerated significantly when targeted with a specific antibody-tagged vehicle carrying chemotherapy agent against antigen expressive cells, such as Bx-PC-3. Finally, it appears that the BxPC-3 cell line is more chemo-sensitive to gemcitabine, as much lower concentrations of gemcitabine was required to cause significant cell death with the same cell density as the Mia Pa Ca-2 cell line.

4.4 Summary

The experiments performed against pancreatic cancer cells *in vitro* in 2D culture prove that cell death can be accelerated effectively by using a specific antibody-tagged gemcitabine-loaded SPION. Furthermore, the experiments demonstrated that the gemcitabine loaded onto the nanohybrids is the only chemotoxic agent the cells are exposed to. This was encouraging results and would lead to further study of the cells; Mia Pa Ca-2 (CA 19-9 antigen negative) and BxPC-3 (CA 19-9 antigen expressive) in both 3D and circulatory models.

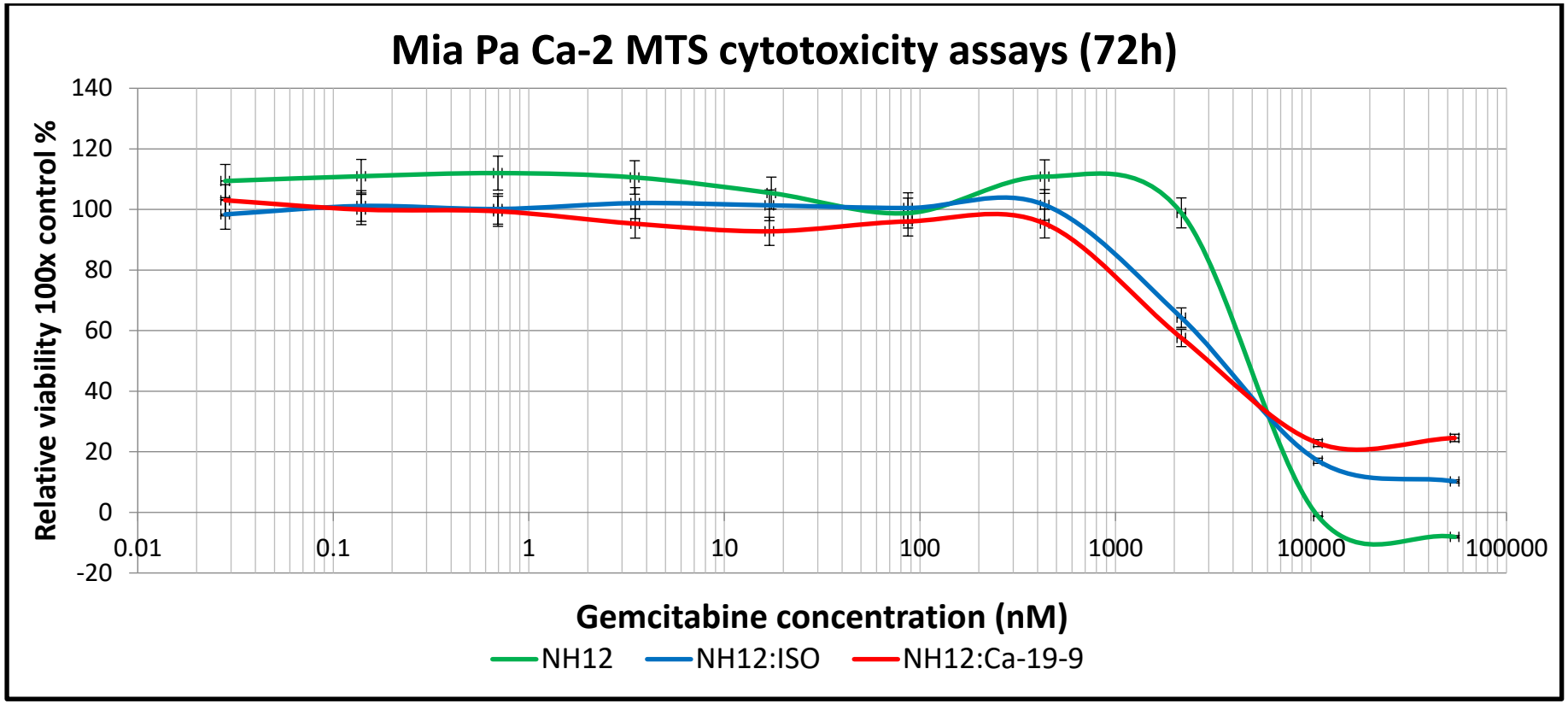

Cell line	Ca-19-9 expressive?	IC_{50} value (nM)			
		Gemcitabine	NH12	NH12:ISO	NH12:Ca-19-9
MIAPACA-2	No	41.79	4,051	3,535	3,090

Figure 16: MTS cytotoxicity curves and table demonstrate no statistically significant alteration in the IC_{50} of Mia Pa Ca-2 cells when treated with either nanohybrids (NH), non-specific isotype antibody-tagged nanohybrids (NH:ISO) or CA 19-9 antibody-conjugated nanohybrids (NH:CA 19-9). Gemcitabine curve is not shown. 95% CI shown. (n=5; p=0.27) nM=nanomolar

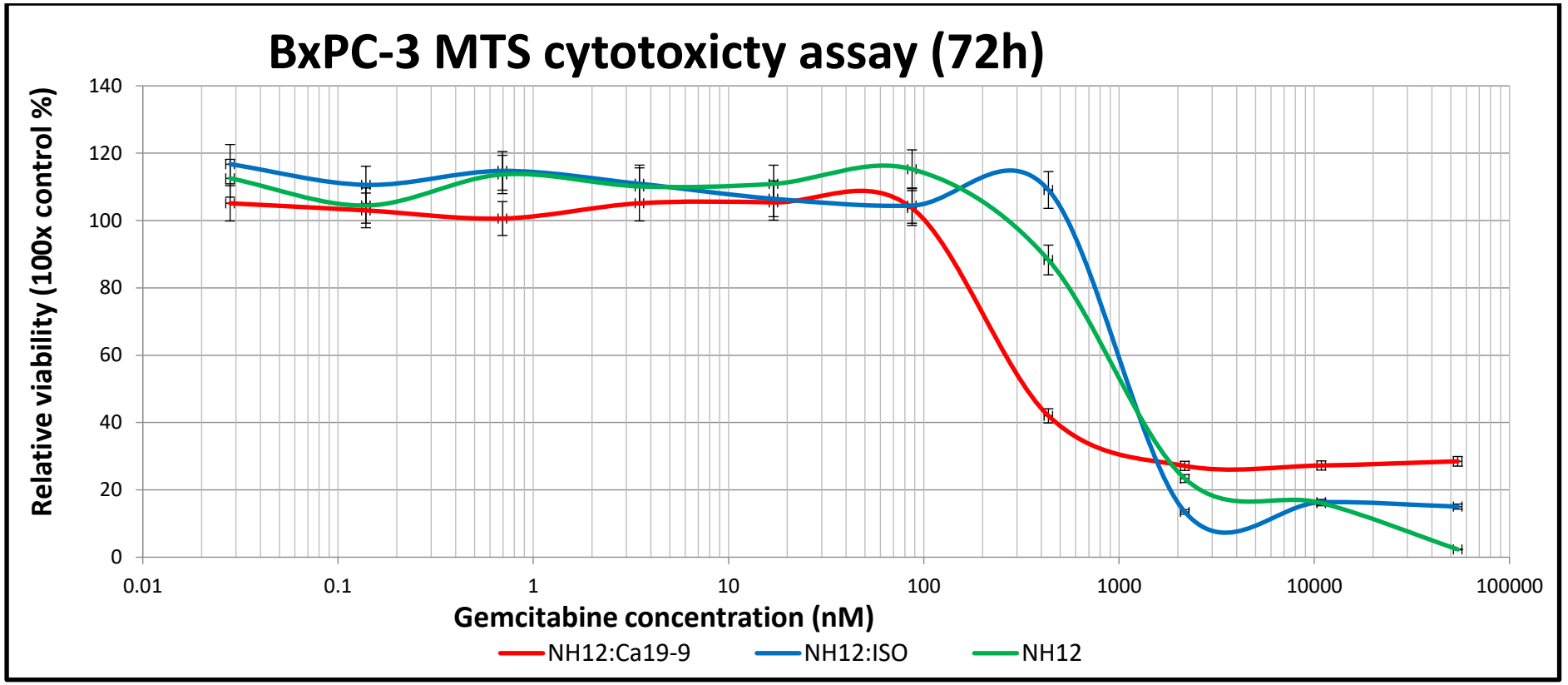

Cell line	Ca-19-9 expressive	IC_{50} value (nM)			
		Gemcitabine	NH12	NH12:ISO	NH12:Ca19.9
BxPC-3	Yes	4.99	1,123	1,175	354

Figure 17: MTS cytotoxicity curves and table demonstrate statistically significant decrease in the IC_{50} of BxPC-3 cells when treated with CA 19-9 antibody-conjugated nanohybrids (NH:CA 19-9) in comparison to nanohybrids (NH) and non-specific isotype antibody-tagged nanohybrids (NH:ISO). Gemcitabine curve is not shown. 95% CI shown (n=6; p<0.001) nM=nanomolar

5 Results III: Cytotoxicity of pancreatic cancer cell lines using Operetta® CLS High-Content Analysis System (including against formed spheroids)

5.1 Visualisation of receptor-mediated endocytosis

5.1.1 SPIONs enter Mia Pa Ca-2 cells and are targeted to the nucleus

We were able to take real-time confocal imagery using the Operetta® CLS High-Content Analysis System and analysed them using the Harmony ® High Content Imaging and Analysis Software. We were able to run the experiment for a total of 17 hours, however, we found that 2 hours after transfection, the SPIONs entered the cells and after 4-6 hours they begin to target the nucleus (figure 18 C-D). Up to 10 hours after transfection, the SPIONs have completely engulfed the cells and only they are visible (figure 18 E-F).

5.2 BxPC-3 form tightly packed spheroids

We experimented with both Mia Pa Ca-2 and BxPC-3 cells and found the BxPC-3 cells formed tight spheroids, probably as they tend to grow with more confluence in normal 2D culture within a T75 flask as shown in section 4.1. We were able to successfully visualise the formation of the BxPC-3 spheroid over a period of 10 hours in the Operetta® CLS High-Content Analysis System. The formation of the spheroid is shown in figure 19.

5.3 Addition of gemcitabine-loaded SPIONs causes dissociation of tight formed spheroids

Once spheroid formation was optimised, the gemcitabine-loaded SPIONs were transfected onto the spheroids, to assess their effect on the tightly packed structure. We were able to successfully visualise the effects of the gemcitabine-loaded SPIONs on the BxPC-3 spheroid over a period of 10 hours in the Operetta® CLS High-Content Analysis System. The formation of the spheroid is shown in figure 19.

Figure 20 shows that over a 14-hour period there is complete dissociation of the spheroid visually indicating cell death.

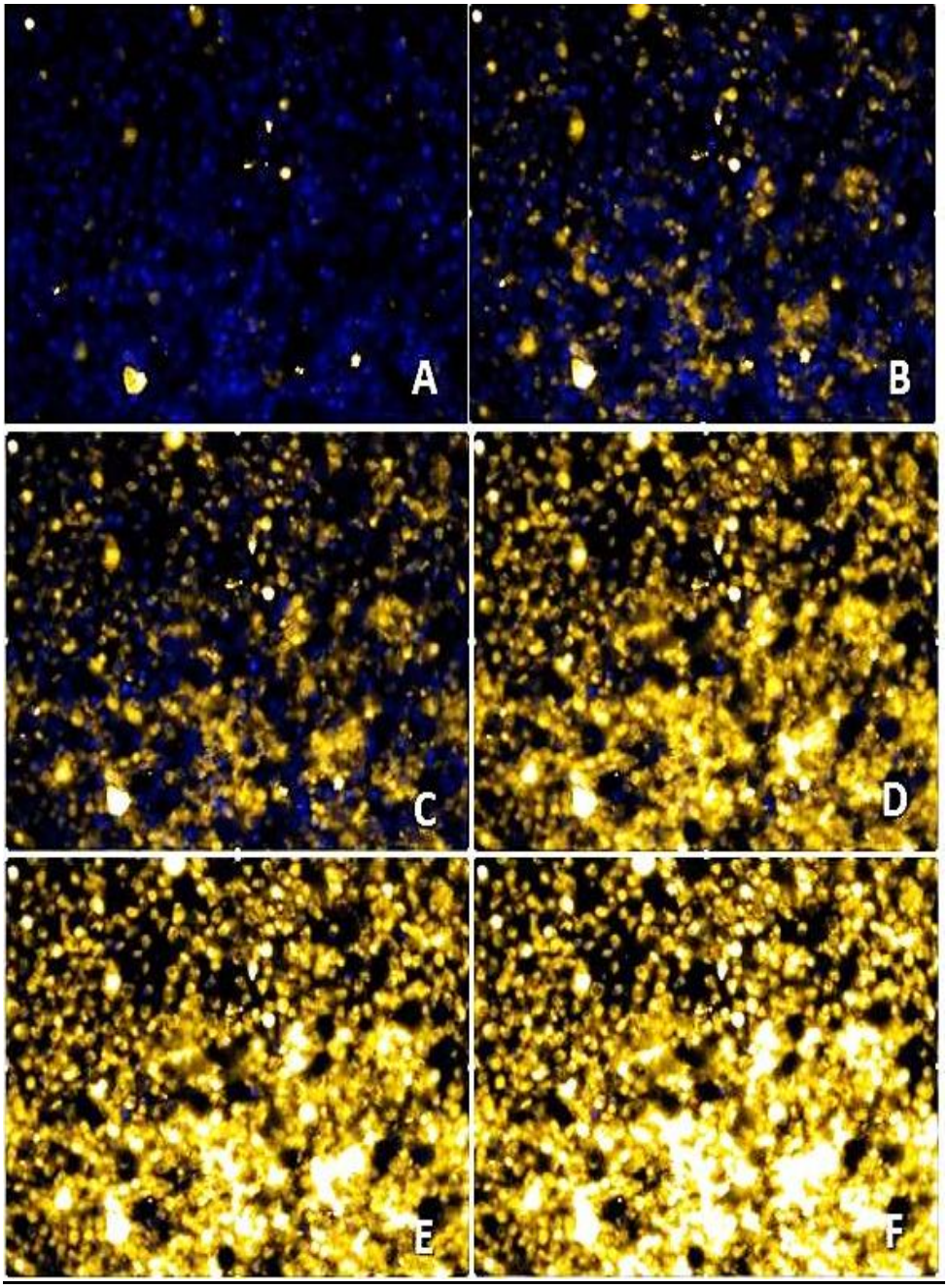

Figure 18: MiaPaCa-2 cells treated with gemcitabine-loaded SPIONS. SPIONs visualised on the Operetta® CLS High-Content Analysis System, and images were produced using Harmony ® High Content Imaging and Analysis Software. Images represent cells at [A] 0 hours [B] 2 hours [C] 4 hours [D] 6 hours [E] 8 hours [F] 10 hours after incubation in Operetta. Blue= Hoescht [2ug/ml] representing cells' nuclei. Yellow= Rhodamine, representing SPIONs. (n=3)

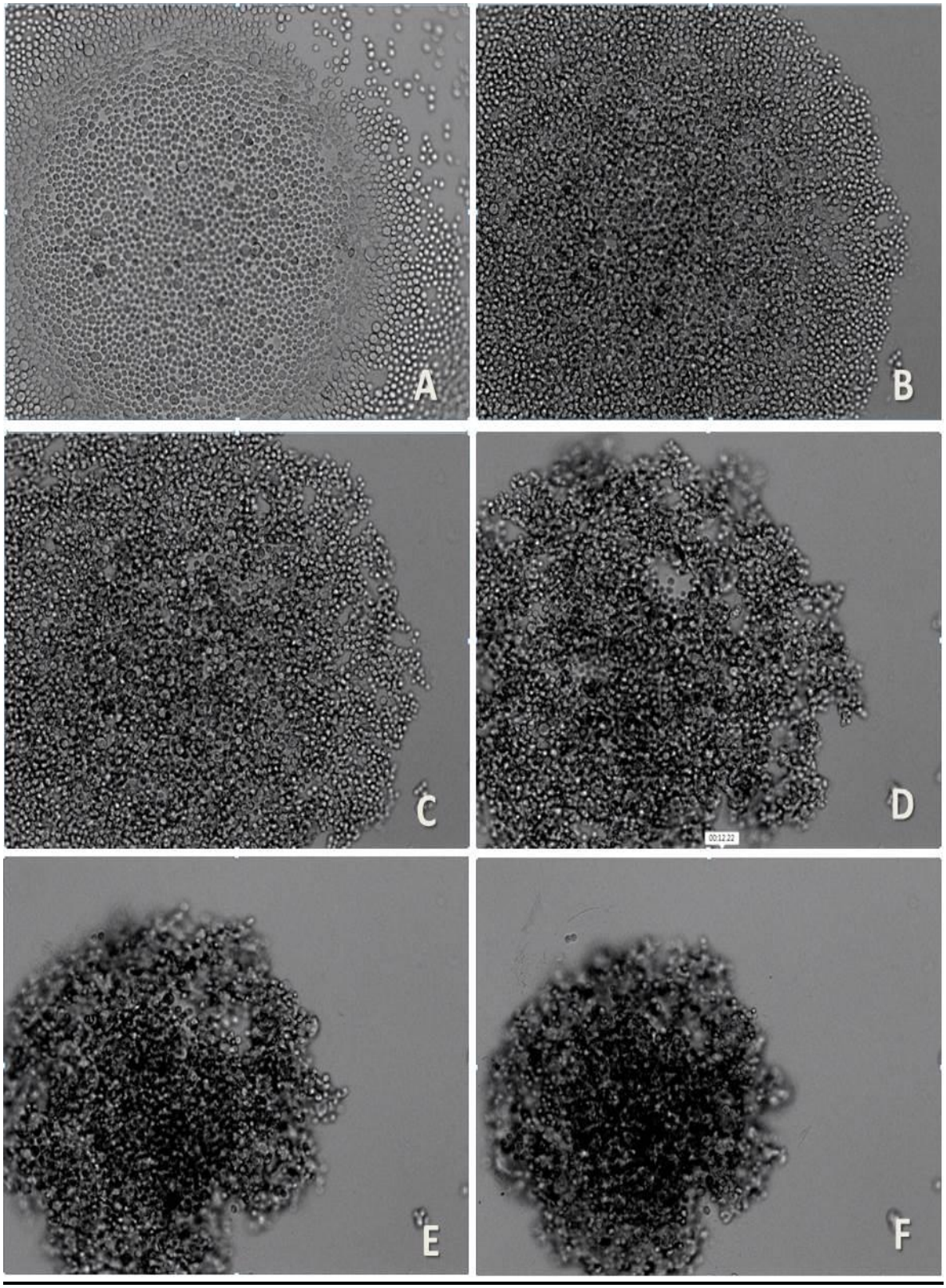

Figure 19: Confocal microscopy imagery demonstrating formation of tightly condensed BxPC-3 spheroids, visualised using Operetta® CLS High-Content Analysis System, and images were produced using Harmony ® High Content Imaging and Analysis Software. Images represent cells at [A] 0 hours [B] 2 hours [C] 3.5 hours [D] 6 hours [E] 8 hours [F] 10 hours after incubation within the Operetta® CLS High-Content Analysis System. Image magnification x150.

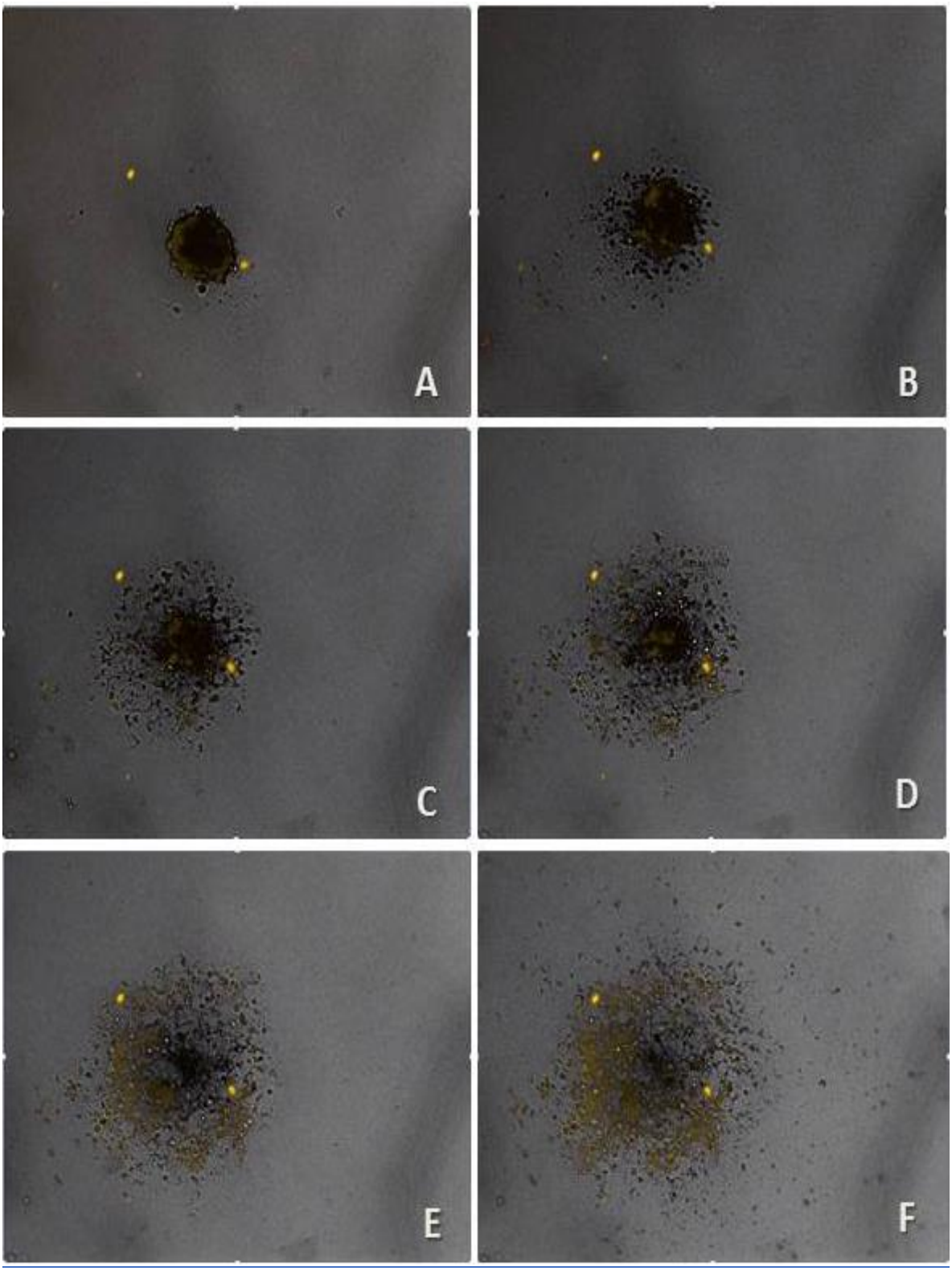

Figure 20: Confocal microscopy imagery demonstrating the dissociation of the tight spheroid using gemcitabine-loaded SPIONS. Cells initially incubated for 2 hours. Images represent [A] 2 hours [B] 5 hours [C] 8 hours [D] 10 hours [E] 12 hours [F] 14 hours after incubation. Visualised using the Operetta® CLS High-Content Analysis System, and images were produced using Harmony® High Content Imaging and Analysis Software. Yellow=rhodamine incorporated within SPION. Image magnification x30

5.4 Summary

These experiments involving the Operetta® CLS High-Content Analysis System were entirely novel, in terms of the use of this piece of equipment to demonstrate real time cell death after transfection with gemcitabine-loaded SPIONs. They certainly needed a great deal of optimisation especially in determining the ideal density of cells to use to form a spheroid initially. Unfortunately, we would have liked to perform further experiments with more cell types.

As a result, the conclusions drawn from these experiments are primarily to exhibit the cell death or destruction of a tightly formed cell spheroid, which would be more in-keeping with a solid *in vivo* tumour after treatment with the gemcitabine-loaded SPIONs.

6 Results IV: Cytotoxicity of pancreatic cancer cell lines (artificial circulation)

6.1 Variables

The artificial circulation model experiments were carried out as described in section 2.9. They created several variables within the experiments to investigate the use of the differing treatments against the pancreatic cancer cells. These are outlined in Table 10 as per section 2.9, however, will be repeated for ease (Table 11).

Time point	Treatment	Magnet	Flow
16 / 24 / 48 / 72 hours	Media with 2% nanoparticle treatment ***or*** media only.	Magnetic field underneath flask present ***or*** absent.	Exposed to 80rpm flow of media ***or*** static only

Table 11: Variables pancreatic cancer cells are exposed to during experiments with an artificial circulatory model.

6.2 Cell lines used

As these experiments were entirely novel and had never been attempted before, a lot of optimisation was required. We found that the Mia Pa Ca-2 cell line grew well and were resilient enough to withstand the flow experimentation. Therefore, efforts were concentrated on using this particular cell line to investigate the magnetic properties of the gemcitabine-loaded SPIONs to increase cell death over time. We experimented extensively with the BxPC-3 cell line, but unfortunately found that the artificial flow element of the experiments gave a detrimental outcome to their normal growth pattern. As we found earlier in 2D culture, much lower concentrations of gemcitabine were required to cause cytotoxicity in the BxPC-3 cell line, this may have had a bearing on the potential results that we were unable to obtain for that particular cell line.

6.3 Light microscopy

6.3.1 Destruction of monolayers when subjected to gemcitabine-loaded SPION treatment; especially over a magnetic field

The cell monolayer at each time point within the experiment was imaged under the light microscope. This was to obtain simple images that could be used to see the progression of potential cell death. The light microscopy images demonstrate that the cell monolayer is destroyed quicker when the treatment has been applied over a magnetic field when transfected with gemcitabine-loaded SPIONs. There is a marked difference between where the magnetic field is at its strongest (centrally) compared to both peripherally obtained images and in cell monolayers without a magnetic field at all. These results were reproduced 3 times and shown in figure 23.

6.3.2 No destruction of the cell monolayer was seen on light microscopy without treatment with gemcitabine-loaded SPIONs

Light micrographs of the cell monolayer obtained at the same time points when only subjected to media only instead of treatment with gemcitabine-loaded SPIONs, did not show any significant destruction or cell death. This is the control arm of the experiments. This indicates that no cytotoxic effect was seen without gemcitabine or that the cells were being damaged by the flow system itself. This is shown in figure 22.

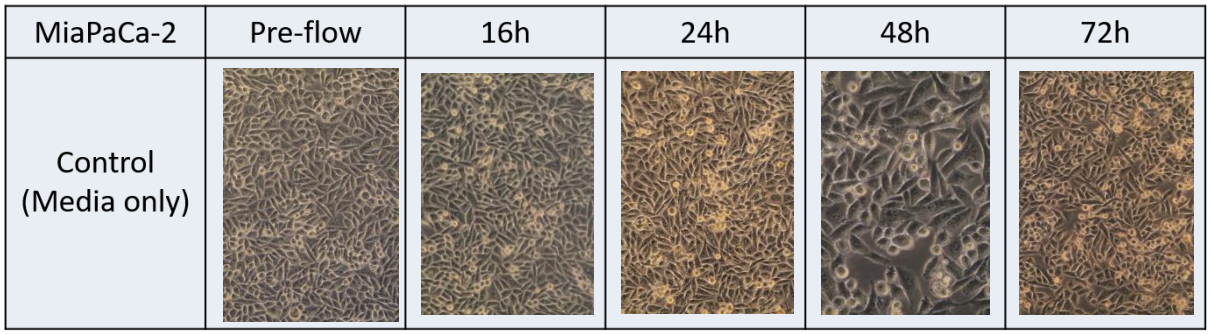

Figure 21: Light micrographs of cellular monolayers subjected to phosphate-buffered saline only within the artificial circulatory model. Images taken before commencing flow and after various time points. Panels demonstrate no significant destruction of the cell monolayer over time.

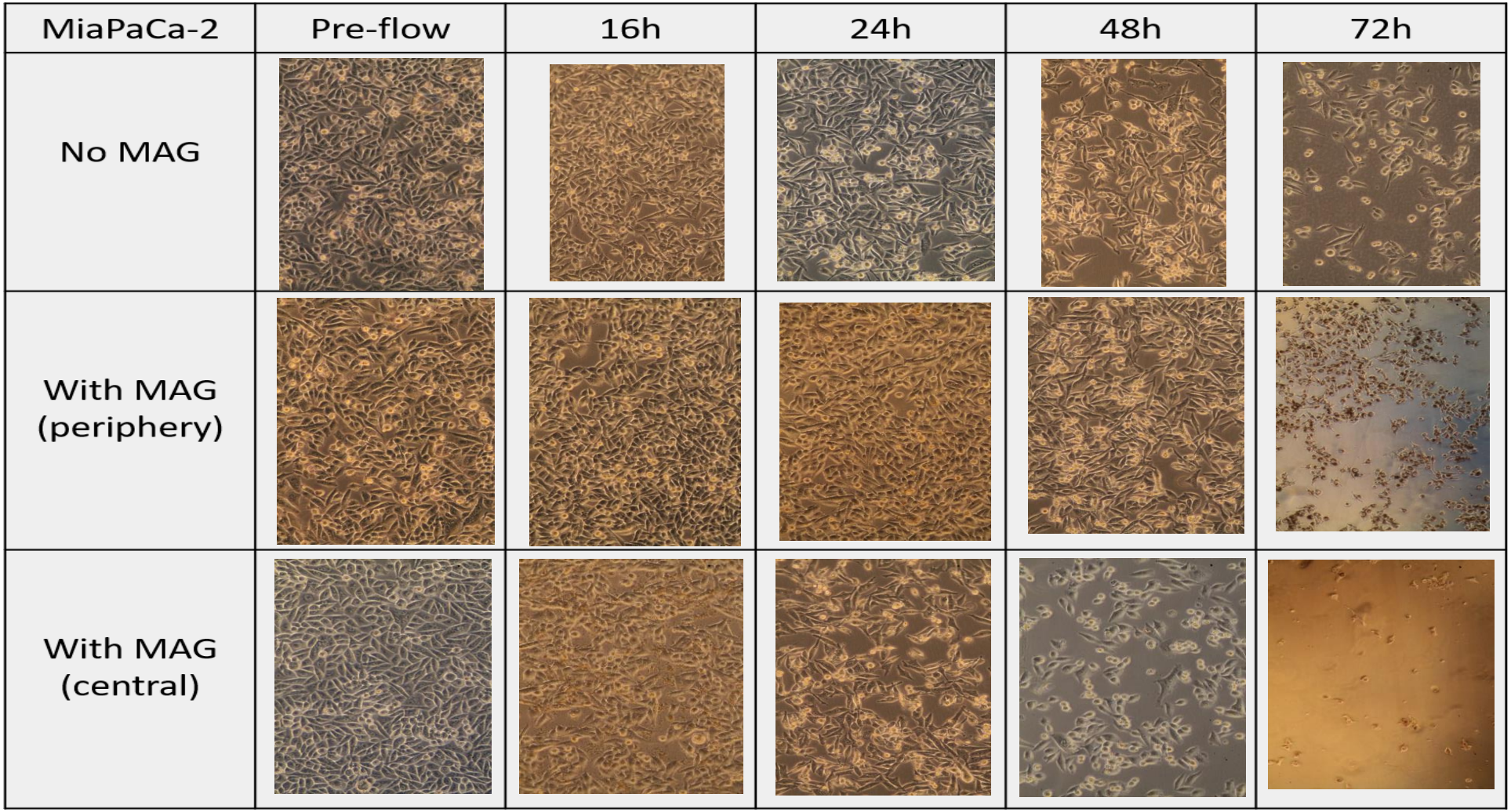

Figure 22: Light micrographs of cellular monolayers subjected to treatment with gemcitabine-loaded SPIONs. Images taken before commencing flow and after various time points. Panels demonstrate increased monolayer destruction over time and with a magnetic field in-situ. MAG = magnetic field in-situ; images taken at both the central aspect of the flask where the magnet in situated and periphery of the flask where the magnetic field is weaker. All micrographs at magnification 20x. n=3

6.4 Co-localisation fluorescent microscopy

6.4.1 Demonstrated uptake of gemcitabine-loaded SPIONs by cells after 72 hours of circulation

Following treatment with gemcitabine-loaded SPIONs, the cell monolayer was imaged using co-localisation fluorescent microscopy. This demonstrated that the SPIONs were up taken by the cells, furthermore, showed that the SPIONs are being drawn to the cells within the artificial circulation model. The images obtained were taken from the periphery of the flask or in experiments without a magnetic field, as after 72 hours the cell monolayers over a magnetic field centrally were essentially destroyed and therefore were unable to be imaged effectively. Nevertheless, the fluorescent microscopy obtained was encouraging showing that even after 72 hours, SPIONs were still in circulation and adherent to cells. This is demonstrated in figure 24.

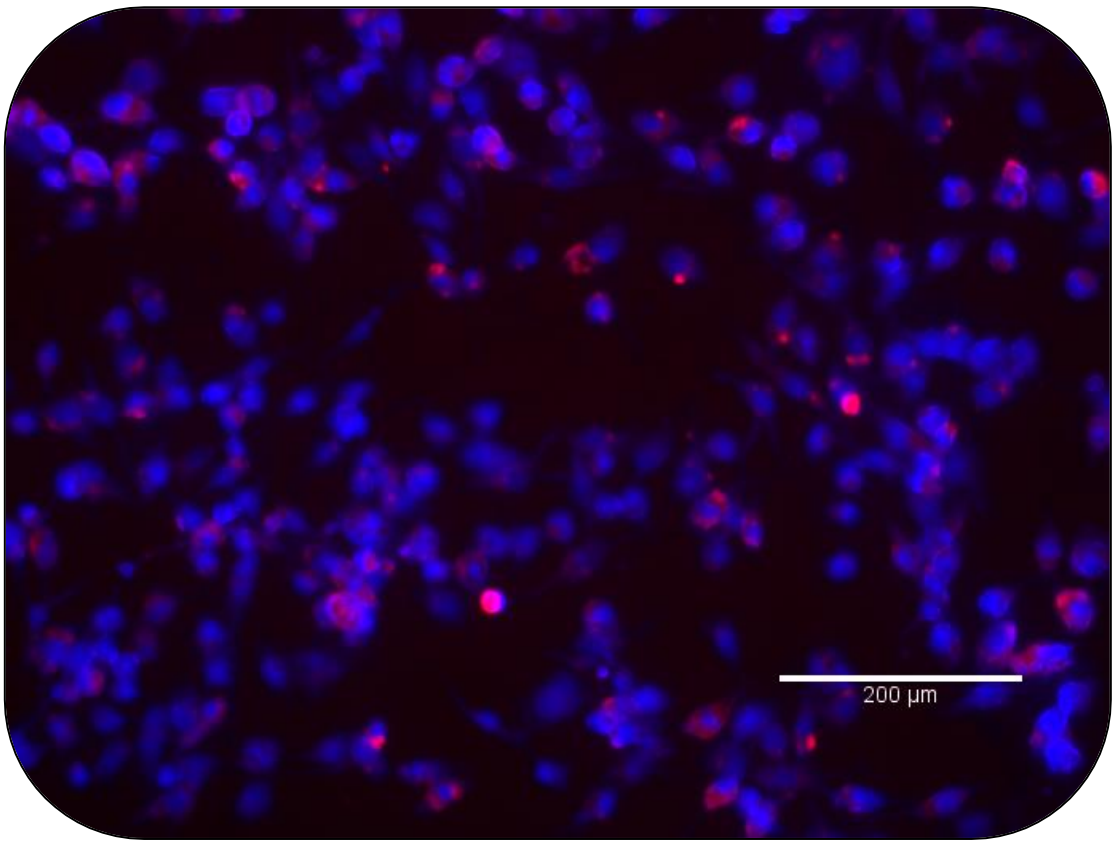

Figure 23: Co-localisation fluorescent micrograph of Mia Pa Ca-2 cellular monolayer subjected to 72 hours of gemcitabine-loaded SPION treatment. Blue=DAPI nuclear staining of cells; red=rhodamine tagged SPIONs.

6.5 LDH assay results

6.5.1 No significant cell death demonstrated in control arm in both static and flow conditions

This was further evidence that the active treatment for cell death is gemcitabine. The control arm (media only) did not show any significant increased cell death despite the other variables in the experiments: use of a magnetic field, time points or use of a flow system. The LDH assay results are represented in figure 25 B and D, where the higher the optical density the greater the cell death.

6.5.2 Use of magnetic field has significant increased cell death in static conditions at early time point

At the 16-hour time point, a statistically significant increase in cell death in static conditions 1.094nm with the magnetic field against 0.752nm without the magnetic field; $p<0.05$. After the 16-hour time point, there was no statistically significant difference in cell death with the use of a magnetic field. This is represented in figure 6.4 C, where the higher the optical density the greater the cell death.

6.5.3 Use of magnetic field demonstrated significant increased cell death within a flow system

There was an increased in cell death when cells were subjected to gemcitabine-loaded SPIONs within the flow system with the use of a magnetic field. At the 16 and 24 hour time points, the results are statistically significant, these are summarised in table 12.

Time point (hours)	Optical density (nm)		p- value
	Magnetic field	No magnetic field	
16	0.751	0.139	<0.001
24	0.798	0.226	0.02
48	1.716	1.375	0.10
72	1.645	1.330	0.11

Table 12: Summary of LDH assay results from flow experiments using gemcitabine-loaded SPION treatment with or without the use of a magnetic field. (nm=nanometre)

Furthermore, the results are represented in graphical form in figure 25 A and highlighted in figure 26.

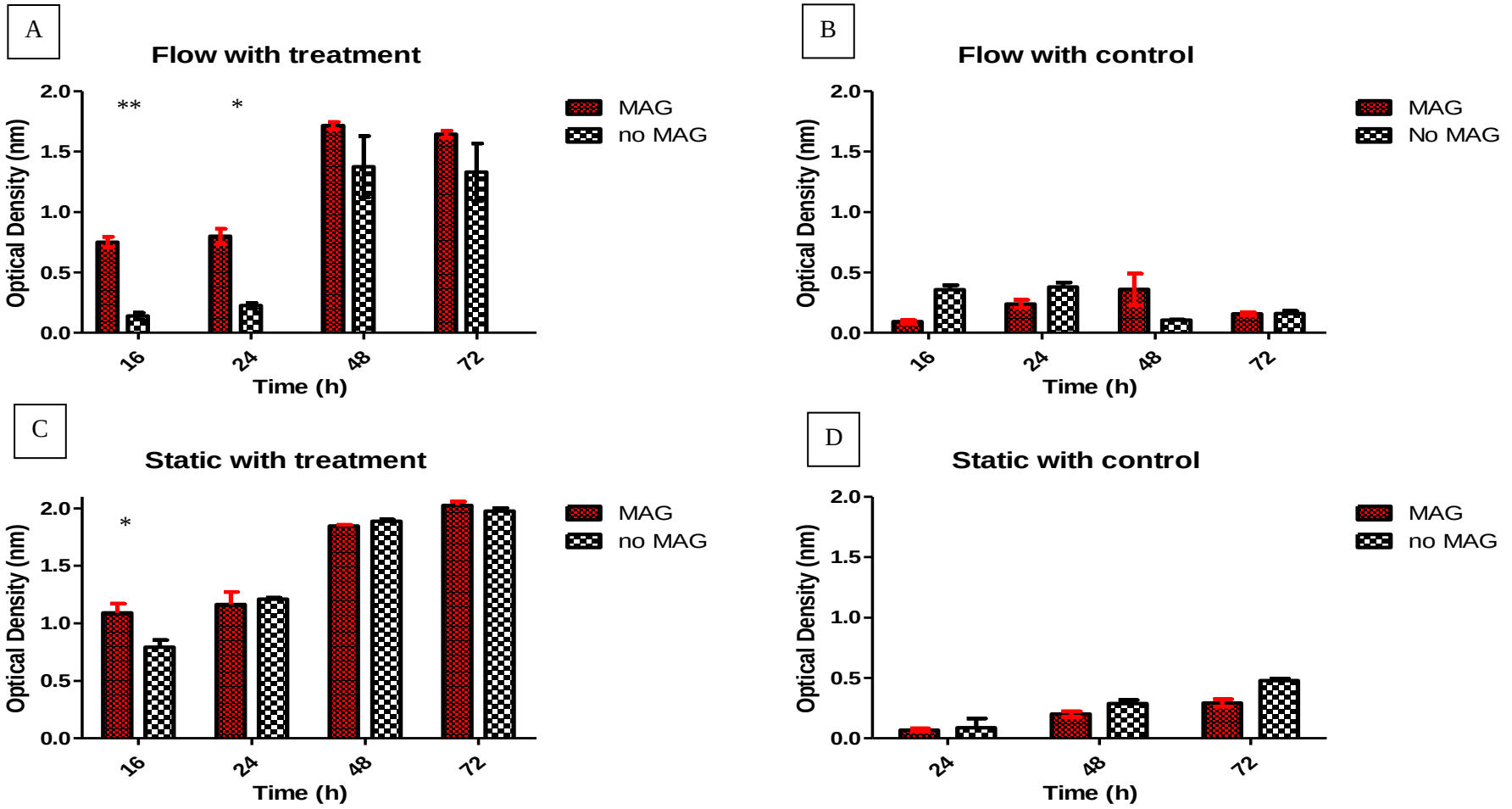

Figure 24: Results from LDH assay performed on all conditions tests. Higher optical density indicates increased cell death. [A] confirms cell death effects of gemcitabine-loaded SPIONs; potentiating effect of magnet in early time points with flow and little effect of magnet in static experiments. n=3 for all experiments. Treatment = 2% gemcitabine-loaded SPIONs. Control = media only. MAG=use of magnetic field. (nm=nanometre) ** p<0.001; * p<0.05.

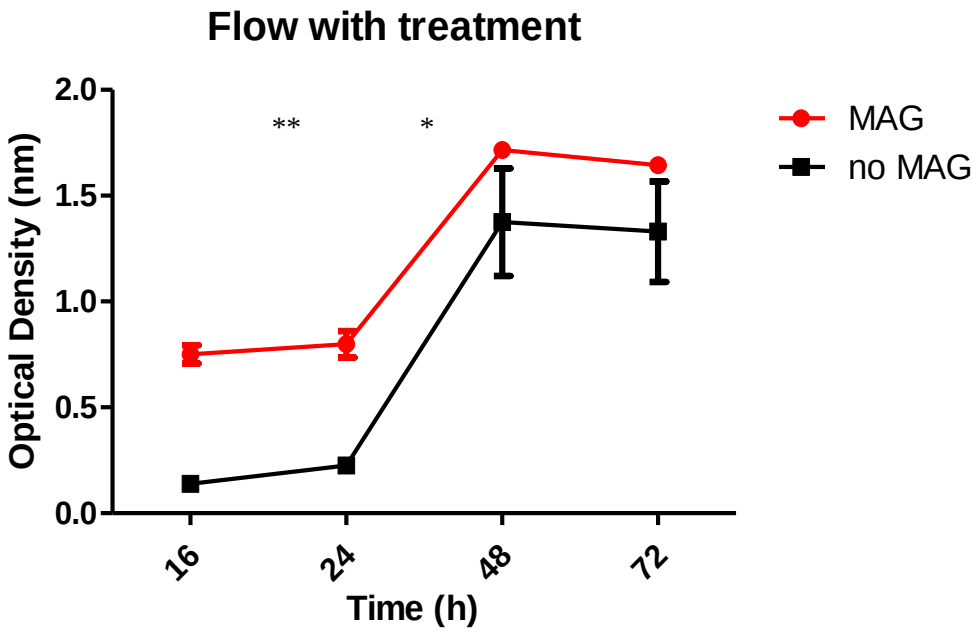

Figure 25: Results from LDH assay highlighting the increased cell death from magnetic targeting at early time points in a flow system. n=3. Higher optical density indicates increased cell death. Treatment = 2% gemcitabine-loaded SPIONs. MAG=use of magnetic field. ** p<0.001; * p<0.05.

6.6 Summary

The artificial circulation model experiments were very encouraging in demonstrating some important negatives. Firstly, that again only the gemcitabine-loaded SPIONs (indirectly gemcitabine) can cause cytotoxicity of the cells. Secondly, that the flow system that the cells are being subjected does not cause harm to them, as shown in the control arm of the experiments. Promisingly, we have demonstrated that the gemcitabine-loaded SPIONs can successfully be drawn from a circulatory model and destroy cell monolayers. This effect is definitely potentiated by the magnetic targeting mechanism and has its greatest effect at early time points (16 and 24 hours) and although has reducing effect, is still present by 72 hours, although not statistically significant.

7 Discussion

7.1 Interpretations

The results presented are predominantly novel experiments into producing cytotoxic effects on pancreatic cell lines using a multifunctional superparamagnetic iron oxide nanoparticles (SPIONs) loaded with gemcitabine. We have shown in a variety of modalities that the manufactured SPIONs are successful in causing cytotoxic effects to desired cells. Importantly, it has been demonstrated that it is only the chemotherapy agent (gemcitabine) alone that is causing the cell damage. By successfully growing specific cancer cell lines for our experimental purposes we have shown the capabilities of the manufactured SPIONs as published by Olariu et al [137]. The pancreatic cancer cells were effectively manipulated to demonstrate the SPIONs ability to cause cytotoxic effects in three differing environments: in 2D culture, 3D culture and within a flow system. This is particularly encouraging as it demonstrates that the SPIONs are adaptable to the environment they have been subjected to and still cause the desired effects – causing cell damage to cancer cells.

7.1.1 Successful uptake of gemcitabine-loaded SPIONS to cancer cells

With the use of co-localisation fluorescent microscopy, we have demonstrated successful cellular uptake – with endocytosis – in both 2D and 3D models. Furthermore, this was shown in real-time confocal imaging using the Operetta® CLS High-Content Analysis System and Harmony ® High Content Imaging and Analysis Software. The real-time imaging showed maximal effect at around 4-6 hours without any active targeting mechanism.

7.1.2 Accelerating effects of gemcitabine-loaded SPIONs

Furthermore, two methods of active targeting of the SPIONs have been demonstrated. Both have indicated an improvement in the absolute reduction in the cell viability of the treated pancreatic cells and also accelerating the process, as proven by the use of MTS assays.

7.1.2.1 Attaching CA 19-9 antibody

Firstly, by attaching a specific target ligand in the form of an anti-CA 19-9 antibody onto the surface coating of the nano-complex, when targeted against a CA 19-9 antigen expressive cell line, such as BxPC-3, as used in these experiments. Conversely, the antibody targeting showed no reduction in cell viability against the Mia Pa Ca-2 cell line, which was proven to be non-expressive of CA 19-9 antigen. Both these cell lines' antigen expressivity was repeatedly demonstrated using indirect immunofluorescence.

7.1.2.2 Magnetic targeting

Secondly, by exploiting the unique magnetic qualities of SPIONs, we were able to draw the SPIONs to accelerate cell damage to the pancreatic cancer cells. This was particularly of interest as this was tested within the artificial circulatory model. These results add to the prior work of my colleague, Mr Paul Sykes, who had successfully demonstrated the aggregation of SPIONs over a static magnet in 2D culture. We both demonstrated that the magnetic targeting effect was relatively swift with the statistically significant benefit in reducing cell viability occurring by 24 hours within a flow system. Finally, the magnetic targeting results were against a cell line (Mia Pa Ca-2) that was non-expressive for CA 19-9 antigen.

7.1.3 Versatility of gemcitabine-loaded SPIONs

As described, the SPIONs were successful in differing environments plus independently demonstrated an effective benefit with two methods of active targeting. These attributes are important going forward for their potential application in the clinic [9, 52], which is discussed in more detail below.

7.2 Implications

The ultimate purpose of these experiments and the results is to showcase the gemcitabine-loaded SPIONs effects *in vitro*, in order to translate the findings onto further experimentation firstly *in vitro* and then ideally into clinical trials.

7.2.1 Translational implications

These results, if extrapolated, can offer exciting implications in the clinic, obviously there is further work to be performed to ensure its safety and efficacy (discussed later). However, initial and ground-breaking results are indeed encouraging. There are several features presented within the results that deserve highlighting.

7.2.1.1 Gemcitabine-loaded SPIONs are of interest in size

The completed nano-complex manufactured are consistently shown to be less than 200nm, even with an IgG antibody attachment. It is well known concerning the molecular biology of pancreatic ductal adenocarcinoma (PDAC), there is a dense peripheral stroma [74, 76, 78]. As a result, chemotherapy drug delivery to a tumour load in PDAC is challenging due the fibrotic stroma. The nano-complexes manufactured are of small enough size to potentially penetrate this dense surrounding peri-tumoural tissue and deliver its payload. This effect tried to be replicated when SPIONs were exposed to tightly formed spheroids, more in keeping with a solid tumoural mass. The SPIONs were successful in destroying the spheroids.

7.2.1.2 Antibody targeting

In these experiments, the anti-CA 19-9 antibody was used, as it is expressed in several PDAC types and is widely available, to showcase the active targeting effects. We found that to achieve the same reduction in cell viability of cancer cells, a significantly lower amount of drug concentration was required when using antibody-conjugated SPIONs compared to when SPIONs with no antibody attachment was used. The attached antibody in certain nano-complexes produced, offer a specific targeting ligand that, like the results presented *in vitro*, could improve specificity in delivery chemotherapy drugs to desired cells or tissues *in vivo*. It offers a strategy for reduced unwanted systemic side effects in certain antigen expressive cancers. This lies within the concept of personalised medicine, where in an individual's certain tumour is fully genotyped with complete immunohistochemistry in order to investigate any potential targetable biomarkers (such as antigens like CA 19-9); with that information nano-complexes can be conjugated with target ligands specific to that tumour. Of interest, any IgG

antibody could be attached to the manufactured nano-complexes with the same chemistry process that I performed.

7.2.1.3 Magnetic targeting

As presented the cellular damage caused when the SPIONs were deployed with a magnetic field was most effective at early time points within the flow system. Furthermore, it was effective against negatively antigen expressive cells. The implications of this significant moving forward to *in vivo* work. As the preferred route of administration of SPIONs in currently via the intravenous route, the artificial circulation model was constructed to mimic blood flow and it is encouragingly that the SPIONs were still able to exert their effects successfully. When considering the results for translational purposes, it shows that SPIONs could be injected with the use of an implantable magnet or even a targeted magnetic field from a supermagnet, for a short period of time, reducing the exposure of chemotherapy drug concentration and subsequent side effects, before the magnet field is withdrawn. If an external magnet field is used, repeated administrations would be achievable being a non-invasive approach.

7.3 Limitations

However, encouraging the results presented are, they naturally only represent a small example in the vast field of nanoparticle-driven drug delivery to cancer. The major limitation in formulating translational implications from these experiments is that they have been performed *in vitro* and obvious cannot replicate the real-life conditions found within complex pancreatic tumours and the blood stream.

7.3.1 Pancreatic cancer cells

As the experiments performed were novel, optimisation was challenging. We were successful in manipulating two cell cancer lines BxPC-3. Obviously, it is well known that PDAC is a complex and heterogenous tumour with a surrounding stroma, that is not fully understood in its mechanism. These experiments were unable to replicate the elaborate nature of a PDAC, as the

SPIONs were tested against a homogeneous mass of cancer cells only. Nevertheless, attempts were made to mimic a solid tumour using the 3D models. Notably, the absence of any stroma replication is important, as it contains several components, including pancreatic stellate cells and growth factors, that may interact with the SPIONs and alter their behaviour.

7.3.2 Artificial circulation

Obviously, within an *in vitro* setting, we attempted to reproduce blood/plasma flow conditions that may be faced *in vivo*, by manufacturing an artificial system. The continuous flow contained media, which was proven not to be detrimental to the SPIONs. However, within the body, plasma contains a multitude of different components, which influence the pharmacokinetics of SPIONs greatly. For example, studies have demonstrated SPIONs are predominantly taken up by phagocytes in the reticuloendothelial systems of the liver, spleen, and lymph tissue [31], which obviously, the SPIONs used in our experimentation were not exposed to.

7.3.3 Excretion and toxicity profile

As the SPIONs were not tested against a biological system, its harmful effects cannot be examined. Therefore, its safe excretion and toxicity cannot be assessed here.

7.3.4 CA 19.9 antigen expression

Further to previous discussion, PDAC remains a complicated reality. There are multiple cell types with a several expressing proteins or biomarkers of interest. Although, CA 19-9 antigen remains the commonest biomarker of interest in PDAC, it is by no means universally expressed. Within tumours there is a variable degree of expression, if at all, like immortalised pancreatic cancer cell line. In the results, non-CA 19-9 expressive Mia Pa Ca-2 cells showed no reduction in cell viability by active targeting using the conjugated antibody. Extrapolated, this indicates that if targeting PDAC, perhaps a variety of targeting ligands need to be attached onto the SPION to counter the variability of the tumoural mass. If only one targeting ligand, in this case CA 19-9 antibody, is conjugated there may only be a partial or indeed no increased effect of the active chemotherapy agent. Nevertheless, despite the above being stated, results using the

CA 19-9 conjugated gemcitabine-loaded SPION against Bx PC-3 cells (CA 19-9 expressive) were very promising and definitively deserves further investigation and testing.

7.4 Recommendations

The results presented are exciting, and due to their novel nature would almost certainly require much more investigation as findings are at a nascent stage, like most nanomedical work into cancer drug delivery.

7.4.1 Further in vitro studies

For completeness, exploration of both active targeting modalities – with an antibody and magnetic field – should be considered to understand if there is any benefit in even more accelerated reduction in cell viability, especially in a flow system. These experiments were attempted, although results are not shown as they were not successfully repeated, preliminary findings showed that the magnetic field drew the SPIONs very early on, negating any effect the targeting antibody had. However, these results are only anecdotal at best.

7.4.2 In vivo studies: murine models

Initial experimentation to further investigate the effects of SPIONs would best be suited using a mouse model, this would be predominantly used to build a toxicity profile for the manufactured gemcitabine-loaded SPIONs.

7.4.2.1 Active targeting

However, if the mice are transfected with pancreatic cancer cells and the tumours allowed to mature, a response to treatment with various conditions (including the gemcitabine-loaded SPIONs), can be measured. Below is an outline for proposed experimentation in a murine mode – figure 27 and table 13.

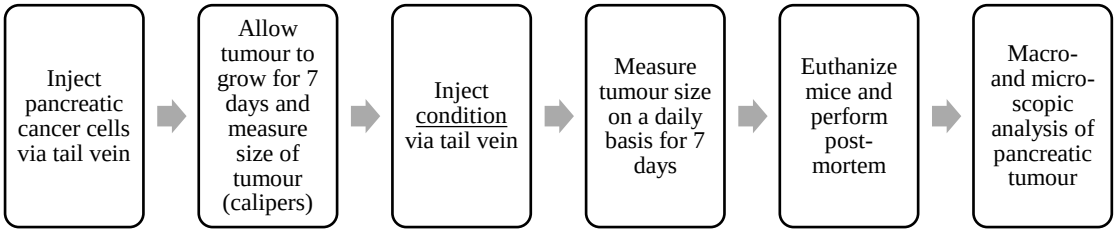

Figure 26: Outline of proposed murine experiment: measuring pancreatic tumour size in nu/nu xenograft mouse model after tail-vein injection of gemcitabine-loaded SPIONs.

Condition	Comment
Non-gemcitabine-loaded SPIONs	Negative control for assessment of toxicity
Gemcitabine-loaded SPIONs	
Gemcitabine-loaded SPIONs with CA 19-9 antibody tag	Active targeting mechanism
Gemcitabine	Positive control

Table 13: Different conditions for proposed murine model. (SPIONs = superparamagnetic iron oxide nanoparticles)

Again, any murine model would have limitations. The pancreatic tumours would again homogenous in nature, which against what is known about PDAC in the clinic. However, the mouse model would provide valuable information regarding the accumulation, biodistribution and excretion of the SPIONs, which would lead to a preliminary toxicity profile. The behaviour of the SPIONs *in vivo* would provide essential knowledge moving forward in eventual clinical work.

The above is addressing one active targeting method, regarding the use of an external magnetic field, there are a variety of methods that could be explored. Most simply, a basic mouse model could be used, and a subcutaneous tumour may be matured. Then the macro- and microscopic response to the tumour of treatment with conditions as per table 13 but with or without an external magnet. This approach would confirm the accelerated tumour damage achieved with a magnet; however, it would not replicate features of a PDAC seen clinically. More sophisticated methods to determine the effects of a magnetic field are available. Chertok et al describe magnet targeting of SPIONs to brain tumours in a tailor-made rat model, a 1.8-fold increase in SPION concentration was seen after intra-arterial administration (carotid artery) compared to intravenous injection. Furthermore, SPION concentrations increased with longer

exposure to the magnetic field [143]. Obviously, the intra-arterial route is invasive and clinically not preferred. For in vivo studies, the application of the magnetic field will possibly require several magnetic field forces targeting an area of the body as opposed to the unidirectional magnetic force used in experiments to date.

However, imaging-guided techniques, which are non-invasive, may be preferred and as previously described SPION treatment can be combined with the use of magnetic resonance imaging (MRI) scanning. This would not only allow one to visualise tumour accumulation or biodistribution of SPIONs, but also measure cancer treatment response.

7.4.3 Future considerations and clinical work

There are substantial hurdles before any early phase clinical trials would be considered, as the manufactured SPIONs toxicity profile would have to be declared. Until this is completed, unfortunately, no clinical research can start.

In the future, clinical work would ideally investigate the effects of the gemcitabine-loaded SPIONs against pancreatic tumours, most likely in the palliative setting initially (where gemcitabine is mostly used), whilst being to image the response simultaneously using MRI. How this is achieved would be either with gemcitabine-loaded SPIONs conjugated with an individualised specific target ligand bound to the drug vehicle; or using an external magnetic field. The magnetic field would either be in the form of an implantable magnet or an external stereotactic-like magnetic field using a supermagnet. It must be noted that it would be unlikely to offer invasive surgery to implant a magnet in the palliative setting. Whatever the active targeting method, it is likely to require repeat sittings. Finally, treatment response ideally would be imaged using MRI, to gauge the response of the treatment against the drug-loaded SPIONs, similar to current practice in several solid tumours following initiation of a chemotherapy regimen.

7.4.3.1 Personalised nanomedicine

It is increasingly clear that no two pancreatic tumours are the same. Current and future work will certainly focus on the individual's tumour and consider a personalised approach to the patient's treatment. As further research reveals more biomarkers and potentially 'drug-able' targets, especially from the abundance of cells from the stroma of a pancreatic tumour, it offers further hope to manufacture tailor-made nanoparticle-based drug delivery systems.

7.4.3.2 Translational goals

This is a completely novel project and potentially has very exciting and wide-ranging consequences. The data gathered from the project will inevitably add considerable knowledge to the potential effectiveness of nanoparticle-based chemotherapy, not exclusive to pancreatic cancer treatment. The concepts being tested in these experiments can be transferred to the treatment to other solid cancers. That is to say, an appropriate chemotherapy agent can be chemically loaded onto a nanoparticle complex with a suitable ligand (such as an expressed antibody) to target a specific cancer. These theories lead to the overall translational goal of this research, which is to be able to safely administer the manufactured nanoparticles in patients, with the capability to kill cancer cells without damaging normal, healthy cells, which causes unwanted effects from conventional chemotherapy. There is a huge potential to improve patients' quality of life, by providing a more precise or personalised approach to the chemotherapy they receive.

8 Conclusions

Pancreatic cancer therapy has poor outcomes despite advancement of chemotherapy agents and surgical interventions. There are a multitude of factors that have maintained the dismal prognosis over the past forty years. Drug delivery of cytotoxic drugs is a major factor. This is in part due to the hostile tumour microenvironment and complex stroma-tumour interactions. This indicates that newer approaches are desperately required in the delivery of anticancer drugs, this research demonstrates initial effective concepts to try to address the issues outlined.

This project has shown that a stable and sophisticated SPION complex has been created and its effects tested on a variety of cellular models, confirming their desired effects. Furthermore, two methods of actively targeting the SPION have also been demonstrated: using an antibody and a magnet. Very encouraging results have been presented in 2D and 3D culture and finally with an artificial circulatory model. Although, the field of nanotechnology is booming there has been few applications towards the treatment pancreatic cancer. This is undoubtedly due to the exhaustive level of prior research and development required before even considering clinical use. Nevertheless, the results will add to the promising nascent work in the field of nanoparticle-driven cancer therapy.

References

1. Gabellieri, C. and H. Frima, *Nanomedicine in the European Commission policy for nanotechnology.* Nanomedicine, 2011. **7**(5): p. 519-20.
2. (ACN), T.A.C.f.N. 2015; Available from: http://www.acn.unsw.edu.au/.
3. Nanomedicine, E.T.P., 2011.
4. Globocan 2012: Estimated Cancer Incidence, M.a.P.W.i., 2012.
5. Cancer Research UK. *Pancreatic cancer statistics*. 2020 [cited 2020 02/01/2020]; Available from: https://www.cancerresearchuk.org/health-professional/cancer-statistics/statistics-by-cancer-type/pancreatic-cancer#heading-One.
6. Global Cancer Observatory. *Cancer Today: Data visualization tools for exploring the global cancer burden in 2018* 2018 [cited 2020 02/01/2020]; Available from: https://gco.iarc.fr/today/home.
7. Shi, J., et al., *Cancer nanomedicine: progress, challenges and opportunities.* Nature Reviews Cancer, 2017. **17**(1): p. 20-37.
8. Haley, B. and E. Frenkel, *Nanoparticles for drug delivery in cancer treatment.* Urologic Oncology: Seminars and Original Investigations, 2008. **26**(1): p. 57-64.
9. Gonda, A., et al., *Engineering Tumor-Targeting Nanoparticles as Vehicles for Precision Nanomedicine.* Med One, 2019. **4**.
10. Lee, G.Y., et al., *Theranostic Nanoparticles with Controlled Release of Gemcitabine for Targeted Therapy and MRI of Pancreatic Cancer.* ACS Nano, 2013. **7**(3): p. 2078-2089.
11. Chenthamara, D., et al., *Therapeutic efficacy of nanoparticles and routes of administration.* Biomaterials research, 2019. **23**: p. 20-20.
12. Wahajuddin and S. Arora, *Superparamagnetic iron oxide nanoparticles: magnetic nanoplatforms as drug carriers.* International journal of nanomedicine, 2012. **7**: p. 3445-3471.
13. Bao, G., S. Mitragotri, and S. Tong, *Multifunctional nanoparticles for drug delivery and molecular imaging.* Annu Rev Biomed Eng, 2013. **15**: p. 253-82.
14. Matsumura, Y. and H. Maeda, *A new concept for macromolecular therapeutics in cancer chemotherapy: mechanism of tumoritropic accumulation of proteins and the antitumor agent smancs.* Cancer Res, 1986. **46**(12 Pt 1): p. 6387-92.
15. Sykes, P.D., et al., *Nanotechnology advances in upper gastrointestinal, liver and pancreatic cancer.* Expert Rev Gastroenterol Hepatol, 2012. **6**(3): p. 343-56.
16. Gradishar, W.J., et al., *Phase III trial of nanoparticle albumin-bound paclitaxel compared with polyethylated castor oil-based paclitaxel in women with breast cancer.* J Clin Oncol, 2005. **23**(31): p. 7794-803.
17. Wang, A.Z., R. Langer, and O.C. Farokhzad, *Nanoparticle delivery of cancer drugs.* Annu Rev Med, 2012. **63**: p. 185-98.
18. Libutti, S.K., et al., *Phase I and pharmacokinetic studies of CYT-6091, a novel PEGylated colloidal gold-rhTNF nanomedicine.* Clin Cancer Res, 2010. **16**(24): p. 6139-49.
19. Yoffe, S., et al., *Superparamagnetic iron oxide nanoparticles (SPIONs): synthesis and surface modification techniques for use with MRI and other biomedical applications.* Curr Pharm Des, 2013. **19**(3): p. 493-509.
20. Mahmoudi, M., et al., *Superparamagnetic iron oxide nanoparticles (SPIONs): Development, surface modification and applications in chemotherapy.* Advanced Drug Delivery Reviews, 2011. **63**(1): p. 24-46.
21. Kodama, R.H., *Magnetic nanoparticles.* Journal of Magnetism and Magnetic Materials, 1999. **200**(1): p. 359-372.
22. Chouly, C., et al., *Development of superparamagnetic nanoparticles for MRI: effect of particle size, charge and surface nature on biodistribution.* J Microencapsul, 1996. **13**(3): p. 245-55.
23. Gupta, A.K. and S. Wells, *Surface-modified superparamagnetic nanoparticles for drug delivery: preparation, characterization, and cytotoxicity studies.* IEEE Trans Nanobioscience, 2004. **3**(1): p. 66-73.

24. Sjogren, C.E., et al., *Crystal size and properties of superparamagnetic iron oxide (SPIO) particles.* Magn Reson Imaging, 1997. **15**(1): p. 55-67.
25. Veiseh, O., J.W. Gunn, and M. Zhang, *Design and fabrication of magnetic nanoparticles for targeted drug delivery and imaging.* Adv Drug Deliv Rev, 2010. **62**(3): p. 284-304.
26. Danhier, F., O. Feron, and V. Preat, *To exploit the tumor microenvironment: Passive and active tumor targeting of nanocarriers for anti-cancer drug delivery.* J Control Release, 2010. **148**(2): p. 135-46.
27. Meng, J., V. Agrahari, and I. Youm, *Advances in Targeted Drug Delivery Approaches for the Central Nervous System Tumors: The Inspiration of Nanobiotechnology.* J Neuroimmune Pharmacol, 2017. **12**(1): p. 84-98.
28. Dobson, J., *Magnetic nanoparticles for drug delivery.* Drug Development Research, 2006. **67**(1): p. 55-60.
29. Zhang, L., W.F. Dong, and H.B. Sun, *Multifunctional superparamagnetic iron oxide nanoparticles: design, synthesis and biomedical photonic applications.* Nanoscale, 2013. **5**(17): p. 7664-84.
30. Prijic, S., et al., *Increased cellular uptake of biocompatible superparamagnetic iron oxide nanoparticles into malignant cells by an external magnetic field.* J Membr Biol, 2010. **236**(1): p. 167-79.
31. Barry, S.E., *Challenges in the development of magnetic particles for therapeutic applications.* Int J Hyperthermia, 2008. **24**(6): p. 451-66.
32. Jain, K.K., *Nanobiotechnology-based strategies for crossing the blood-brain barrier.* Nanomedicine (Lond), 2012. **7**(8): p. 1225-33.
33. Briley-Saebo, K., et al., *Hepatic cellular distribution and degradation of iron oxide nanoparticles following single intravenous injection in rats: implications for magnetic resonance imaging.* Cell Tissue Res, 2004. **316**(3): p. 315-23.
34. Levy, M., et al., *Degradability of superparamagnetic nanoparticles in a model of intracellular environment: follow-up of magnetic, structural and chemical properties.* Nanotechnology, 2010. **21**(39): p. 395103.
35. Levy, M., et al., *Long term in vivo biotransformation of iron oxide nanoparticles.* Biomaterials, 2011. **32**(16): p. 3988-99.
36. Viota, J.L., et al., *Functionalized magnetic nanoparticles as vehicles for the delivery of the antitumor drug gemcitabine to tumor cells. Physicochemical in vitro evaluation.* Materials Science and Engineering: C, 2013. **33**(3): p. 1183-1192.
37. Jordan, A., et al., *Presentation of a new magnetic field therapy system for the treatment of human solid tumors with magnetic fluid hyperthermia.* Journal of Magnetism and Magnetic Materials, 2001. **225**(1): p. 118-126.
38. Alexiou, C., et al., *Locoregional cancer treatment with magnetic drug targeting.* Cancer Res, 2000. **60**(23): p. 6641-8.
39. Gupta, A.K. and M. Gupta, *Cytotoxicity suppression and cellular uptake enhancement of surface modified magnetic nanoparticles.* Biomaterials, 2005. **26**(13): p. 1565-73.
40. Cole, A.J., et al., *Polyethylene glycol modified, cross-linked starch-coated iron oxide nanoparticles for enhanced magnetic tumor targeting.* Biomaterials, 2011. **32**(8): p. 2183-93.
41. Guthi, J.S., et al., *MRI-visible micellar nanomedicine for targeted drug delivery to lung cancer cells.* Mol Pharm, 2010. **7**(1): p. 32-40.
42. Pradhan, P., et al., *Targeted temperature sensitive magnetic liposomes for thermo-chemotherapy.* J Control Release, 2010. **142**(1): p. 108-21.
43. Cinteza, L.O., et al., *Diacyllipid micelle-based nanocarrier for magnetically guided delivery of drugs in photodynamic therapy.* Mol Pharm, 2006. **3**(4): p. 415-23.
44. Wang, L., et al., *Bifunctional Nanoparticles with Magnetization and Luminescence.* The Journal of Physical Chemistry C, 2009. **113**(10): p. 3955-3959.
45. Cherukuri, P., E.S. Glazer, and S.A. Curley, *Targeted hyperthermia using metal nanoparticles.* Adv Drug Deliv Rev, 2010. **62**(3): p. 339-45.
46. Gonzalez-Fernandez, M.A., et al., *Magnetic nanoparticles for power absorption: Optimizing size, shape and magnetic properties.* Journal of Solid State Chemistry, 2009. **182**(10): p. 2779-2784.

47. Takeda, S.-i., et al., *Development of magnetically targeted drug delivery system using superconducting magnet.* Journal of Magnetism and Magnetic Materials, 2007. **311**(1): p. 367-371.
48. Yellen, B.B., et al., *Targeted drug delivery to magnetic implants for therapeutic applications.* Journal of Magnetism and Magnetic Materials, 2005. **293**(1): p. 647-654.
49. Price, P.M., et al., *Magnetic Drug Delivery: Where the Field Is Going*. Frontiers in chemistry, 2018. **6**: p. 619-619.
50. Mahmoudi, M., et al., *Superparamagnetic Iron Oxide Nanoparticles with Rigid Cross-linked Polyethylene Glycol Fumarate Coating for Application in Imaging and Drug Delivery.* The Journal of Physical Chemistry C, 2009. **113**(19): p. 8124-8131.
51. Solanki, A., M. Das, and S. Thakore, *A review on carbohydrate embedded polyurethanes: An emerging area in the scope of biomedical applications.* Carbohydrate Polymers, 2018. **181**: p. 1003-1016.
52. Palanisamy, S. and Y.-M. Wang, *Superparamagnetic iron oxide nanoparticulate system: synthesis, targeting, drug delivery and therapy in cancer.* Dalton Transactions, 2019. **48**(26): p. 9490-9515.
53. Reddy, L.H., et al., *Magnetic Nanoparticles: Design and Characterization, Toxicity and Biocompatibility, Pharmaceutical and Biomedical Applications.* Chemical Reviews, 2012. **112**(11): p. 5818-5878.
54. Liu, S.Y., et al. *Toxicology studies of a superparamagnetic iron oxide nanoparticle in vivo*. in *Advanced Materials Research*. 2008. Trans Tech Publ.
55. Singh, N., et al., *Potential toxicity of superparamagnetic iron oxide nanoparticles (SPION).* Nano Rev, 2010. **1**.
56. Elgert, K.D., *Immunology : understanding the immune system*. 2nd ed. ed. 2009, Hoboken, N.J.: Wiley-Blackwell.
57. Edelman, G.M. and M.D. Poulik, *Studies on structural units of the gamma-globulins.* J Exp Med, 1961. **113**: p. 861-84.
58. Edelman, G.M., et al., *Structural differences among antibodies of different specificities.* Proc Natl Acad Sci U S A, 1961. **47**: p. 1751-8.
59. Zhong, Y., et al., *Ligand-directed active tumor-targeting polymeric nanoparticles for cancer chemotherapy.* Biomacromolecules, 2014. **15**(6): p. 1955-69.
60. Nicolas, J., et al., *Design, functionalization strategies and biomedical applications of targeted biodegradable/biocompatible polymer-based nanocarriers for drug delivery.* Chemical Society Reviews, 2013. **42**(3): p. 1147-1235.
61. Arruebo, M., M. Valladares, and A. Gonzalez-Fernandez, *Antibody-Conjugated Nanoparticles for Biomedical Applications.* Journal of Nanomaterials, 2009.
62. Hassan, M.M., et al., *Risk factors for pancreatic cancer: case-control study.* Am J Gastroenterol, 2007. **102**(12): p. 2696-707.
63. Batty, G.D., et al., *Risk factors for pancreatic cancer mortality: extended follow-up of the original Whitehall Study.* Cancer Epidemiol Biomarkers Prev, 2009. **18**(2): p. 673-5.
64. Genkinger, J.M., et al., *Alcohol intake and pancreatic cancer risk: a pooled analysis of fourteen cohort studies.* Cancer Epidemiol Biomarkers Prev, 2009. **18**(3): p. 765-76.
65. Landi, S., *Genetic predisposition and environmental risk factors to pancreatic cancer: A review of the literature.* Mutat Res, 2009. **681**(2-3): p. 299-307.
66. Riva, G., et al., *Histo-molecular oncogenesis of pancreatic cancer: From precancerous lesions to invasive ductal adenocarcinoma.* World J Gastrointest Oncol, 2018. **10**(10): p. 317-327.
67. Goggins, M., *Molecular markers of early pancreatic cancer.* J Clin Oncol, 2005. **23**(20): p. 4524-31.
68. Cicenas, J., et al., *KRAS, TP53, CDKN2A, SMAD4, BRCA1, and BRCA2 Mutations in Pancreatic Cancer.* Cancers (Basel), 2017. **9**(5).
69. Vincent, A., et al., *Pancreatic cancer.* Lancet, 2011. **378**(9791): p. 607-20.
70. Statistics, O.f.N. 2012; Available from: http://www.ons.gov.uk/ons/rel/vsob1/cancer-statistics-registrations--england--series-mb1-/index.html.
71. Neoptolemos, J.P., et al., *A randomized trial of chemoradiotherapy and chemotherapy after resection of pancreatic cancer.* N Engl J Med, 2004. **350**(12): p. 1200-10.

72. Ghaneh, P., et al., *Neoadjuvant and adjuvant strategies for pancreatic cancer.* Eur J Surg Oncol, 2008. **34**(3): p. 297-305.
73. Li, J., M.G. Wientjes, and J.L.S. Au, *Pancreatic Cancer: Pathobiology, Treatment Options, and Drug Delivery.* Aaps Journal, 2010. **12**(2): p. 223-232.
74. Gore, J. and M. Korc, *Pancreatic cancer stroma: friend or foe?* Cancer Cell, 2014. **25**(6): p. 711-2.
75. Hwang, R.F., et al., *Cancer-associated stromal fibroblasts promote pancreatic tumor progression.* Cancer Res, 2008. **68**(3): p. 918-26.
76. Helm, O., et al., *Tumor-associated macrophages exhibit pro- and anti-inflammatory properties by which they impact on pancreatic tumorigenesis.* Int J Cancer, 2014. **135**(4): p. 843-61.
77. Li, X., et al., *Sonic Hedgehog Paracrine Signaling Activates Stromal Cells to Promote Perineural Invasion in Pancreatic Cancer.* Clin Cancer Res, 2014.
78. Rhim, A.D., et al., *Stromal elements act to restrain, rather than support, pancreatic ductal adenocarcinoma.* Cancer Cell, 2014. **25**(6): p. 735-47.
79. Apte, M.V., et al., *Periacinar stellate shaped cells in rat pancreas: identification, isolation, and culture.* Gut, 1998. **43**(1): p. 128-33.
80. Stromnes, I.M., et al., *Stromal reengineering to treat pancreas cancer.* Carcinogenesis, 2014. **35**(7): p. 1451-1460.
81. Komar, G., et al., *Decreased blood flow with increased metabolic activity: a novel sign of pancreatic tumor aggressiveness.* Clin Cancer Res, 2009. **15**(17): p. 5511-7.
82. Spivak-Kroizman, T.R., et al., *Hypoxia triggers hedgehog-mediated tumor-stromal interactions in pancreatic cancer.* Cancer Res, 2013. **73**(11): p. 3235-47.
83. Park, M.S., et al., *Perfusion CT: noninvasive surrogate marker for stratification of pancreatic cancer response to concurrent chemo- and radiation therapy.* Radiology, 2009. **250**(1): p. 110-7.
84. Olive, K.P., et al., *Inhibition of Hedgehog signaling enhances delivery of chemotherapy in a mouse model of pancreatic cancer.* Science, 2009. **324**(5933): p. 1457-61.
85. Tredan, O., et al., *Drug resistance and the solid tumor microenvironment.* J Natl Cancer Inst, 2007. **99**(19): p. 1441-54.
86. Amrutkar, M. and I. Gladhaug, *Pancreatic Cancer Chemoresistance to Gemcitabine.* Cancers, 2017. **9**(11): p. 157.
87. Clark, C.E., et al., *Dynamics of the immune reaction to pancreatic cancer from inception to invasion.* Cancer Res, 2007. **67**(19): p. 9518-27.
88. Engels, B., D.A. Rowley, and H. Schreiber, *Targeting stroma to treat cancers.* Semin Cancer Biol, 2012. **22**(1): p. 41-9.
89. McCarroll, J., et al., *Potential applications of nanotechnology for the diagnosis and treatment of pancreatic cancer.* Front Physiol, 2014. **5**: p. 2.
90. Jenkinson, C., et al., *Biomarkers for early diagnosis of pancreatic cancer.* Expert Rev Gastroenterol Hepatol, 2015. **9**(3): p. 305-15.
91. Steinberg, W., *The clinical utility of the CA 19-9 tumor-associated antigen.* Am J Gastroenterol, 1990. **85**(4): p. 350-5.
92. Poruk, K.E., et al., *The clinical utility of CA 19-9 in pancreatic adenocarcinoma: diagnostic and prognostic updates.* Current molecular medicine, 2013. **13**(3): p. 340-351.
93. Baghbanian, M., et al., *Serum CA19-9 in patients with solid pancreatic mass.* Gastroenterology and hepatology from bed to bench, 2013. **6**(1): p. 32-35.
94. Farley, A.M., et al., *Antibodies to a CA 19-9 Related Antigen Complex Identify SOX9 Expressing Progenitor Cells In Human Foetal Pancreas and Pancreatic Adenocarcinoma.* Scientific Reports, 2019. **9**(1): p. 2876.
95. *Tumour markers in gastrointestinal cancers--EGTM recommendations. European Group on Tumour Markers.* Anticancer Res, 1999. **19**(4a): p. 2811-5.
96. van den Bosch, R.P., et al., *Serum CA19-9 determination in the management of pancreatic cancer.* Hepatogastroenterology, 1996. **43**(9): p. 710-3.
97. Franco, O.E., et al., *Cancer associated fibroblasts in cancer pathogenesis.* Semin Cell Dev Biol, 2010. **21**(1): p. 33-9.

98. Kraman, M., et al., *Suppression of antitumor immunity by stromal cells expressing fibroblast activation protein-alpha.* Science, 2010. **330**(6005): p. 827-30.
99. LeBeau, A.M., et al., *Targeting the cancer stroma with a fibroblast activation protein-activated promelittin protoxin.* Mol Cancer Ther, 2009. **8**(5): p. 1378-86.
100. Hofheinz, R.D., et al., *Stromal antigen targeting by a humanised monoclonal antibody: an early phase II trial of sibrotuzumab in patients with metastatic colorectal cancer.* Onkologie, 2003. **26**(1): p. 44-8.
101. Lee, H.O., et al., *FAP-overexpressing fibroblasts produce an extracellular matrix that enhances invasive velocity and directionality of pancreatic cancer cells.* BMC Cancer, 2011. **11**: p. 245.
102. Apte, M.V., et al., *Extracellular matrix composition significantly influences pancreatic stellate cell gene expression pattern: role of transgelin in PSC function.* Am J Physiol Gastrointest Liver Physiol, 2013. **305**(6): p. G408-17.
103. Provenzano, P.P., et al., *Enzymatic targeting of the stroma ablates physical barriers to treatment of pancreatic ductal adenocarcinoma.* Cancer Cell, 2012. **21**(3): p. 418-29.
104. Strimpakos, A.S. and M.W. Saif, *Update on phase I studies in advanced pancreatic adenocarcinoma. Hunting in darkness?* Jop, 2013. **14**(4): p. 354-8.
105. ClinicalTrials.gov. *PEGPH20 Plus Nab-Paclitaxel Plus Gemcitabine Compared With Nab-Paclitaxel Plus Gemcitabine in Subjects With Stage IV Untreated Pancreatic Cancer (HALO-109-202)*. 2014; Available from: http://www.clinicaltrials.gov/ct2/show/NCT01839487?term=NCT01839487&rank=1.
106. Michl, P. and T.M. Gress, *Improving drug delivery to pancreatic cancer: breaching the stromal fortress by targeting hyaluronic acid.* Gut, 2012. **61**(10): p. 1377-9.
107. Mielgo, A. and M.C. Schmid, *Impact of tumour associated macrophages in pancreatic cancer.* BMB Rep, 2013. **46**(3): p. 131-8.
108. Protti, M.P. and L. De Monte, *Immune infiltrates as predictive markers of survival in pancreatic cancer patients.* Front Physiol, 2013. **4**: p. 210.
109. Kusmartsev, S., et al., *Antigen-specific inhibition of CD8+ T cell response by immature myeloid cells in cancer is mediated by reactive oxygen species.* J Immunol, 2004. **172**(2): p. 989-99.
110. Stromnes, I.M., et al., *Targeted depletion of an MDSC subset unmasks pancreatic ductal adenocarcinoma to adaptive immunity.* Gut, 2014.
111. Beyer, M. and J.L. Schultze, *Regulatory T cells in cancer.* Blood, 2006. **108**(3): p. 804-11.
112. Sica, A., et al., *Macrophage polarization in tumour progression.* Semin Cancer Biol, 2008. **18**(5): p. 349-55.
113. Beatty, G.L., et al., *CD40 agonists alter tumor stroma and show efficacy against pancreatic carcinoma in mice and humans.* Science, 2011. **331**(6024): p. 1612-6.
114. Heinemann, V., et al., *Comparison of the cellular pharmacokinetics and toxicity of 2',2'-difluorodeoxycytidine and 1-beta-D-arabinofuranosylcytosine.* Cancer Res, 1988. **48**(14): p. 4024-31.
115. Gandhi, V. and W. Plunkett, *Modulatory activity of 2',2'-difluorodeoxycytidine on the phosphorylation and cytotoxicity of arabinosyl nucleosides.* Cancer Res, 1990. **50**(12): p. 3675-80.
116. Huang, P., et al., *Action of 2',2'-difluorodeoxycytidine on DNA synthesis.* Cancer Res, 1991. **51**(22): p. 6110-7.
117. Schy, W.E., et al., *Effect of a template-located 2',2'-difluorodeoxycytidine on the kinetics and fidelity of base insertion by Klenow (3'-->5'exonuclease-) fragment.* Cancer Res, 1993. **53**(19): p. 4582-7.
118. Gandhi, V., et al., *Excision of 2',2'-difluorodeoxycytidine (gemcitabine) monophosphate residues from DNA.* Cancer Res, 1996. **56**(19): p. 4453-9.
119. NICE. *GEMCITABINE: Indications and doses*. [cited 2020 03/01/2020]; Available from: https://bnf.nice.org.uk/drug/gemcitabine.html.
120. Neoptolemos, J.P., et al., *Comparison of adjuvant gemcitabine and capecitabine with gemcitabine monotherapy in patients with resected pancreatic cancer (ESPAC-4): a multicentre, open-label, randomised, phase 3 trial.* Lancet, 2017. **389**(10073): p. 1011-1024.

121. U.S Food & Drug Administration. *GEMCITABINE HYDROCHLORIDE*. 2018 [cited 2019 20.12.2019]; Available from: https://www.accessdata.fda.gov/scripts/cder/daf/index.cfm?event=overview.process&ApplNo=020509.
122. Maksimenko, A., et al., *Gemcitabine-based therapy for pancreatic cancer using the squalenoyl nucleoside monophosphate nanoassemblies.* International Journal of Pharmaceutics, 2015. **482**(1): p. 38-46.
123. Das, M., et al., *Macromolecular bipill of gemcitabine and methotrexate facilitates tumor-specific dual drug therapy with higher benefit-to-risk ratio.* Bioconjug Chem, 2014. **25**(3): p. 501-9.
124. Koizumi, K., et al., *Activation of p38 mitogen-activated protein kinase is necessary for gemcitabine-induced cytotoxicity in human pancreatic cancer cells.* Anticancer Res, 2005. **25**(5): p. 3347-53.
125. García-Manteiga, J., et al., *Nucleoside transporter profiles in human pancreatic cancer cells: role of hCNT1 in 2', 2'-difluorodeoxycytidine-induced cytotoxicity.* Clinical Cancer Research, 2003. **9**(13): p. 5000-5008.
126. Mackey, J.R., et al., *Functional nucleoside transporters are required for gemcitabine influx and manifestation of toxicity in cancer cell lines.* Cancer research, 1998. **58**(19): p. 4349-4357.
127. Rauchwerger, D.R., et al., *Equilibrative-sensitive nucleoside transporter and its role in gemcitabine sensitivity.* Cancer Res, 2000. **60**(21): p. 6075-9.
128. Poplin, E., et al., *Randomized, multicenter, phase II study of CO-101 versus gemcitabine in patients with metastatic pancreatic ductal adenocarcinoma: including a prospective evaluation of the role of hENT1 in gemcitabine or CO-101 sensitivity.* J Clin Oncol, 2013. **31**(35): p. 4453-61.
129. Wattanawongdon, W., et al., *Establishment and characterization of gemcitabine-resistant human cholangiocarcinoma cell lines with multidrug resistance and enhanced invasiveness.* Int J Oncol, 2015. **47**(1): p. 398-410.
130. Mackey, J.R., et al., *Gemcitabine transport in xenopus oocytes expressing recombinant plasma membrane mammalian nucleoside transporters.* Journal of the National Cancer Institute, 1999. **91**(21): p. 1876-1881.
131. Ritzel, M.W., et al., *Recent molecular advances in studies of the concentrative Na+-dependent nucleoside transporter (CNT) family: identification and characterization of novel human and mouse proteins (hCNT3 and mCNT3) broadly selective for purine and pyrimidine nucleosides (system cib).* Molecular membrane biology, 2001. **18**(1): p. 65-72.
132. NICE. *Pancreatic cancer in adults: diagnosis and management*. February 2018 [cited 2020 03/01/2020]; Available from: https://www.nice.org.uk/guidance/ng85/chapter/Recommendations#managing-resectable-and-borderline-resectable-pancreatic-cancer.
133. Hoy, S.M., *Albumin-bound paclitaxel: a review of its use for the first-line combination treatment of metastatic pancreatic cancer.* Drugs, 2014. **74**(15): p. 1757-68.
134. Hoffman, R.M. and M. Bouvet, *Nanoparticle albumin-bound-paclitaxel: a limited improvement under the current therapeutic paradigm of pancreatic cancer.* Expert opinion on pharmacotherapy, 2015. **16**(7): p. 943-947.
135. Von Hoff, D.D., et al., *Gemcitabine plus nab-paclitaxel is an active regimen in patients with advanced pancreatic cancer: a phase I/II trial.* Journal of clinical oncology : official journal of the American Society of Clinical Oncology, 2011. **29**(34): p. 4548-4554.
136. Olariu, C.I., Yiu, H.P.P., Bouffier, L., Nedjadi, T., Costello, E., Halloran, C.M., Rosseinsky, M.J. , *Multifunctional nanoparticles for healthcare applications.* European Cells and Materials, 2010. **20**: p. 192.
137. Olariu, C.I., et al., *Multifunctional Fe3O4 nanoparticles for targeted bi-modal imaging of pancreatic cancer.* Journal of Materials Chemistry, 2011. **21**(34): p. 12650-12659.
138. Meng, H., et al., *Two-Wave Nanotherapy To Target the Stroma and Optimize Gemcitabine Delivery To a Human Pancreatic Cancer Model in Mice.* ACS Nano, 2013. **7**(11): p. 10048-10065.

139. Von Hoff, D.D., et al., *Increased survival in pancreatic cancer with nab-paclitaxel plus gemcitabine.* N Engl J Med, 2013. **369**(18): p. 1691-703.
140. Lee, G.Y., et al., *Theranostic nanoparticles with controlled release of gemcitabine for targeted therapy and MRI of pancreatic cancer.* ACS Nano, 2013. **7**(3): p. 2078-89.
141. Cabral, H., et al., *Targeted therapy of spontaneous murine pancreatic tumors by polymeric micelles prolongs survival and prevents peritoneal metastasis.* Proc Natl Acad Sci U S A, 2013. **110**(28): p. 11397-402.
142. Zhu, S., et al., *The effect of the acid-sensitivity of 4-(N)-stearoyl gemcitabine-loaded micelles on drug resistance caused by RRM1 overexpression.* Biomaterials, 2013. **34**(9): p. 2327-39.
143. Chertok, B., A.E. David, and V.C. Yang, *Brain tumor targeting of magnetic nanoparticles for potential drug delivery: effect of administration route and magnetic field topography.* J Control Release, 2011. **155**(3): p. 393-9.

Published Abstracts

Nandi S, Sykes PD, Hasan E, Barrow M, Costello E, Rosseinsky MJ, Hunt JA,Halloran CM. (2016). Investigating gemcitabine-loaded superparamagnetic iron oxide nanoparticles against pancreatic cancer cells in artificial circulation. Pancreas, 44(8), 1401.

Nandi S, Sykes PD, Hasan E, Rubbi C, Barrow M, Neoptolemos JP, Costello E, Rosseinsky M, Halloran CM. (2016). Gemcitabine-loaded and antibody-tagged superparamagnetic iron oxide nanoparticles as targeted drug vehicles in pancreatic cancer cell lines. HPB, 18(S2), e776.

Nandi S, Sykes P, Hasan E, Barrow M, Neoptolemos J, Costello E, Rosseinsky M, Hunt J, Halloran C. (2015). Use of gemcitabine-loaded superparamagnetic iron oxide nanoparticles against pancreatic cancer cells in an artificial circulatory model. Pancreatology, 15(3), S22.